Structure of Finite Nuclei in the Local-Density Approximation*

J. W. NEGELE†‡
Laboratory of Nuclear Studies, Cornell University, Ithaca, New York 14850

(Received 25 August 1969)

A new theory is presented for calculating the structure of finite nuclei from the nucleon-nucleon interaction. The essential features of the reaction matrix in finite nuclei are obtained from nuclear-matter theory through the local-density approximation. The resulting density- and energy-dependent effective interaction is justified in detail, and it is shown that the tensor force plays an important role in saturation. The effective interaction is cast into two different forms, one convenient for use in calculating matrix elements and the other specialized for a Hartree-Fock calculation in position space. The density-dependent Hartree-Fock equations are derived by variation of the ground-state expectation value of the energy, and in addition to the usual Hartree-Fock terms, one obtains rearrangement terms arising from the variation of the density appearing in the density-dependent interaction. The appropriate angular-momentum reduction for closed j-shell nuclei is performed. The need for modifying the effective interaction to account for higher-order corrections is discussed, and the constraints imposed on this modification by the properties of nuclear matter are examined. The results of this theory for O^{16}, Ca^{40}, Ca^{48}, Zr^{90}, and Pr^{208} are shown to yield very satisfactory agreement with experimental binding energies, single-particle energies, and electron scattering cross sections. The rearrangement terms in the density-dependent theory are demonstrated to have two essential effects on nuclear structure: a significant reduction in the central density of the nucleus, and a modification of the usual Hartree-Fock relation between single-particle energies and the binding energy. Equivalent local single-particle potentials are calculated and are shown to have significant state dependence.

I. INTRODUCTION

ONE of the most fundamental and elusive problems in theoretical nuclear physics has been to understand the structure of finite nuclei in terms of the nucleon-nucleon interaction. Whereas the theory of Brueckner and co-workers[1,2] establishes the essential framework which, in principle, relates nuclear structure to the two-nucleon interaction, previous calculations have failed to produce reasonable binding energies, single-particle energies, and charge-density distributions for finite nuclei.

The significance of the density dependence of the reaction matrix was recognized in the early calculations, which were consequently performed in position space. Using a reaction matrix based on the Gammel-Thaler potential,[3] Brueckner, Gammel, and Weitzner,[4] and Brueckner and Goldman[5] developed a Hartree-Fock (HF) theory which included density dependence through the rearrangement potential. The fundamental limitation of this work was the inclusion only of the density dependence of the core repulsion, thereby omitting the strong density dependence of the tensor force which will prove crucial in our subsequent theory. The manifestation of this omission in the calculations of O^{16}, Ca^{40}, and Zr^{90} by Brueckner, Lockett, and Rotenberg[6] and Pb^{208} by Masterson and Lockett[7] is far too little saturation, leading to unrealistically high central densities. A rather similar theory by Köhler[8] suffered from the same difficulty, since his simplified force included only a central S-state interaction.

More recent calculations have been performed in a harmonic-oscillator representation because of the computational advantage of the convenient decomposition into relative partial waves. The essential weakness of calculations thus far using this approach is the complete omission of the rearrangement potential, resulting in even less saturation than in the previous calculations. The basic theory and results for simplified forces are presented by Davies, Krieger, and Baranger, and by Tarbutton and Davies.[9] Calculations using reaction matrices instead of simplified forces have been performed by Irvine[10] for light nuclei, and by Davies, Baranger, Tarbutton, and Kuo[11] for closed-shell nuclei up to Pb^{208}. The serious lack of saturation is evident from their excessive central densities.

In view of these previous results, our present theory places special emphasis upon the density dependence of the reaction matrix in finite nuclei. Our approach is predicated upon the conviction that the essential properties of the reaction matrix in finite nuclei may be obtained from nuclear-matter theory, and this connection is established in detail in our subsequent discussion

† National Science Foundation Graduate Fellow.
* Work supported in part by the National Science Foundation and in part by the Office of Naval Research.
‡ Present address: Niels Bohr Institute, Copenhagen, Denmark.
[1] K. A. Brueckner and C. A. Levinson, Phys. Rev. **97**, 1344 (1955); K. A. Brueckner, *ibid.* **97**, 1353 (1955).
[2] K. A. Brueckner and J. L. Gammel, Phys. Rev. **109**, 1023 (1958).
[3] J. L. Gammel and R. M. Thaler, Phys. Rev. **107**, 291 (1957); **107**, 1337 (1957).
[4] K. A. Brueckner, J. L. Gammel, and H. Weitzner, Phys. Rev. **110**, 431 (1958).
[5] K. A. Brueckner and D. T. Goldman, Phys. Rev. **116**, 424 (1959).
[6] K. A. Brueckner, A. M. Lockett, and M. Rotenberg, Phys. Rev. **121**, 255 (1961).
[7] K. A. Masterson and A. M. Lockett, Phys. Rev. **129**, 776 (1963).
[8] H. S. Köhler, Phys. Rev. **137**, B1145 (1965); **138**, B831 (1965).
[9] K. T. R. Davies, S. J. Krieger, and M. Baranger, Nucl. Phys. **84**, 545 (1966); R. M. Tarbutton and K. T. R. Davies, *ibid.* **A120**, 1 (1968).
[10] J. M. Irvine, Nucl. Phys. **A120**, 576 (1968).
[11] K. T. R. Davies, M. Baranger, R. M. Tarbutton, and T. T. S. Kuo, Phys. Rev. **177**, 1519 (1969).

of the local-density approximation (LDA). The primary limitation of this philosophy is that it is necessary to account in some way for the discrepancy between the two-body contribution to nuclear-matter binding energy of 11.0 MeV and the total binding energy we expect from the semiempirical mass formula of 15.68 MeV. In this work, we make the assumption that when higher-order corrections have been evaluated carefully, nuclear-matter theory will indeed produce the correct binding, and thus we modify the effective interaction to produce the proper binding. This assumption is the weakest point in our theory, but is somewhat substantiated by our results which yield satisfactory energies and densities for nuclei from O^{16} to Pb^{208}. Even without modifying the effective interaction, our results are a significant improvement over the previous calculations.

Results similar to those in this paper have been obtained by Meldner,[12] on the basis of a completely different philosophy. He takes only the general form of the interaction from nuclear-matter theory—exchange, density dependence, etc.—and then fixes five parameters to achieve agreement. His agreement with binding energies of selected nuclei is extremely good, better than ours, and he also gets very good agreement with mean square radii. His parameters are adjusted to yield $0s$ proton energies of approximately 80 MeV, which we believe to be incorrect. There are significant differences in the shape of the density distributions: We believe Meldner's central densities for Ca^{40} and Pb^{208} are about 20% too high, his half-density radius for Pb is about 4% lower than ours, and his surface thickness for Pb is only about $\frac{2}{3}$ of ours. Since our results have been tested against electron scattering, which is sensitive to the half-density radius and the surface thickness, we believe our results on shape to be more reliable. This in no way detracts from Meldner's use of his theory for an extrapolation to superheavy nuclei, like $Z=114$.

II. CONSTRUCTION OF AN EFFECTIVE TWO-BODY INTERACTION FROM NUCLEAR-MATTER THEORY

Elements of Nuclear-Matter Theory

In seeking to develop a theory of the structure of finite nuclei, the natural starting point is the existing theory of nuclear matter. Thus, we shall sidestep the questions of the nature of the fundamental nucleon-nucleon interaction, whether the meson degrees of freedom may legitimately be suppressed, and whether the three-body and higher many-body forces are, in fact, negligible,[13] and instead, assume that the nucleon-nucleon interaction may be adequately described nonrelativistically by a phenomenological two-body potential.

Throughout this work, the Reid soft-core potential is used.[14] The nonlocality in angle, with each partial wave having simple functions of the radial coordinate multiplying unity, $\mathbf{l}\cdot\mathbf{s}$ and $\mathbf{S}_{12}$ affords sufficient flexibility to fit scattering phase shifts and the deuteron quadrupole moment, and is computationally much more convenient than potentials with explicit momentum dependence or general nonlocality in the two-particle coordinates. The potential satisfies the minimal conditions one might demand from the present understanding of meson theory, in that the long-range behavior is consistent with one-pion exchange and the short-range repulsion is generated by Yukawas corresponding to bosons of sensible mass. One should bear in mind that the $T=0$ states are not as well determined by experimental data as the $T=1$ states and, in particular, the $^3S_1$-$^3D_1$ potentials, to which the structure of finite nuclei is particularly sensitive, are not strongly determined.

Since nuclear-matter theory is extensively described in the literature,[1,2,15–19] with Day's review article[17] providing an ideal introduction for the uninitiated, we shall only note the features which are most relevant to our subsequent work. The essential quantity entering into the theory is the reaction matrix G, which sums all orders of ladder diagrams containing the bare interaction and unoccupied intermediate states. Denoting Q as the projector onto unoccupied two-body states and defining the positive-definite operator e such that $e\,|\,pq\rangle=(E_p+E_q+W)\,|\,pq\rangle$, where the starting energy W is written with the opposite sign from the usual convention and is defined by the particular Goldstone diagram under consideration, then

$$G(W)=V-V(Q/e)V+V(Q/e)V(Q/e)V-\cdots$$
$$=V-V(Q/e)G(W). \qquad (2.1)$$

For nuclear matter the Goldstone expansion is particularly simple since translational invariance specifies the unperturbed wave functions as plane waves, and momentum conservation eliminates a large class of diagrams. It is convenient to introduce the following notation:

$$\Phi_{mn}(\mathbf{r}_1,\mathbf{r}_2)=(1/\Omega)\exp(i\mathbf{k}_m\cdot\mathbf{r}_1)\exp(i\mathbf{k}_n\cdot\mathbf{r}_2)$$
$$=(1/\Omega)\exp(i\mathbf{K}_{mn}\cdot\mathbf{R})\exp(i\mathbf{k}_{mn}\cdot\mathbf{r}), \qquad (2.2)$$

where

$$\mathbf{R}=(\mathbf{r}_1+\mathbf{r}_2)/2, \qquad \mathbf{r}=\mathbf{r}_1-\mathbf{r}_2,$$
$$\mathbf{K}_{mn}=\mathbf{k}_m+\mathbf{k}_n, \qquad \mathbf{k}_{mn}=\tfrac{1}{2}(\mathbf{k}_m-\mathbf{k}_n),$$

[12] H. Meldner, Phys. Rev. **178**, 1815 (1969).
[13] G. E. Brown, A. M. Green, and W. J. Gerace, Nucl. Phys. **A115**, 435 (1968); G. E. Brown and A. M. Green, *ibid.* **A137**, 1 (1969).
[14] R. V. Reid, Ann. Phys. (N.Y.) **50**, 411 (1968).
[15] J. Goldstone, Proc. Roy. Soc. (London) **A239**, 267 (1957).
[16] H. A. Bethe, B. H. Brandow, and A. G. Petschek, Phys. Rev. **129**, 225 (1963), hereafter referred to as BBP.
[17] B. D. Day, Rev. Mod. Phys. **39**, 719 (1967).
[18] B. H. Brandow, Rev. Mod. Phys. **39**, 771 (1967).
[19] G. Dahll, E. Østgaard, and B. Brandow, Nucl. Phys. **A124**, 481 (1969).

and to define the correlated wave function Ψ by

$$v\Psi_{mn}=G\Phi_{mn}. \tag{2.3}$$

Separation of c.m. coordinates and resolution into partial waves is accomplished most conveniently in the entrance-channel description[2,16] in which we obtain

$$\Psi_{mn}{}^{M}=(1/\Omega)\exp(i\mathbf{K}_{mn}\cdot\mathbf{R})\sum_{JLL'} i^{L}[4\pi(2L+1)]^{1/2}$$
$$\times C(L1J:0MM)\mathcal{Y}_{L',J}{}^{M}(1/k_{mn}r)u_{L',J}{}^{(L)}(\mathbf{k}_{mn},\mathbf{r}). \tag{2.4}$$

For the singlet case, the Clebsch-Gordan coefficients and $\mathcal{Y}_{L',J}{}^{M}$ simplify to the usual form involving only Y_{L0}. Introducing the angle-averaged Pauli operator $Q_{\rm av}$, $u_{L'J}{}^{(L)}$ satisfies the coupled equations

$$u_{L'J}{}^{(L)}(k,r)=\delta_{LL'}\mathcal{J}_{L}(kr)$$
$$-(Q_{\rm av}/e)\sum_{L''} v_{L',L''}{}^{J}u_{L'',J}{}^{(L)}, \tag{2.5}$$

where

$$v_{L',L''}{}^{J}=\langle\mathcal{Y}_{L'J}{}^{M}\mid v\mid\mathcal{Y}_{L''J}{}^{M}\rangle.$$

All of the numerical results of this work utilize solutions to the Bethe-Goldstone equation (2.5), obtained from a computer program written by Siemens[20] based on the iterative method of Kallio and Day.[21]

Although the unperturbed wave functions are uniquely specified by translation invariance, the single-particle energies in the Goldstone expansion are chosen with the intent of minimizing the effect of contributions beyond lowest order. For states below the Fermi momentum, it is shown in Appendix B of BBP that the familiar HF potential

$$\langle m\mid U_{\rm HF}\mid m\rangle=\sum_{n<k_F}[\langle mn\mid G\mid mn\rangle-\langle mn\mid G\mid nm\rangle] \tag{2.6}$$

with G evaluated on the energy shell, i.e.,

$$W=(-E_m-E_n),$$

corresponds to the exact cancellation of a large class of diagrams. The lowest-order effect of $U_{\rm HF}$ is to cancel a single off-energy-shell G interaction connected to a hole loop, and higher-order diagrams are cancelled in which additional G matrices are added below the level of $U_{\rm HF}$ and alternate in level with original or additional G interactions in the main diagram. $U_{\rm HF}$ defined in this way must satisfy a self-consistency condition since G depends on $U_{\rm HF}$ through W and $U_{\rm HF}$ is defined in terms of G.

For states above the Fermi sea, the single-particle energy does not exactly cancel any class of diagrams, but rather is selected to roughly compensate the total contribution of three-body diagrams. We shall refer to three-body diagrams as the set of diagrams in which the first two G interactions produce three-particle and three-hole lines, any number of additional interactions occur between the particle lines with the provision that only particle states are allowed and two interactions may not occur consecutively between the same pair of lines and, finally, the last two interactions return the system to the state with no particles or holes. Bethe[22,23] has shown that these three-body diagrams do not converge order by order, but rather must be summed by means of the Faddeev equation. Since Dahlblom[24] has calculated the total contribution to be -0.7 MeV at $k_F=1.36$ F^{-1}, it is simplest to cancel the three-body terms on the average by using zero nuclear potential energy for excited states.

Local-Density Approximation

There are two basic approaches available for constructing an analogous theory for finite nuclei. The most straightforward and accurate approach, which we shall call the state-dependent approach, is to begin with a suitable basis of finite wave functions and solve the Bethe-Goldstone equation for all two-body states in this basis. In the special case of a harmonic-oscillator basis, the formalism becomes particularly simple since the Brody-Moshinsky transformation[25] allows exact decomposition of a two-body product wave function into relative and c.m. coordinates. More general bases are conveniently treated by expanding in a harmonic-oscillator basis, possibly using different $\hbar\omega$ for various states to reduce the required number of terms. Numerous calculations using this approach have been performed in light nuclei,[26–31] but the method becomes computationally cumbersome in heavy nuclei.

The alternative approach, which this work pursues, is to apply the nuclear-matter reaction matrix to finite nuclei through the LDA. This approximation is motivated by the fact that two-body correlations are of relatively short range compared with nuclear dimensions. Thus, it is reasonable to assume that for a given starting energy W, in the small region about some c.m. coordinate in which the correlated and uncorrelated wave functions differ significantly, the dominant many-body effect is simply that obtained in nuclear matter of the density occurring at the c.m.

The LDA approximates the propagator Q/e in a

[20] P. Seimens, Nucl. Phys. **A141,** 225 (1970).
[21] A. Kallio and B. D. Day, Phys. Letters **25B,** 72 (1967); Nucl. Phys. **A124,** 177 (1969).
[22] H. A. Bethe, Phys. Rev. **138,** B804 (1965); **158,** 941 (1967).
[23] R. Rajaraman and H. A. Bethe, Rev. Mod. Phys. **39,** 745 (1967).
[24] T. Dahlblom, Acta Acad. Aboensis, Math. Phys. **29,** 6 (1969).
[25] T. A. Brody and M. Moshinsky, *Tables of Transformation Brackets* (Gordon and Breach Science Publishers, Inc., New York, 1967).
[26] T. T. S. Kuo and G. E. Brown, Nucl. Phys. **85,** 40 (1966).
[27] T. T. S. Kuo, Nucl. Phys. **A103,** 71 (1967).
[28] R. L. Becker, A. D. MacKellar, and B. M. Morris, Phys. Rev. **174,** 1264 (1968).
[29] R. J. McCarthy, Nucl. Phys. **A130,** 305 (1969).
[30] C. W. Wong, Nucl. Phys. **A91,** 399 (1967).
[31] R. J. Eden and V. J. Emery, Proc. Roy. Soc. (London) **A248,** 266 (1958).

finite nucleus by that in nuclear matter, and thus requires the use of plane-wave intermediate states. Although conceptually the unoccupied states should be orthogonal to the occupied states, in practice, one expects significant corrections only for excitations to the lowest unoccupied states, to which the theory is not critically sensitive. The energy denominator e is essentially exact since the difference between nuclear matter and a finite nucleus is contained in W.

The most serious assumption in the LDA is approximating the exclusion operator in a finite nucleus Q by the nuclear-matter Pauli operator, and has been treated in detail by Wong.[30] For an $A=18$ nucleus, in which a harmonic-oscillator basis is valid, Wong compares the Pauli operator in LDA with an essentially exact global approximation in which $(1-Q)$ is expressed purely in terms of harmonic-oscillator states. By means of the Brody-Moshinsky transformation, $(1-Q)$ is transformed into relative and c.m. coordinates for calculation of the reaction matrix. The comparison of results computed in this global approximation with those obtained in the LDA thus provides a direct evaluation of the error introduced by the seemingly inconsistent LDA prescription. For states concentrated well within the interior of the nucleus, the two methods agree very closely, whereas in the surface the LDA gives slightly too much attraction.

Given the uncertainty in cancelling the three-body contributions, which have never been evaluated in finite nuclei, it is felt that the small error created by the LDA in the surface may be neglected. Hence, for our purposes, we shall now proceed to construct an effective interaction for finite nuclei based on the nuclear-matter propagator Q/e.

Construction of Effective Local Interaction

As has already been pointed out, one may expand the most general two-body matrix element into sums of matrix elements between product wave functions of relative and c.m. coordinates. Since the bare interaction only involves relative coordinates, the reaction matrix at a given c.m. point does not depend on the c.m. wave function. Hence, the general problem is to evaluate the matrix elements of G at a given density between arbitrary relative wave functions. Treating for the moment only singlet matrix elements between relative wave functions denoted by $|\phi_{nl}\rangle$ and having radial functions $R_{nl}(r)$, and bearing in mind that the following equations pertain to a specific density and starting energy, we may insert two complete sets of plane-wave states as follows:

$$\begin{aligned}\langle\phi_{nl}\,|\,G\,|\,\phi_{n'l}\rangle&=\sum_{\mathrm{k}k_0}\langle\phi_{nl}\,|\,\phi_{\mathrm{k}}\rangle\langle\phi_{\mathrm{k}}\,|\,G\,|\,\phi_{\mathrm{k}_0}\rangle\langle\phi_{\mathrm{k}_0}\,|\,\phi_{n'l}\rangle\\&=\int dr\int dr'\int dr''\sum_{kk_0}R_{nl}(r)\mathcal{J}_l(kr)\\&\times\mathcal{J}_l(kr'')v_l(r'')u_l(r'',k_0)\mathcal{J}_l(k_0r')R_{n'l}(r').\end{aligned}\quad(2.7)$$

The sum over k yields $\delta(r-r'')$, but the effective potential is nonlocal in r.

$$\langle\phi_{nl}\,|\,G\,|\,\phi_{n'l}\rangle=\int dr\int dr'R_{nl}(r)R_{n'l}(r')v_l(r,r'),\quad(2.8)$$

where

$$v_l(r,r')=\sum_{k_0}v_l(r)u_l(r,k_0)\mathcal{J}_l(k_0r').$$

In order to construct a potential which is local in r, one must make the approximation

$$u_l(r,k_0)=f_l(r)\mathcal{J}_l(k_0r),\quad(2.9)$$

where $f_l(r)$ is as yet unspecified. Then,

$$\langle\phi_{nl}\,|\,G\,|\,\phi_{n'l}\rangle=\int drR_{nl}(r)R_{n'l}(r)v_l^{\mathrm{eff}}(r),\quad(2.10)$$

where

$$v_l^{\mathrm{eff}}(r)=v_l(r)f(r).$$

In practice, the precise prescription for $f(r)$ is not critical. An effective force suggested by Brandow[32] corresponds to defining $f(r)$ at some average momentum:

$$\begin{aligned}f_l(r)&=u_l(r,k_{\mathrm{av}})/\mathcal{J}_l(k_{\mathrm{av}}r),\\v_l^{\mathrm{eff}}(r)&=v_lu_l(r,k_{\mathrm{av}})/\mathcal{J}_l(k_{\mathrm{av}}r).\end{aligned}\quad(2.11)$$

The zeros in the denominator constitute no serious problem since they occur at sufficiently large r that u_l has healed essentially to $\mathcal{J}_l$ and v_l^{eff} is simply v_l. The validity of this approximation is most easily understood by considering the defect function $\chi_l=\mathcal{J}_l-u_l$ in the simple case of a pure hard core. Clearly, (2.9) is equivalent to specifying

$$\chi=g(r)\mathcal{J}_l(kr).\quad(2.12)$$

Inside the core radius, $\chi_l=\mathcal{J}_l$ so (2.12) is satisfied identically. Outside the core radius, χ_l is equal to a decaying Hankel function with the normalization specified by continuity at the core radius c. Thus, beyond c, the ratio of the approximate χ_l given by (2.12) to the true hard core χ_l is

$$\mathcal{J}_l(k_{\mathrm{av}}c)\mathcal{J}_l(kr)/\mathcal{J}_l(kc)\mathcal{J}_l(k_{\mathrm{av}}r).$$

For all k of physical interest, this ratio varies insignificantly within the range of the Hankel function so that (2.12) is an excellent approximation. For a realistic force, one cannot make a similar simple analytical argument, but the general features should remain the same and (2.12) should still be a reasonably good approximation to χ_l. Since χ_l is much smaller than $\mathcal{J}_l$, (2.9) must be an excellent approximation to u_l.

---

[32] B. H. Brandow, in *Proceedings of the International School of Physics "Enrico Fermi", Course XXXVI* (Academic Press Inc., New York, 1966).

An alternative definition for $f(r)$ has been used by Siemens[20] in the context of Thomas-Fermi theory.

$$f_l(r)=\sum_{k_1<k_F}\sum_{k_2<k_F}|\tfrac{1}{2}(\mathbf{k}_1-\mathbf{k}_2)|^{-2}\mathcal{J}_l(\tfrac{1}{2}|\mathbf{k}_1-\mathbf{k}_2|r)u_l(r,\tfrac{1}{2}|\mathbf{k}_1-\mathbf{k}_2|)/\sum_{k_1<k_F}\sum_{k_2<k_F}|\tfrac{1}{2}(\mathbf{k}_1-\mathbf{k}_2)|^{-2}\mathcal{J}_l^2(\tfrac{1}{2}|\mathbf{k}_1-\mathbf{k}_2|r). \quad (2.13)$$

Written in this form, it is clear that instead of defining an average k, we are averaging f over all the normally occupied states in nuclear matter. For notational convenience we shall transform from $\mathbf{k}_1$ and $\mathbf{k}_2$ to relative $\mathbf{k}$ according to (2.2). Then

$$\int^{k_F}d^3k_1\int^{k_F}d^3k_2F(\tfrac{1}{2}|\mathbf{k}_1-\mathbf{k}_2|)=\int_0^{k_F}k^2dk\,W(k,k_F)F(k), \quad (2.14)$$

where

$$W(k,k_F)=(64\pi^2/3)(2k_F{}^3+k^3-3k_F{}^2k).$$

In this notation,

$$v_l{}^{\text{eff}}(r)=\frac{\int dk\,W(k,k_F)\mathcal{J}_l(kr)v_l(r)u_l(r,k)}{\int dk\,W(k,k_F)\mathcal{J}_l{}^2(kr)}. \quad (2.15)$$

The argument for the validity of this choice is analogous to that given for Brandow's prescription, and, in practice, there is negligible numerical difference between the two definitions of $v_l{}^{\text{eff}}$. The present choice has the technical advantage that the denominator is positive definite and, in addition, the lowest-order contribution to nuclear-matter binding energy is exact, as follows trivially from the definition

$$\begin{aligned}&\tfrac{1}{2}\sum_{k_1<k_F}\sum_{k_2<k_F}\langle\mathbf{k}_1\mathbf{k}_2|v^{\text{eff}}|\mathbf{k}_1\mathbf{k}_2-\mathbf{k}_2\mathbf{k}_1\rangle\\&=\sum_l\int dk\,W(k,k_F)(2l+1)\int dr\,\mathcal{J}_l{}^2(kr)v_l{}^{\text{eff}}(r)\\&=\sum_l(2l+1)\int dk\,W(k,k_F)\int dr\,\mathcal{J}_l(kr)v_l(r)u_l(r,k)\\&=\tfrac{1}{2}\sum_{k_1<k_F}\sum_{k_2<k_F}\langle\mathbf{k}_1\mathbf{k}_2|G|\mathbf{k}_1\mathbf{k}_2-\mathbf{k}_2\mathbf{k}_1\rangle. \quad (2.16)\end{aligned}$$

It is instructive at this point to note the simple structure in momentum space implied by (2.9). In general,

$$\langle k|G|k'\rangle=\int\mathcal{J}_l(kr)\mathcal{J}_l(k'r)v_l{}^{\text{eff}}(r)\,dr, \quad (2.17)$$

and for S states, the k dependence is particularly simple,

$$\langle k|G|k'\rangle=F(k-k')-F(k+k'), \quad (2.18)$$

where

$$F(k)=\tfrac{1}{2}\int\cos(kr)v_0{}^{\text{eff}}(r)\,dr.$$

Equation (2.18) provides another check on the basic approximation in (2.9), and calculations in the singlet S state, as well as the triplet S state which is explained below, have yielded good agreement.

In order to generalize to the triplet case with the tensor force, plane-wave matrix elements of G are written in terms of the wave function in (2.4) and averaged over M:

$$\begin{aligned}&\sum_M\langle\mathcal{Y}_{L'J}{}^M\mathcal{J}_{L'}(kr)|G|\mathcal{J}_L(k_0r)\mathcal{Y}_{LJ}{}^M\rangle\\&\quad=\int dr\,\mathcal{J}_{L'}(kr)\sum_{L''}v_{L',L''}{}^J(r)u_{L'',J}{}^{(L)}(r,k_0). \quad (2.19)\end{aligned}$$

Since the reaction matrix G is Hermitian for constant W, (2.19) implies

$$\begin{aligned}&\int dr\,\mathcal{J}_{L'}(kr)\sum_{L''}v_{L'L''}{}^J(r)u_{L'',J}{}^{(L)}(r,k_0)\\&\quad=\int dr\,\mathcal{J}_L(k_0r)\sum_{L''}v_{LL''}{}^Ju_{L'',J}{}^{(L')}(r,k). \quad (2.20)\end{aligned}$$

Constructing the diagonal effective interaction in the same manner as (2.15), we obtain

$${}^3v_{\text{eff}_{L,L}}{}^J(r)=\int dk\,W(k,k_F)\mathcal{J}_L(kr)\sum_{L''}v_{LL''}{}^J(r)u_{L'',J}{}^{(L)}(r,k)/\int dk\,W(k,k_F)\mathcal{J}_L{}^2(kr). \quad (2.21)$$

Although this definition clearly reproduces the correct lowest-order contribution to nuclear-matter binding energy, the basic approximation in (2.9) must be reexamined since we assume

$$\begin{aligned}&v_{LL}{}^J(r)u_{L,J}{}^{(L)}(r,k)+v_{LL'}{}^J(r)u_{L',J}{}^{(L)}(r,k)\\&\quad=[v_{LL}{}^J(r)f_L(r)+v_{LL'}{}^J(r)f_{L'}(r)]\mathcal{J}_L(kr), \quad (2.22)\end{aligned}$$

where

$$L'=J\pm1 \quad \text{for} \quad L=J\mp1.$$

Whereas the argument in the singlet case still applies to the f_L term, there is no correspondingly simple argument for the k dependence of the coupled wave $u_{L',J}{}^{(L)}(r,k)$. Instead, we consider the contribution of the tensor force to the perturbation series (2.1), noting that the only nonlocality arises from the operator Q/e. The tensor force is most conveniently treated by considering the long- and short-range parts separately. The short-range part is very strong and contributes significantly in the second and all higher orders, but since it excites very-high-energy intermediate states, Q is of negligible consequence and the average e is large compared with the range of significant intermediate states. The long-range tensor force, on the other hand, is sufficiently weak that its dominant contribution is in second order. Kuo and Brown[26]

have examined this second-order contribution and show that here, too, nonlocality is negligible since the closure approximation is a good approximation.

$$\langle V_{TL}(Q/e)\,V_{TL}\rangle \cong (1/e_{\rm eff})\langle V_{TL}{}^2\rangle, \qquad e_{\rm eff}=220\ \text{MeV}. \tag{2.23}$$

Thus, we conclude that even the coupled wave component of (2.22) is reasonably accurate, and feel that the definition of $f_{L'}(r)$ implied by (2.21) provides a sensible average over the small amount of nonlocality.

The nondiagonal effective interaction is defined analogously to (2.21),

$$^3v_{{\rm eff}L',L}{}^J(r)=\int dk\,W(k,k_F)\mathcal{J}_{L'}(kr)\sum_{L''}v_{L'L''}{}^J(r)u_{L'',J}{}^{(L)}(r,k)/\int dk\,W(k,k_F)\mathcal{J}_{L'}(kr)\mathcal{J}_L(kr). \tag{2.24}$$

According to (2.20), an equivalent definition should be obtained by interchanging L and L', and, in practice, this provides a useful check on numerical calculations. The argument concerning the local approximation given above still applies for the short-range tensor force, and we now note that the main contribution of the long-range force is in first order and is thus necessarily local. The particular average chosen in (2.24) no longer is justified on the basis of contribution to nuclear-matter binding energy, since the nondiagonal tensor force does not contribute to the lowest-order binding energy, but it still appears to be a reasonable average. Finally, we note that the zeros in the denominator, due to the fact that the integral with $L\neq L'$ is not positive definite, are of no practical importance since in the $S-D$ case at $k_F=1.4$ F^{-1} the first zero is beyond 6 F, and the zeros of higher angular-momentum states are correspondingly farther from the origin.

Thus far, we have insisted that the effective interaction defined in general in (2.24) be calculated for a specific starting energy W. In practice, the available nuclear-matter matrix elements involved self-consistent starting energies, as discussed in connection with (2.6). Hence, the actual $v_{{\rm eff}L'L}{}^J$ that has been computed involves an average over a range of starting energies where the average starting energy is approximately 2.4 F^{-2}. Corrections for this averaging will be considered below. The individual interactions $v_{{\rm eff}L'L}{}^J$ in all partial waves through $L=2$ are tabulated by Siemens.[20]

Matrix Elements of Effective Interaction in a Finite Nucleus

One of the two main applications of the effective interaction is the calculation of matrix elements in a finite nucleus. Since the above development pertains to the construction of an effective interaction at a particular density and starting energy, it is now necessary to consider a computationally simple method of including the dependence on k_F and W, which does not necessitate complete reaction matrix calculations at a large number of values of these parameters.

Since any finite wave function can be expanded in terms of harmonic-oscillator wave functions, we need consider only matrix elements between two-body antisymmetrized and normalized harmonic-oscillator product wave functions which are coupled to specified angular momentum J and isospin T. The matrix element between such states may be written as follows[26]:

$$\begin{aligned}\langle n_al_aj_a,\,n_bl_bj_b;JT\,|\,v_{\rm eff}\,|\,n_cl_cj_cn_dl_dj_d;JT\rangle&=[(1+\delta_{ab})(1+\delta_{cd})]^{-1/2}\\
\times\sum_{LL'S}&\begin{Bmatrix} l_a & \tfrac12 & j_a\\ l_b & \tfrac12 & j_b\\ L & S & J\end{Bmatrix}\begin{Bmatrix} l_c & \tfrac12 & j_c\\ l_d & \tfrac12 & j_d\\ L' & S & J\end{Bmatrix}(-1)^{L+L'}\hat S(\hat L\hat j_a\hat j_b\hat L'\hat j_c\hat j_d)^{1/2}\sum_{nln'l',N\mathcal{L}N'}\langle nlN\mathcal{L},L\,|\,n_al_an_bl_b,L\rangle\\
\times\langle n'l'N'\mathcal{L},L'\,|\,n_cl_cn_dl_d,L'\rangle&(-1)^{l+l'}[1-(-1)^{l+S+T}]\sum_{\mathcal{J}}U(\mathcal{L}lJS;L\mathcal{J})\,U(\mathcal{L}l'JS;L'\mathcal{J})\\
&\times\langle N\mathcal{L}\,|\,\langle nl\,|^{(2S+1)}v_{{\rm eff}ll'}{}^{\mathcal{J}}\,|\,n'l'\rangle\,|\,N'\mathcal{L}\rangle,\end{aligned} \tag{2.25}$$

where

$$\delta_{ab}=\delta_{l_al_b}\delta_{j_aj_b}\delta_{n_an_b},$$

$$\hat L=2L+1,$$

$\langle nlN\mathcal{L},L\,|\,n_al_an_bl_b,L\rangle$ is a Brody-Moshinsky bracket,[25]

$$U(\mathcal{L}lJS;L\mathcal{J})=(-1)^{\mathcal{L}+l+J+S}\hat L\hat{\mathcal{J}}\begin{Bmatrix}\mathcal{L} & l & L\\ S & J & \mathcal{J}\end{Bmatrix},$$

and relative and c.m. coordinates are defined

$$\mathbf{r}=(\mathbf{r}_1-\mathbf{r}_2)/\sqrt2, \qquad \mathbf{R}=(\mathbf{r}_1+\mathbf{r}_2)/\sqrt2.$$

The various terms in (2.25) arise because of the different coupling of angular momentum required for the over-all two-body matrix element, for the transformation to relative and c.m. coordinates, and for the matrix element of the two-body force. The factors for particles a and b arise as follows. The 9-j symbol is

TABLE I. Coefficients for density and starting energy dependence in Eq. (2.33). The last two entries are the nondiagonal tensor components.

State	F^S	F^L	C_1^S	C_2^S	C_3^S	C_1^L	C_2^L	C_3^L
$^1S_0$	0.866	1.030	0.723	0.128	−0.0011	1.014	−0.0101	0.0018
$^3S_1$	0.703	1.212	0.156	0.429	−0.0205	1.020	−0.0256	0.0075
$^1P_1$	0.867	0.919	0.539	0.236	−0.0122	1.140	−0.0637	0.0000
$^3P_0$	0.963	1.006	0.888	0.0552	−0.0019	0.997	0.0009	0.0003
$^3P_1$	0.908	0.976	0.799	0.1129	−0.0099	1.009	−0.0042	−0.0001
$^3P_2$	1.058	1.055	1.405	−0.209	0.0115	0.977	0.0075	0.0014
$^1D_2$	1.032	1.004	1.061	−0.0741	0.0211	1.003	−0.0016	0.0001
$^3D_1$	0.566	0.990	1	0	0	1	0	0
$^3D_2$	1.098	1.015	1	0	0	1	0	0
$^3D_3$	0.902	0.833	1	0	0	1	0	0
S-D	1.025	0.985	1	0	0	1	0	0
P-F	1.01	1.01	1	0	0	1	0	0

used to couple l_a and l_b to L, $\frac{1}{2}$ and $\frac{1}{2}$ to S, and j_a and j_b to J. The Brody-Moshinsky transformation conserves L, so that l and $\mathfrak{L}$ are coupled to L. Because of the 9-j symbol, L in turn is coupled with S to form J. Hence, the 6-j symbol is used to recouple the angular momenta to J, so that S and l first couple to $\mathcal{J}$, and then $\mathcal{J}$ and $\mathfrak{L}$ couple to J. The S, l, $\mathcal{J}$ coupling is then appropriate for the relative matrix element of the two-body interaction. Finally, $(1+\delta_{ab})^{-1/2}$ takes into account the extra factor required for normalization when a and b are identical particles.

The essential simplification employed in evaluating the reduced matrix element

$$\langle N\mathfrak{L} \mid \langle nl \mid v_{\mathrm{eff}ll'}{}^{\mathcal{J}} \mid n'l' \rangle \mid N'\mathfrak{L} \rangle$$

is to factorize the density dependence so as to perform the relative and c.m. integrals independently. Simply multiplying the effective interaction at some k_F by a function of k_F is *a priori* a poor approximation because of the different physics of the excitations by short-range and long-range parts of the force. However, because of the fact that the c.m. integral always includes the product of v_{eff} with harmonic-oscillator functions whose range of variation is strictly limited by physically sensible values of $\hbar\omega$, the reduced matrix element cannot be extremely sensitive to the detailed spatial distribution of density dependence. Hence, in this work, the effective interaction is divided at 1 F into a long- and a short-range part, each having the spatial dependence of $v_{\mathrm{eff}}(k_F, r)$ at $k_F=1.4$ F^{-1}, but being multiplied by separate functions of k_F. It should be noted that the resulting discontinuities in $v_{\mathrm{eff}}(k_F, r)$ at other densities at which the multiplicative functions may not agree are physically quite acceptable, corresponding only to discontinuities in the second derivatives of wave functions.

In the spirit of approximation which has been established above, the multiplicative density factors at any k_F are defined such that the nuclear-matter average of this factor times $v_{\mathrm{eff}}(k_F=1.4, r)$ is identical to the nuclear-matter average of $v_{\mathrm{eff}}(k_F, r)$. Thus,

$$\int_0^1 dr \int_0^{k_F} dk\, W(k, k_F) F^S(k_F) \times \mathcal{J}_l(kr) v_{\mathrm{eff}ll'}{}^J(k_F=1.4, r) \mathcal{J}_{l'}(kr) = \int_0^1 dr \int_0^{k_F} dk\, W(k, k_F) \mathcal{J}_l(kr) v_{\mathrm{eff}ll'}{}^J(k_F, r) \mathcal{J}_{l'}(kr), \tag{2.26}$$

and similarly for F^L. By definition, $F(k_F=1.4)=1$. Values of $F(k_F)$ have been computed at $k_F=1.0$ F^{-1} and $k_F=1.7$ F^{-1} for partial waves through $L=2$, and the $k_F=1.0$ F^{-1} values are tabulated in Table I. In considering the entries in this Table, it is important to note that the separation at 1 F often results in a great deal of cancellation between attractive and repulsive contributions. For this reason and because of the angular-momentum barrier in the P and D states, the numerical contribution of the short-range part is usually small, so that the large change in F^S does not really imply a large density dependence.

Since $k_F=1.4$ and 1.0 F^{-1} roughly correspond to nuclear-matter density and $\frac{1}{3}$ nuclear-matter density, respectively, requiring that a simple function for $F(k_F)$ reproduce the calculated results at these points, assures that the physically significant contributions to the reduced matrix element will be adequately approximated. Although rough qualitative arguments[33] suggest quadratic dependence on k_F, we find that a linear function fit to $k_F=1.4$ and 1.0 F^{-1} yields much better agreement with the calculated values at the unphysical Fermi momentum, $k_F=1.7$ F^{-1}. The most serious extrapolation error at $k_F=1.7$ F^{-1} is a 10% discrepancy which occurs for the $^3S_1$ long-range contribution, in which the change from $k_F=1.4$ to 1.7 F^{-1} is much less than expected on the basis of the change from $k_F=1.0$ to 1.4 F^{-1}. This is easily understood since the $^3S_1$ saturation arises principally from the Pauli operator cutting off the attraction from the

second-order tensor contribution through intermediate states close to the Fermi momentum, and such saturation cannot continue to increase linearly in k_F. Dahlblom's calculations in Table I of Ref. 33 exhibit the same feature at $k_F=1.7$ F^{-1}, and are very accurately linear from 0.9 to 1.5 F^{-1}. Hence, we conclude that linear interpolation is adequate for the present work.

The above prescription results in the following simple structure for the c.m. part of the reduced matrix element:

$$\int_0^\infty (\sqrt{2}/b) R_{N\mathcal{L}}(\sqrt{2}R/b) R_{N'\mathcal{L}}(\sqrt{2}R/b) \times\{[(1.4F-1)/0.4]+k_F(\rho(R))[(1-F)/0.4]\}dR, \quad (2.27)$$

where F is the appropriate long- or short-range density factor at $k_F=1.0$, b is the harmonic-oscillator size parameter $(\hbar/M\omega)^{1/2}$, and k_F is related to ρ by the usual relation

$$k_F=(\tfrac{3}{2}\pi^2\rho)^{1/3}. \quad (2.28)$$

The function $\rho(R)$ is taken to be a simple Fermi function

$$\rho(R)=\frac{\rho_0}{1+\exp[(R-c)/a]}, \quad (2.29)$$

where

$$a=0.54,$$
$$c=(0.978+0.0206A^{1/3})A^{1/3},$$
$$\rho_0=\frac{3A}{4\pi c^3(1+\pi^2a^2/c^2)},$$

by normalization. The form for c in (2.29) is chosen to fit proton charge distributions throughout the Periodic Table,[34] with the assumption that proton and neutron distributions are sufficiently similar for this application. The contribution to (2.27) by the term independent of k_F is simply $\delta_{NN'}$ by orthogonality of the harmonic-oscillator functions, with the nondiagonal contributions arising from the integral over $\rho(R)^{1/3}$. For most applications, the size parameter in the harmonic-oscillator wave functions is determined by Bethe's[35] formula for the harmonic-oscillator energy,

$$\hbar\omega=1.85+35.5A^{-1/3}. \quad (2.30)$$

Starting energy dependence is treated similarly to the density dependence described above. We again assume a separate multiplicative function for the short- and long-range parts of the effective interaction. Rather than explicitly investigating the density dependence of the starting energy factors, we assume that their dependence is adequately approximated by the over-all density factors. Since the starting energy dependence arises from the second- and higher-order terms in (2.1), we expect the functional form of the factor to be roughly

$$A+B/(E+W). \quad (2.31)$$

For least-squares fitting of parameters, it is much more convenient to use a polynomial in W, and thus we use a second-degree polynomial to roughly preserve the generality of (2.31). In order to evaluate the six coefficients for each angular-momentum component of $v_{\rm eff}$, nuclear-matter calculations have been carried out at $k_F=1.36$ F^{-1} for $k=0.136$, 0.476, 0.884, and 1.224 F^{-1} and $W=0.48$, 1.69, and 2.40 F^{-2}, where these values have been selected to cover the physically most significant range of W and k. Correcting $v_{\rm eff}$ at $k_F=1.4$ F^{-1} to $k_F=1.36$ F^{-1} using the density factors in Table I, we then require

$$\langle k\mid G(W)\mid k\rangle=(C_1{}^S+C_2{}^SW+C_3{}^SW^2)(0.9+0.1F^S) \times\int_0^1 \mathcal{J}_l{}^2(kr)v_{\rm eff}{}^{(J)}(k_F=1.4,r)+(C_1{}^L+C_2{}^LW+C_3{}^LW^2) \times(0.9+0.1F^{-1})\int_1^\infty \mathcal{J}_l{}^2(kr)v_{\rm eff}{}^{(J)}(k_F=1.4,r). \quad (2.32)$$

For the $^3S_1$ state, the six coefficients are defined to obtain a best least-squares fit to the 12 matrix elements specified above. For the $^1S_0$ and P states, the starting energy dependence is sufficiently weak that it is satisfactory to allow only four free parameters by requiring $C_1+C_2(2.4)+C_3(2.4)^2=1$ and to fit the six matrix elements with $k=0.476$ and 0.884 F^{-1}. The starting energy dependence of the off-diagonal contributions and D states are neglected.

The final form of density and starting energy dependence of the reduced matrix element is as follows:

$$\begin{aligned}&\langle N\mathcal{L}\mid\langle nl\mid{}^{(2S+1)}v_{{\rm eff}ll'}(W)\mid n'l'\rangle\mid N'\mathcal{L}\rangle\\&=(C_1{}^S+C_2{}^SW+C_3{}^SW^2)\\&\quad\times\{[(1.4F^S-1)/0.4]\delta_{NN'}+[(1-F^S)/0.4]\langle k_F\rangle\}\\&\quad\times(1/\sqrt{2}b)\int_0^1 R_{nl}(r/\sqrt{2}b)R_{n'l'}(r/\sqrt{2}b)\\&\quad\times v_{{\rm eff}ll'}{}^J(k_F=1.4,r)dr+(C_1{}^L+C_2{}^LW+C_3{}^LW^2)\\&\quad\times\{[(1.4F^L-1)/0.4]\delta_{NN'}+[(1-F^L)/0.4]\langle k_F\rangle\}\\&\quad\times(1/\sqrt{2}b)\int_1^\infty R_{nl}(r/\sqrt{2}b)R_{n'l'}(r/\sqrt{2}b)\\&\quad\times v_{{\rm eff}ll'}{}^J(k_F=1.4,r)dr, \quad (2.33)\end{aligned}$$

where

$$\langle k_F\rangle=(\sqrt{2}/b)\int dR\, R_{N\mathcal{L}}(\sqrt{2}R/b)R_{N'\mathcal{L}}(\sqrt{2}R/b) \times\left[\frac{\frac{2}{3}\pi^2\rho_0}{1+\exp[(R-c)/a]}\right]^{1/3}dR$$

and C, F are tabulated in Table I. For partial waves

[33] H. A. Bethe, Phys. Rev. **167**, 879 (1968).
[34] M. A. Preston, *Physics of the Nucleus* (Addison-Wesley Publishing Company, Inc., Reading, Mass., 1962).
[35] H. A. Bethe (private communication).

TABLE II. $1s$-$0d$ shell matrix elements $\langle ab \mid G \mid cd\text{-}dc \rangle$ in MeV, as defined in Eq. (2.26). The contributions of the nondiagonal tensor force, partial waves higher than $l=2$, and finite nucleus starting energy corrections are omitted in the partial matrix elements and included in the total matrix elements. Kuo's results are from Ref. 27. The single-particle states are denoted $0d_{5/2}=4$, $1s_{1/2}=5$, and $0d_{3/2}=6$.

T	J	a	b	c	d	Partial	Total	Kuo	T	J	a	b	c	d	Partial	Total	Kuo
0	1	4	4	4	4	−0.29	−0.40	−0.30	0	5	4	4	4	4	−2.47	−3.38	−3.42
		4	4	5	5	−0.34	−0.34	−0.27	1	0	4	4	4	4	−1.26	−1.54	−1.24
		4	4	6	4	−2.27	−3.02	−2.60			4	4	5	5	−0.69	−0.77	−0.63
		4	4	6	5	0.11	−0.04	0.11			4	4	6	6	−3.16	−3.33	−3.02
		4	4	6	6	2.50	2.02	2.10			5	5	5	5	−2.04	−2.26	−2.05
		5	5	5	5	−2.23	−3.24	−3.01			5	5	6	6	−0.56	−0.64	−0.53
		5	5	6	4	−1.30	−2.06	−1.61			6	6	6	6	0.03	−0.23	−0.09
		5	5	6	5	0.65	−0.23	0.08	1	1	6	4	6	4	−0.41	−0.50	−0.33
		5	5	6	6	−0.19	−0.53	−0.42			6	4	6	5	−0.02	−0.13	−0.17
		6	4	6	4	−3.06	−5.23	−4.33			6	5	6	5	−0.27	−0.36	−0.33
		6	4	6	5	−0.58	−1.80	−1.42	1	2	4	4	4	4	−0.95	−1.12	−1.01
		6	4	6	6	0.18	0.25	0.11			4	4	5	4	−0.60	−0.64	−0.56
		6	5	6	5	−2.09	−3.01	−3.02			4	4	6	4	0.35	0.40	0.41
		6	5	6	6	−0.41	−0.81	−0.82			4	4	6	5	0.52	0.58	0.55
		6	6	6	6	−0.46	−0.13	−0.22			4	4	6	6	−0.70	−0.64	−0.60
0	2	5	4	5	4	−0.49	−0.62	−0.53			5	4	5	4	−1.21	−1.26	−1.17
		5	4	6	4	1.20	1.32	1.30			5	4	6	4	0.15	0.22	0.18
		5	4	6	5	2.24	2.46	2.51			5	4	6	5	1.40	1.48	1.45
		6	4	6	4	−2.35	−4.14	−3.59			5	4	6	6	−0.75	−0.79	−0.75
		6	4	6	5	−1.47	−1.63	−1.59			6	4	6	4	−0.46	−0.42	−0.36
		6	5	6	5	−1.40	−1.65	−1.57			6	4	6	5	−0.71	−0.70	−0.66
0	3	4	4	4	4	−0.90	−1.01	−0.79			6	4	6	6	0.73	0.85	0.78
		4	4	5	4	−0.89	−1.35	−1.24			6	5	6	5	−0.63	−0.66	−0.59
		4	4	6	4	−1.16	−1.53	−1.47			6	5	6	6	0.04	0.08	0.04
		4	4	6	6	0.51	0.31	0.39			6	6	6	6	−0.14	−0.28	−0.28
		5	4	5	4	−2.57	−3.30	−3.12	1	3	5	4	5	4	−0.31	−0.34	−0.29
		5	4	6	4	−0.56	−1.00	−1.01			5	4	6	4	0.07	0.09	0.06
		5	4	6	6	0.36	0.32	0.12			6	4	6	4	−0.58	−0.54	−0.40
		6	4	6	4	−0.80	−1.33	−1.11	1	4	4	4	4	4	−0.42	−0.47	−0.43
		6	4	6	6	−1.01	−1.63	−1.72			4	4	6	4	1.02	1.09	1.05
		6	6	6	6	−1.72	−2.37	−2.43			6	4	6	4	−1.95	−2.12	−2.02
0	4	6	4	6	4	−2.93	−3.98	−4.16									

higher than 2, we simply take OPEP with no density or starting energy dependence.

Using the effective interaction summarized in (2.33), a general computer program has been written to calculate matrix elements according to (2.25). Matrix elements from this program will be used later in this work to calculate spin-orbit splittings. In addition, for the sake of comparison with other work, we tabulate s-d shell matrix elements obtained from this theory in Table II. In this calculation, $W=(E_a+E_b+E_c+E_d)/2$, where $E_{0d_{5/2}}=-0.269$ F^{-2}, $E_{1s_{1/2}}=-0.244$ F^{-2}, and $E_{0d_{3/2}}=-0.146$ F^{-2}, $\hbar\omega=14$ MeV, and the half-density radius of the nucleon distribution is 3.04 F. The spacing of the single-particle energies relative to $0d_{5/2}$ was obtained from the O^{17} data reported by Cohen *et al.*,[36] and the energy for $0d_{5/2}$ was obtained by computing the average removal energy for protons and neutrons throughout the $0d_{5/2}$ shell from binding energies[37] and correcting by 1 MeV to account for rearrangement. To indicate the contribution of the off-diagonal tensor force, partial waves beyond $L=2$, and starting energy dependence, matrix elements without these contributions are also tabulated. For comparison, Kuo's[27] state-dependent matrix elements using a LDA with the Hamada-Johnston force are also presented, and although the over-all agreement is good, our matrix elements generally tend to be stronger. This seems to be primarily due to our treatment of the tensor force which is more complete than his second-order closure approximation. Finally, calculation[38] of the core-polarization corrections which are discussed in Ref. 26 using our matrix elements yields results 10–30% larger than those obtained by Kuo, which yields a further increase of the contribution of our effective interaction to finite nuclei in comparison with his.

[36] B. L. Cohen, R. H. Fulmer, A. L. McCarthy, and P. Mukherjee, Rev. Mod. Phys. **35**, 332 (1963).

[37] J. H. E. Mattauch, W. Thiele, and A. H. Wapstra, Nucl. Phys. **67**, 1 (1965).

[38] E. C. Halbert (private communication).

Even- and Odd-State Forces

The second major application of the effective interaction in this work is to calculate the self-consistent structure of nuclei. One possible approach which has been used in recent HF calculations[9–11] is to work in an harmonic-oscillator basis, in which case the separate interactions in each partial wave discussed in the last section would be directly applicable. However, since in deriving the self-consistent density distribution from a variational principle, it is much simpler to include the density dependence of the effective interaction in coordinate space, we now consider the construction of an effective interaction which does not require projection into separate relative partial waves.

The simplest way to motivate our development is to consider the HF choice of the occupied state potentials (2.6) for nuclear matter and a finite nucleus. Even though we shall modify this prescription subsequently, it still contains the most essential features, and serves as a useful guide. Writing out in detail the nuclear-matter contribution indicated in (2.16) and neglecting over-all normalization, we obtain

$$\sum_{STJl}[1-(-)^{l+S+T}](2T+1)(2J+1)\int W(k,k_F)\,dk \times \int dr^{(2S+1)}v_{\mathrm{eff}_{ll}}{}^{J}(r)\mathcal{J}_l{}^2(kr). \quad (2.34)$$

Since the triplet interactions always contribute in the same combination, it is useful to define an average triplet interaction

$${}^3v_{\mathrm{eff}_{ll}}(r)=\Big[\sum_{J=l-1}^{l+1}(2J+1)\,{}^3v_{\mathrm{eff}_{ll}}{}^{J}(r)\Big]\Big/\Big[\sum_{J=l-1}^{l+1}(2J+1)\Big]. \quad (2.35)$$

Then, (2.34) may be rewritten

$$\sum_{STl}[1-(-)^{l+S+T}](2T+1)(2S+1)(2l+1) \times \int W(k,k_F)\,dk\int dr^{(2S+1)}v_{\mathrm{eff}_{ll}}(r)\mathcal{J}_l{}^2(kr). \quad (2.36)$$

For the case of a finite nucleus comprised of harmonic-oscillator functions,

$$\sum_{12}\langle 12\mid v_{\mathrm{eff}}\mid 12-21\rangle=\sum_{n_1l_1j_1m_1\tau_1TM_T,n_2l_2j_2m_2\tau_2JM_J}\begin{pmatrix}\frac{1}{2}&\frac{1}{2}&T\\ \tau_1&\tau_2&M_T\end{pmatrix}^2\begin{pmatrix}j_1&j_2&J\\ m_1&m_2&M_J\end{pmatrix}^2(2T+1)(2J+1) \times(1+\delta_{n_1n_2}\delta_{l_1l_2}\delta_{j_1j_2})\langle n_1l_1j_1n_2l_2j_2;JT\mid v_{\mathrm{eff}}\mid n_1l_1j_1n_2l_2j_2;JT\rangle, \quad (2.37)$$

where the antisymmetrized matrix element is given in (2.25). Removing the 3-j symbols by summing over τ_1, τ_2, m_1, and m_2, the 9-j symbols by summing over j_1 and j_2, and the 6-j symbols by summing over J, one obtains

$$\sum_{12}\langle 12\mid v_{\mathrm{eff}}\mid 12-21\rangle=\sum_{nlN\mathfrak{L}ST}C(nlN\mathfrak{L})[1-(-)^{l+S+T}](2T+1)(2S+1) \times\int(\sqrt{2}/b)[R_{N\mathfrak{L}}{}^{HO}(\sqrt{2}R/b)]^2dR\int(1/\sqrt{2}b)[R_{nl}{}^{HO}(r/\sqrt{2}b)]^2\,{}^{(2S+1)}v_{\mathrm{eff}_{ll}}(r)\,dr, \quad (2.38)$$

where

$$C(nlN\mathfrak{L})=\sum_{n_1n_2l_1l_2L}(2L+1)\langle nlN\mathfrak{L},L\mid n_1l_1n_2l_2,L\rangle^2.$$

Equations (2.36) and (2.38) exhibit the explicit wave function weighting of the effective interaction in individual partial waves specified by the HF potential. Since Ca^{40} is the largest nucleus which is accurately represented by harmonic-oscillator functions of a single $\hbar\omega$, we consider (2.38) to yield the true weighting of individual partial waves in Ca^{40} and compare with the contributions specified by the nuclear-matter weighting (2.36) at the local density. It is important to note that different ranges of the effective interaction have different partial waves emphasized. This is most obvious in (2.36), since as $r\to 0$, $\mathcal{J}_0(kr)$ is the only nonvanishing contribution, whereas for large r many partial waves are significant. Hence, we shall consider two values of the relative coordinate, $r=0.526$ and 1.578 F, which indicate the typical weighting of the short-range repulsion and long-range attraction, respectively. Taking the harmonic-oscillator size parameter $b=1.86$ F, which yields the best agreement with electron scattering, we obtain the relative weighting of the effective interaction in individual partial waves as a function of the c.m. coordinate indicated in Fig. 1.

The most important result indicated in Fig. 1 is that in the interior of the nucleus the nuclear-matter and harmonic-oscillator compositions roughly agree, with the long-range interaction wave function weighting being approximately 65% in S wave, 30% in P, and 5% in D and with the short-range interaction weighting being 95% in S wave and 5% in D. Hence, if one considers separate even- and odd-state forces, the odd-state force need only reproduce the P-wave contribution accurately, whereas the even-state force must reproduce the S-state effective interaction very accurately, and give reasonable results for the D state. Since the nuclear-matter weighting is roughly correct in the interior and has the correct qualitative features in the surface, it is natural to define even- and odd-state effective interactions with the same nuclear-matter weighting prescription which we have used previously. This argument then motivates the definition used

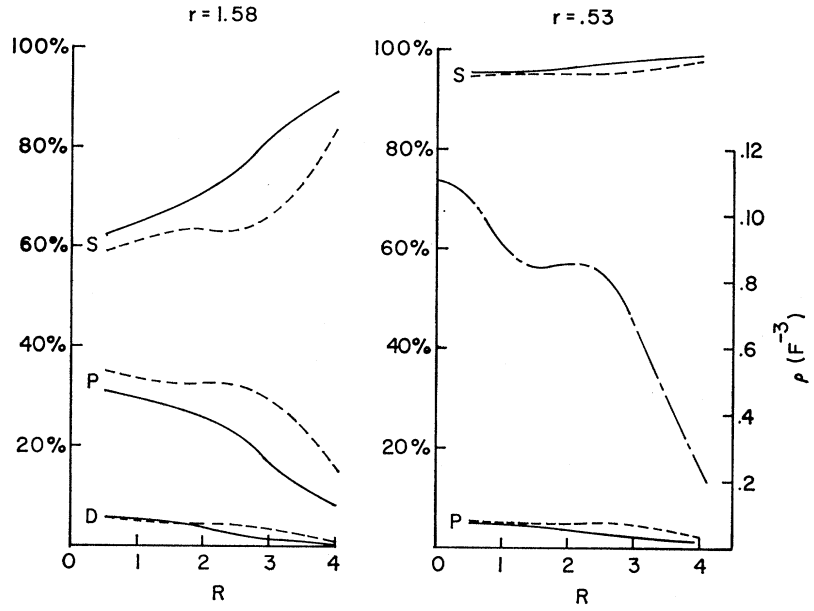

FIG. 1. Weighting of S, P, and D states of the two-body interaction in Ca^{40} as a function of the distance from the center of the nucleus R for relative coordinates of $r=1.58$ F and $r=0.53$ F. Nuclear-matter weighting corresponding to the local density is indicated by the dashed lines, and the solid lines denote harmonic-oscillator weighting. The harmonic-oscillator density distribution is shown for reference in dot-dash lines.

previously by Lin[39] and Siemens[20]

$$v_{\rm ev}(r)=\{\sum_{l\ \rm even}[1-(-)^{l+S+T}](2T+1)(2S+1)(2l+1)\,{}^{(2S+1)}v_{{\rm eff}_{ll}}(r)$$
$$\times\int dk\,W(k_F,k)\mathcal{J}_l^2(kr)\}/\{\sum_{l\ \rm even}[1-(-)^{l+S+T}](2T+1)(2S+1)(2l+1)\int dk\,W(k_F,k)\mathcal{J}_l^2(kr)\}. \quad (2.39)$$

$v_{\rm odd}(r)$ is defined by the analogous sum over odd l. We use OPEP for all partial waves higher than $l=2$ by noting the relation for sums of spherical Bessel functions

$$\sum_{l({\rm even,odd})}(2l+1)j_l^2(z)=\tfrac{1}{2}(1\pm\sin 2z/2z) \quad (2.40)$$

and writing the sum of partial waves greater than $l=2$ as the sum of all partial waves minus those with l less than or equal to 2. Thus, we obtain

$$v_{\rm ev}(r)=[\int dk\,W(k,k_F)\{\tfrac{1}{2}\mathcal{J}_0^2(kr)\,({}^1v_{00}(r)+{}^3v_{00}(r)+6V_{\rm OPEP}(r))+\tfrac{5}{2}\mathcal{J}_2^2(kr)\,({}^1v_{22}(r)+{}^3v_{22}(r)+6V_{\rm OPEP}(r))$$
$$-\tfrac{3}{2}(kr)^2(1+\sin(2kr)/(2kr))V_{\rm OPEP}(r)\}]/[\int dk\,W(k,k_F)\tfrac{1}{2}(kr)^2(1+\sin(2kr)/(2kr))],$$
$$v_{\rm odd}(r)=[\int dk\,W(k,k_F)\{\tfrac{3}{10}\mathcal{J}_1^2(kr)\,({}^1v_{11}(r)+9^3v_{11}(r)-18V_{\rm OPEP}(r))$$
$$+\tfrac{9}{10}(kr)^2(1-\sin(2kr)/(2kr))V_{\rm OPEP}(r)\}]/[\int dk\,W(k,k_F)\tfrac{1}{2}(kr)^2(1-\sin(2kr)/(2kr))], \quad (2.41)$$

where $V_{\rm OPEP}(r)=(10.4/3)(e^{-0.7r}/0.7r)$ and ${}^{(2S+1)}v_{ll}(r)$ is understood to be ${}^{(2S+1)}v_{{\rm eff}_{ll}}(r,k_F)$.

Having motivated the construction of even- and odd-state forces by our basic philosophy of nuclear-matter averages, it is important at this point to examine the quantitative accuracy of this approximation. Considering first the even-state force, it is clear that the short-range part is almost entirely from the S-state interaction, because of the Bessel-function weighting. Hence, the short-range contribution to S-state matrix elements should be very accurate, and there should be negligible short-range contribution to D-state matrix elements. The S-state and D-state weightings become equal at 3 F, and for very large r the situation is exactly reversed with only the D-state force contributing to the effective interaction and the interaction only significantly contributing to D-state matrix elements. However, the long-range part of the nuclear interaction contributes strongly in the region inside 3 F, and there is no *a priori* reason to expect an even-state force to reproduce correctly the separate S- and D-state interactions. However, it is a very fortunate property of the nucleon-nucleon force we are considering, that the long-range behavior of the S- and D-state interactions are sufficiently similar that individual S- and D-state matrix elements are very accurately reproduced. The situation for the P and F waves with the odd effective interaction is analogous.

[39] Y. C. Lin, thesis, Cornell University (unpublished); Y. C. Lin, Nucl. Phys. **A140**, 359 (1970).

TABLE III. Matrix elements of the full effective interaction and the even- and odd-state interactions multiplied by the appropriate statistical factor, F. U^{NM} is the contribution of each partial wave to nuclear-matter binding at $k_F=1.4$ F^{-1}. The sums of the even- and odd-state contributions to U^{NM} are identically reproduced by V_{ev} and V_{odd}, respectively, and are not tabulated.

l	F	V	$F\int \mathcal{J}_l^2(kr)\,V dr$ $k=1.40$	$k=1.05$	$k=0.70$	U^{NM} (MeV)
0	3/16	$^1v_{\text{eff}00}$	−1.115	−3.754	−3.503	−16.42
0	3/16	$^3v_{\text{eff}00}$	0.146	−3.370	−3.361	−15.32
		sum	−0.969	−7.124	−6.864	
0	3/8	V_{ev}	−0.856	−6.942	−6.833	
1	3/16	$^1v_{\text{eff}11}$	6.032	2.300	0.465	2.72
1	27/16	$^3v_{\text{eff}11}$	1.477	−0.298	−0.183	−0.45
		sum	7.509	2.002	0.282	
1	15/8	V_{odd}	7.698	2.238	0.519	
2	15/16	$^1v_{\text{eff}22}$	−5.119	−2.208	−0.600	−2.85
	15/16	$^3v_{\text{eff}22}$	−5.986	−2.948	−0.870	−3.97
		sum	−11.105	−5.156	−1.470	
	15/8	V_{ev}	−13.522	−5.101	−1.297	
Even>2		OPEP				−0.90
Odd>2		OPEP				1.94

In Table III, individual matrix elements of the even- and odd-state interactions are compared with matrix elements of the individual effective interactions in the lowest three partial waves for $k_F=1.4$ F^{-1}. In comparing these matrix elements, it is important to note that the c.m. phase-space weighting function $W(k, k_F)$ specified in (2.14) goes to zero quadratically at $k=k_F$ so that the most significant S-state contributions arise from k in the range 0.7–1.0 F^{-1}. From Table III, we note that in this range the even-state force underbinds by at most 3%. For P and D states, the matrix elements become very small at low k, so the region of most significant contribution is shifted to somewhat higher k. In this region, the agreement in Table III is again seen to be quite good. Finally, to demonstrate the relative contributions of various partial waves to nuclear-matter potential energy, in contrast to the wave function weightings shown in Fig. 1, these energy contributions are also tabulated in Table III. Because of the nuclear-matter average, the total contribution to the nuclear-matter potential energy must be exact.

The even- and odd-state forces defined above contain the averaged central contribution of the tensor force but no explicit off-diagonal contribution. This is consistent not only for nuclear matter, in which the off-diagonal tensor force does not contribute to the lowest-order HF energy, but also in spin-saturated finite nuclei, where it also does not contribute. For the spin-unsaturated nuclei we shall consider, the off-diagonal tensor force can only contribute to the potential of the few nucleons in the unsaturated shells, and we feel that this has a sufficiently small effect on the over-all nuclear structure that it may reasonably be neglected.

As a result of the average in (2.35), the explicit two-body spin-orbit force has also been averaged out of the effective even- and odd-state forces. This averaging causes negligible error when we consider the total contribution of both levels in a completely filled l shell, but requires the introduction of an effective one-body spin-orbit potential when only the lower state of a spin-orbit couplet is filled.

In contrast to the previous section, the detailed spatial distribution of the starting energy dependence is important for the present application. Since almost all of the binding energy arises from the S-state contributions, as evidenced in Table III, the total starting energy dependence is adequately approximated by that of the triplet S state. Considering the average nuclear-matter starting energy to be $W=2.4$ F^{-2}, we may write, using an average k as in (2.11),

$$\Delta^3v_{\text{eff}00}(W,r)={}^3v_{\text{eff}}(W,r)-{}^3v_{\text{eff}}(2.4,r)$$
$$=\big[{}^3v_{00}{}^1(r)\,(u_{0,1}{}^{(0)}(r,k_{\text{av}},W)-u_{0,1}{}^{(0)}(r,k_{\text{av}},2.4))$$
$$+{}^3v_{02}{}^1(r)\,(u_{2,1}{}^{(0)}(r,k_{\text{av}},W)-u_{2,1}{}^{(0)}(r,k_{\text{av}},2.4))\big]/\mathcal{J}_0(k_{\text{av}}r). \quad (2.42)$$

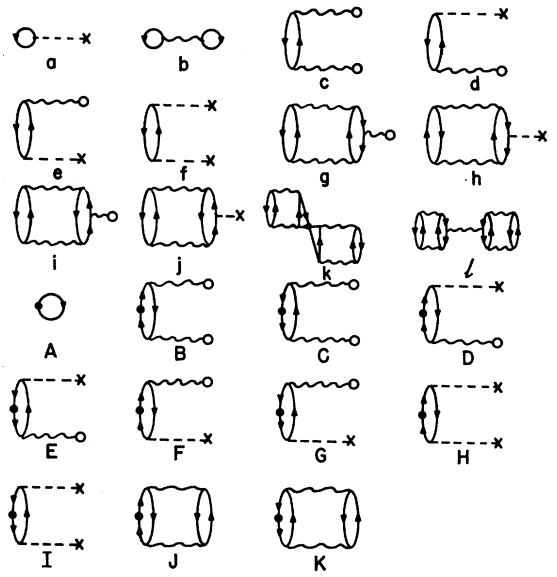

FIG. 2. Goldstone diagrams for the first few terms in the energy and density expansions.

The correction $\Delta^3 v_{\rm eff}(W, r)$ has been calculated at $k_F = 1.4$ F^{-1} for $W = 0.48$ and 1.69 F^{-2}. The long-range part is well fit by

$$\Delta v_{\rm long}(W, r) = (-285.+159.5W-17.1W^2) \times[(r-0.7)^2/(0.69+r^{8.6})] \text{ MeV} \quad (2.43)$$

for $r \geq 0.7$ F and W in F^{-2}. For convenience in subsequent calculations, we lump the short-range part and the difference between (2.43) and the true long-range part into a delta function. For the strength of this delta function, we obtain

$$\Delta v_\delta(W) = \int r^2 (\Delta^3 v_{\rm eff_{00}}(E, r) - \Delta v_{\rm long}(W, r))dr = -5.86+2.64W-0.0805W^2 \text{ MeV}. \quad (2.44)$$

From (2.39), it is evident that the starting energy dependence of the even-state force is

$$\Delta v_{\rm ev}(W, |\mathbf{r}_1-\mathbf{r}_2|) = \tfrac{1}{2}\Delta^3 v_{\rm eff_{00}}(W, |\mathbf{r}_1-\mathbf{r}_2|) = 2\pi v_\delta(W)\delta^3(\mathbf{r}_1-\mathbf{r}_2) + \tfrac{1}{2}\Delta v_{\rm long}(W, |\mathbf{r}_1-\mathbf{r}_2|). \quad (2.45)$$

In this work, we do not include the density dependence of $\Delta v_{\rm ev}(W, r)$ but, rather, use (2.45) at all densities. Physically, it is clear that at low densities the starting energy correction should become even larger for a given W less than 2.4 F^{-2}, since the Pauli operator allows more attraction through the second-order tensor force. Since, however, the contribution to the nuclear potential depends on $\Delta v_{\rm ev}\rho$, the increase in the low density correction receives such little weight that it may be legitimately neglected.

III. DENSITY-DEPENDENT HARTREE-FOCK THEORY OF CLOSED-SHELL NUCLEI

Variational Principle for Single-Particle Potential

In order to utilize the effective interaction in a practical calculation of the binding energies and density distributions of finite nuclei, it is useful to consider in greater detail some formal aspects of the many-body theory of finite nuclei.

Although a formalism exists to treat the case of a degenerate or nearly degenerate ground state,[18,40–42] we shall restrict our attention to closed-shell nuclei for which the Goldstone expansion is applicable. Noting that in the finite nucleus no diagrams are excluded by momentum conservation and adopting the notation that the single-particle potential U is denoted by a $\times$ and the density operator is denoted by a heavy dot, the lowest-order diagrams for the energy and density expansions[43] are shown in Fig. 2. The fundamental problem, of course, is to select the optimal definition of the potential U.

First, we consider the HF potential for occupied states and zero potential for unoccupied states. Because of the lack of momentum conservation, we generalize (2.6) to

$$\langle m \mid U \mid m' \rangle = \tfrac{1}{2}\sum_n \langle mn \mid G(E_m+E_n) + G(E_{m'}+E_n) \mid m'n-nm' \rangle,$$
$$\langle m \mid U \mid a \rangle = \sum_n \langle mn \mid G(E_m+E_n) \mid an-na \rangle, \quad (3.1)$$
$$\langle a \mid U \mid b \rangle = 0,$$

where m, m', n are occupied and a, b are unoccupied. As a result of the BBP cancellation, diagram h in Fig. 2 cancels g and k plus an infinite series of higher-order diagrams. Baranger[44] has generalized the BBP result, showing that for the potential (3.1) diagrams c, d, e, and f sum identically to zero. This cancellation also occurs in the density expansion so that diagrams B–I yield zero contribution. Despite the appeal of this large cancellation of diagrams, there is no real evidence, either intuitive or formal, that this choice of single-particle potential is optimal.

Brandow[42] has recently improved this situation by formulating a many-body variational principle for the single-particle potential. One important observation relevant to this work is the fact that all of the on-energy-shell contributions to the single-particle mass operator have the cancellation property displayed above for the HF potential which is simply the lowest such on-energy-shell insertion. Since the variational principle specifies

[40] C. Bloch and J. Horowitz, Nucl. Phys. **8**, 91 (1958).
[41] B. D. Day, thesis, Cornell University (unpublished).
[42] B. H. Brandow, in *Lectures in Theoretical Physics* (Gordon and Breach Science Publishers, New York, 1969), Vol. XI.
[43] D. J. Thouless, *The Quantum Mechanics of Many Body Systems* (Academic Press Inc., New York, 1961).
[44] M. Baranger, 1967 Varenna Lectures (unpublished).

the potential to be the particular on-energy-shell insertion obtained by functionally differentiating a set of skeletal diagrams approximating the energy, we do not sacrifice any cancellation and have a formally motivated method for extending beyond the HF prescription. The next-order contribution beyond the HF potential in this formalism, where we assume momentum conservation for convenience, is

$$U_m=\sum_n \langle \Phi_{mn} \mid G \mid \Phi_{mn}-\Phi_{nm}\rangle \times[1-\tfrac{1}{2}\sum_{abl}\langle nl-ln \mid G/e \mid ab\rangle\langle ab \mid G/e \mid nl-ln\rangle]. \tag{3.2}$$

To cast this into a more useful form, we introduce the integral of the defect function, κ. Defining $\zeta_{ab}=\Phi_{ab}-\Psi_{ab}$, with partial wave components χ already defined above

$$\kappa=(1/A)\sum_{mn}\langle \zeta_{mn} \mid \zeta_{mn}-\zeta_{nm}\rangle=(1/A)\sum_n \kappa_n = \sum_{lSTJ}(1-(-1)^{l+S+T})(2T+1)(2J+1)9\rho/(32\pi k_F{}^6) \times \iint W(k,k_F)\sum_{l'=J-S}^{J+S}\chi_{l'J}{}^{(l)}(kr)\,dk\,dr \tag{3.3}$$

in nuclear matter. From Eqs. (2.1) and (2.3) it follows that $(QG/e)\mid \Phi_{ab}\rangle=\mid \zeta_{ab}\rangle$. Then, evaluating (3.2) on the energy shell,

$$U_m=\sum_n \langle \Phi_{mn} \mid G \mid \Phi_{mn}-\Phi_{nm}\rangle[1-\sum_l \langle \zeta_{nl} \mid \zeta_{nl}-\zeta_{ln}\rangle] = \sum_n \langle mn \mid G \mid mn-nm\rangle(1-\kappa_n). \tag{3.4}$$

Since $\kappa=0.136$ in nuclear matter at $k_F=1.4$ F^{-1}, the potential (3.2) is roughly 14% more repulsive than the HF potential in a finite nucleus. Thus, the additional term has precisely the effect of the Brueckner rearrangement potential[4] and will contribute significantly to saturation. Although we shall use an alternative potential which is more convenient for numerical calculations, (3.4) will be quite useful because the extent to which our modification of the HF prescription reproduces the κ correction will indicate the extent to which we may expect the cancellation in this formalism to carry over into our theory.

Since we have developed an effective interaction which is a function of relative coordinate and density, the most straightforward and intuitively appealing definition of the single-particle potential is to write the lowest-order contribution to the binding energy, Fig. 2(b), in coordinate space and vary the wave functions. [One should note that Fig. 2(a) contributes to the change in energy from the unperturbed energy $\epsilon_0=\sum\langle n \mid T+U \mid n\rangle$, but it exactly cancels the sum over U in ϵ_0, so that it does not contribute to the binding energy.] The variation of the wave functions in the kets yields the ordinary HF potential, whereas the variation of the wave functions which comprise ρ in the density-dependent interaction leads to additional $\delta V/\delta\rho$ terms. Since only the lowest-order contribution to the total ground-state energy is being minimized, one should expect finite nuclei to be underbound by an amount comparable to that which occurs in nuclear matter. Since the potential energy determines the single-particle eigenvalues, which in turn determine the tails of finite nucleus wave functions, it is clear that a significant error in energy will seriously affect the density. Hence, we shall take into account higher-order contributions to the binding energy in a very crude way, by adjusting the strength of the two-body effective interaction in the energy expression which we vary so as to reproduce nuclear-matter binding energy. The precise adjustment of the effective interaction is discussed in the following section.

In order to calculate higher-order diagrams in Fig. 2 correctly with this potential, it is necessary to note that the two-body effective interaction is only increased in the definition of the potential and not in the reaction matrices explicitly occurring in the diagrams. Thus, the ground-state energy obtained by varying the energy expression with the enhanced interaction is not equal to the contribution of Fig. 2(b); rather we expect it to be close to the total contribution of the entire series of diagrams. If one were to undertake a serious program to calculate the diagrams in Fig. 2, which we do not attempt in this work, it would be most efficient to write our potential as (3.2) plus an additional term. Then the cancellation described above would occur for the component corresponding to (3.2), and a much smaller class of diagrams would remain involving the small additional term. Since we do not systematically evaluate the perturbation series, this work cannot claim to be a fundamental theory of nuclear structure. However, the higher-order terms we do evaluate in a later section turn out extremely small, and this one choice of potential yields reasonably good results throughout the periodic table. To this extent, then, our intuitively motivated procedure maintains contact with the formal many-body theory.

Direct and Exchange Forces

Having defined the single-particle potential in terms of the variation of coordinate space wave functions, we now consider the appropriate modification and parameterization of the effective interaction for this purpose.

To motivate our construction in the more complicated general case, we now consider spin-saturated nuclei with equal numbers of neutrons and protons. As mentioned previously, the absence of a two-body spin-orbit potential results in a single radial function corresponding to the weighted average of the two radial functions of a spin-orbit doublet. Denoting

$$\mid M\rangle=R_{NL}(r)\,Y_{Lm}(\Omega)\chi_m\tau_m$$

and

$$|m\rangle = R_{NL}(r)\,Y_{Lm}(\Omega) = \psi_m, \tag{3.5}$$

where χ_m and τ_m are spin and isospin functions, respectively, and writing

$$V = \tfrac{1}{2}(1+P_m)v_{\rm ev} + \tfrac{1}{2}(1-P_m)v_{\rm odd}, \tag{3.6}$$

where P_m is the Majorana space exchange operator, the space and spin functions separate trivially.

$$\begin{aligned}
&\langle MN \mid V \mid MN-NM\rangle \\
&= \iint d^3r_1 d^3r_2 \psi_m^\dagger(1)\psi_n^\dagger(2)\chi_m^\dagger(1)\chi_n^\dagger(2)\tau_m^\dagger(1)\tau_n^\dagger(2) \\
&\quad\times[\tfrac{1}{2}(1+P_m)v_{\rm ev}+\tfrac{1}{2}(1-P_m)v_{\rm odd}] \\
&\quad\times[\psi_m(1)\psi_n(2)\chi_m(1)\chi_n(2)\tau_m(1)\tau_n(2) \\
&\qquad -\psi_m(2)\psi_n(1)\chi_m(2)\chi_n(1)\tau_m(2)\tau_n(1)] \\
&= \langle mn \mid \tfrac{1}{2}(1-\delta_\tau\delta_\chi)v_{\rm ev}+\tfrac{1}{2}(1+\delta_\tau\delta_\chi)v_{\rm odd} \mid mn\rangle \\
&\quad + \langle mn \mid \tfrac{1}{2}(1-\delta_\tau\delta_\chi)v_{\rm ev}-\tfrac{1}{2}(1+\delta_\tau\delta_\chi)v_{\rm odd} \mid nm\rangle,
\end{aligned} \tag{3.7}$$

where $\delta_\tau = \delta_{\tau_m\tau_n}$ and similarly for δ_χ. To the extent to which neutron and proton radial functions are identical, it is sensible to define the spin and isospin average of (3.7). Then,

$$\begin{aligned}
\tfrac{1}{4}\sum_{\tau_m\chi_m}\langle MN \mid V \mid MN-NM\rangle &= \langle mn \mid \tfrac{3}{8}v_{\rm ev}+\tfrac{5}{8}v_{\rm odd} \mid mn\rangle \\
&\quad + \langle mn \mid \tfrac{3}{8}v_{\rm ev}-\tfrac{5}{8}v_{\rm odd} \mid nm\rangle.
\end{aligned} \tag{3.8}$$

Noting our convention of adding instead of subtracting the exchange term, it is convenient to define average direct and exchange forces

$$v_{\rm (dir,ex)}{}^{\rm av} = \tfrac{3}{8}v_{\rm ev} \pm \tfrac{5}{8}v_{\rm odd}. \tag{3.9}$$

At this point an important numerical consideration arises. When matrix elements are expanded in relative coordinates, $v_{\rm odd}$ is always multiplied by a product of radial functions which behave at small r as $\mathcal{J}_1^2(kr)$ so that the contribution is never as singular at short range as the bare V. However, in (3.8) the even and odd projectors have already been used to eliminate the spin and isospin dependence so that the strong short-range contributions of the odd force in the direct and exchange terms must very closely cancel. Whereas the formal cancellation is clear in (3.8), numerical calculations would have to use an exceedingly fine grid to accomplish such cancellation in practice.

Physically it is clear that to the extent to which the short-range force is represented by a delta function the matrix element in (3.8) only depends upon the sum of $v_{\rm dir}+v_{\rm ex}$ so that the distinction between direct and exchange is completely arbitrary. Since the direct numerical integral is much simpler than the exchange integral, it is clearly desirable to place all of the short-range contribution in the direct force. For realistic forces of nonzero range this modification amounts to arbitrarily changing the short-range part of $v_{\rm odd}$ which does not contribute significantly. Since $v_{\rm odd}$ coincides with $\frac{3}{5}v_{\rm ev}$ in the region of $r=0.5$ F without any modification, this is a natural point to begin adjustment of $v_{\rm odd}$. Hence, we modify $v_{\rm odd}$ as follows:

$$\begin{aligned}
v_{\rm odd}' &= \tfrac{3}{5}v_{\rm ev} \quad \text{for} \quad r \leq 0.45 \text{ F}, \\
v_{\rm odd}' &= v_{\rm odd} \quad \text{for} \quad r \geq 0.60 \text{ F},
\end{aligned} \tag{3.10}$$

and $v_{\rm odd}'$ is joined smoothly between 0.45 and 0.60 F. This change in $v_{\rm odd}$ results in 0.043-MeV error in nuclear-matter binding at $k_F=1.4$, which is clearly negligible. With this modification, $v_{\rm ex}$ is identically zero inside 0.45 F and is attractive at all larger r.

The direct force obtained in this way is highly repulsive inside approximately 0.75 F and attractive outside. For numerical purposes it is useful to separate the direct force into a repulsive short-range part, which is identically zero beyond 0.85 F, and an attractive long-range part, which is zero inside 0.70 F. In the region between 0.70 and 0.85 F, the two potentials are defined so as to approach zero smoothly and to yield the proper sum. The direct integral of the strong short-range direct force may then be performed in relative coordinates, and the direct and exchange integrals of the long-range forces may be easily performed in the individual particle coordinates. The direct and exchange forces so defined are tabulated in Table IV for $k_F=1.0$ and 1.4 F^{-1} and are graphed in Fig. 3 for $k_F=1.4$ F^{-1}.

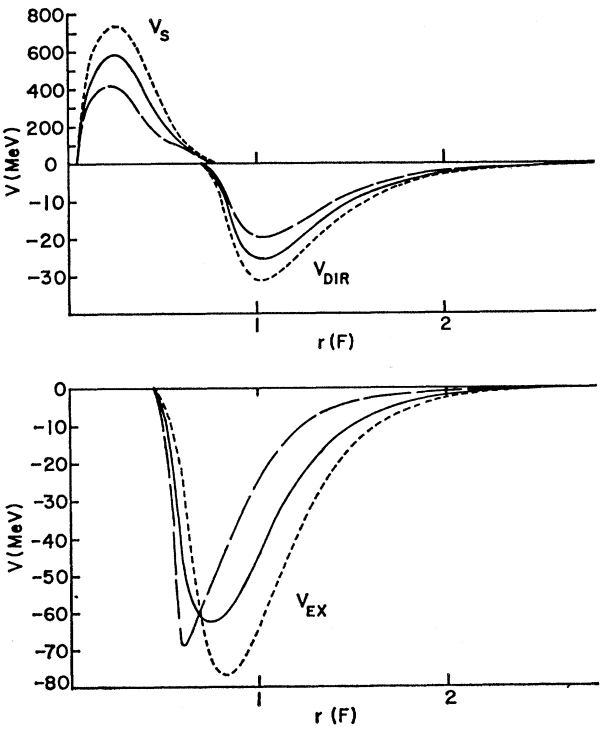

FIG. 3. The short-range direct interaction V_S, the long-range direct interaction $V_{\rm dir}$, and the long-range exchange interaction $V_{\rm ex}$. The solid lines, short dashes, and long dashes correspond to the average, unlike, and like interactions, respectively. Note that the scale for V_S is contracted by a factor of 20.

TABLE IV. The short-range direct interaction V_S, the long-range direct interaction V_{dir}, and the exchange interaction V_{ex}, at $k_F=1.4$ and 1.0 F^{-1}. The form "A (b)" means $A\times10^{b}$.

r (F)	$V_S(k_F=1.4)$ (MeV)	$V_{\text{ex}}(k_F=1.4)$ (MeV)	$V_S(k_F=1.0)$ (MeV)	$V_{\text{ex}}(k_F=1.0)$ (MeV)
0.05	−5.9062 (−1)		3.2625 (−1)	
0.10	3.6950 (2)		3.1127 (2)	
0.15	4.7712 (2)		4.3070 (2)	
0.20	5.5064 (2)		5.1961 (2)	
0.25	5.7730 (2)		5.6089 (2)	
0.30	5.5507 (2)		5.5015 (2)	
0.35	4.9327 (2)		4.9571 (2)	
0.40	4.0697 (2)		4.1280 (2)	
0.45	3.1142 (2)	0.0000 (−1)	3.1748 (2)	0.0000 (−1)
0.50	2.2549 (2)	−6.7949 (0)	2.2773 (2)	−4.8500 (0)
0.55	1.5966 (2)	−2.3097 (1)	1.5437 (2)	−1.6500 (1)
0.60	1.1618 (2)	−4.7282 (1)	1.0556 (2)	−3.8437 (1)
0.65	7.2956 (1)	−5.6382 (1)	6.2314 (1)	−5.0273 (1)
0.70	4.0086 (1)	−6.1533 (1)	2.9605 (1)	−5.7758 (1)
0.75	1.7848 (1)	−6.3154 (1)	1.3827 (1)	−6.1233 (1)
0.80	5.1576 (0)	−6.1999 (1)	4.2306 (0)	−6.1472 (1)
0.85	0.0000 (−1)	−5.8882 (1)	0.0000 (−1)	−5.9345 (1)

r	$V_{\text{dir}}(k_F=1.4)$	$V_{\text{ex}}(k_F=1.4)$	$V_{\text{dir}}(k_F=1.0)$	$V_{\text{ex}}(k_F=1.0)$
0.70	0.0000 (−1)		0.0000 (−1)	
0.75	−1.8831 (0)		−7.9952 (0)	
0.80	−6.1964 (0)		−1.4890 (1)	
0.85	−1.2437 (1)		−2.1423 (1)	
0.90	−1.9561 (1)	−5.4527 (1)	−2.7829 (1)	−5.5646 (1)
0.95	−2.3523 (1)	−4.9515 (1)	−3.1037 (1)	−5.1036 (1)
1.00	−2.5225 (1)	−4.4279 (1)	−3.1986 (1)	−4.6014 (1)
1.10	−2.4569 (1)	−3.4267 (1)	−2.9885 (1)	−3.6058 (1)
1.20	−2.1180 (1)	−2.5624 (1)	−2.5314 (1)	−2.7273 (1)
1.30	−1.7188 (1)	−1.8779 (1)	−2.0343 (1)	−2.0183 (1)
1.40	−1.3457 (1)	−1.3568 (1)	−1.5852 (1)	−1.4725 (1)
1.50	−1.0317 (1)	−9.7080 (0)	−1.2134 (1)	−1.0644 (1)
1.60	−7.8179 (0)	−6.9031 (0)	−9.1973 (0)	−7.6500 (0)
1.70	−5.8935 (0)	−4.8923 (0)	−6.9417 (0)	−5.4790 (0)
1.80	−4.4415 (0)	−3.4665 (0)	−5.2373 (0)	−3.9179 (0)
1.90	−3.3591 (0)	−2.4649 (0)	−3.9618 (0)	−2.8034 (0)
2.00	−2.5547 (0)	−1.7627 (0)	−3.0068 (0)	−2.0057 (0)
2.20	−1.5255 (0)	−9.5232 (−1)	−1.7715 (0)	−1.0514 (0)
2.40	−9.5678 (−1)	−5.7555 (−1)	−1.0790 (0)	−5.8047 (−1)
2.60	−6.3098 (−1)	−4.0252 (−1)	−6.8237 (−1)	−3.5233 (−1)
2.80	−4.3375 (−1)	−3.1978 (−1)	−4.4838 (−1)	−2.4333 (−1)
3.00	−3.0656 (−1)	−2.7410 (−1)	−3.0536 (−1)	−1.9094 (−1)
3.40	−1.5867 (−1)	−2.1533 (−1)	−1.5438 (−1)	−1.4773 (−1)
3.80	−8.2451 (−2)	−1.6646 (−1)	−8.3878 (−2)	−1.2344 (−1)
4.20	−4.2428 (−2)	−1.2416 (−1)	−4.6900 (−2)	−1.0030 (−1)
4.60	−2.1735 (−2)	−9.0338 (−2)	−2.6311 (−2)	−7.8246 (−2)
5.00	−1.1190 (−2)	−6.4890 (−2)	−1.4664 (−2)	−5.9108 (−2)
5.40	−5.8311 (−3)	−4.6364 (−2)	−8.1103 (−3)	−4.3680 (−2)
5.80	−3.0867 (−3)	−3.3073 (−2)	−4.4641 (−3)	−3.1833 (−2)
6.20	−1.6600 (−3)	−2.3589 (−2)	−2.4546 (−3)	−2.3011 (−2)
6.60	−9.0475 (−4)	−1.6833 (−2)	−1.3535 (−3)	−1.6565 (−2)
7.00	−4.8781 (−4)	−1.1919 (−2)	−7.3219 (−4)	−1.1803 (−2)

Having motivated the construction of direct and exchange forces by the simple case of identical wave functions for neutrons and protons, it is now straightforward to generalize to arbitrary closed-shell nuclei. Instead of simply defining even- and odd-state interactions as in (2.41), we now define separate singlet even (SE), triplet even (TE), singlet odd (SO), and triplet odd (TO) interactions. The formal definition is Eq. (2.39) with the sums over S omitted. These separate even and odd interactions reproduce individual matrix elements somewhat less accurately than the composite even and odd interactions, but the average contributions should be sufficiently accurate for our needs. Then (3.6) is replaced by

$$V=\tfrac{1}{4}(1+P_m)(1+P_\sigma)V_{\mathrm{TE}}+\tfrac{1}{4}(1+P_m)(1-P_\sigma)V_{\mathrm{SE}}+\tfrac{1}{4}(1-P_m)(1+P_\sigma)V_{\mathrm{TO}}+\tfrac{1}{4}(1-P_m)(1-P_\sigma)V_{\mathrm{SO}}, \tag{3.11}$$

where P_σ is the spin-exchange operator, and we obtain

$$\begin{aligned}\langle MN \mid V \mid MN-NM\rangle &= \tfrac{1}{4}[(1-\delta_\tau\delta_\chi+\delta_\chi-\delta_\tau)\langle mn \mid V_{\mathrm{TE}} \mid mn\rangle \\ &+(1-\delta_\tau\delta_\chi+\delta_\chi-\delta_\tau)\langle mn \mid V_{\mathrm{TE}} \mid nm\rangle \\ &+(1-\delta_\tau\delta_\chi-\delta_\chi+\delta_\tau)\langle mn \mid V_{\mathrm{SE}} \mid mn\rangle \\ &+(1-\delta_\tau\delta_\chi-\delta_\chi+\delta_\tau)\langle mn \mid V_{\mathrm{SE}} \mid nm\rangle \\ &+(1+\delta_\tau\delta_\chi+\delta_\chi+\delta_\tau)\langle mn \mid V_{\mathrm{TO}} \mid mn\rangle \\ &+(-1-\delta_\tau\delta_\chi-\delta_\chi-\delta_\tau)\langle mn \mid V_{\mathrm{TO}} \mid nm\rangle \\ &+(1+\delta_\tau\delta_\chi-\delta_\chi-\delta_\tau)\langle mn \mid V_{\mathrm{SO}} \mid mn\rangle \\ &+(-1-\delta_\tau\delta_\chi+\delta_\chi+\delta_\tau)\langle mn \mid V_{\mathrm{SO}} \mid nm\rangle].\end{aligned} \tag{3.12}$$

For unlike particles, $\delta_\tau=0$ so that averaging over spin yields

$$\begin{aligned}\tfrac{1}{2}\sum_{\chi m}\langle MN \mid V \mid MN-NM\rangle^{\mathrm{un}} &= \langle nm \mid \tfrac{3}{8}V_{\mathrm{TE}}+\tfrac{1}{8}V_{\mathrm{SE}}+\tfrac{3}{8}V_{\mathrm{TO}}+\tfrac{1}{8}V_{\mathrm{SO}} \mid nm\rangle \\ &+\langle nm \mid \tfrac{3}{8}V_{\mathrm{TE}}+\tfrac{1}{8}V_{\mathrm{SE}}-\tfrac{3}{8}V_{\mathrm{TO}}-\tfrac{1}{8}V_{\mathrm{SO}} \mid mn\rangle.\end{aligned} \tag{3.13}$$

For like particles, $\delta_\tau=1$, and averaging over spin yields

$$\tfrac{1}{2}\sum_{\chi m}\langle MN \mid V \mid MN-NM\rangle^{\mathrm{lk}} = \langle nm \mid \tfrac{1}{4}V_{\mathrm{SE}}+\tfrac{3}{4}V_{\mathrm{TO}} \mid nm\rangle+\langle nm \mid \tfrac{1}{4}V_{\mathrm{SE}}-\tfrac{3}{4}V_{\mathrm{TO}} \mid mn\rangle. \tag{3.14}$$

We now define the interactions within the direct and exchange integrals in (3.13) as $v_{\mathrm{dir}}{}^{\mathrm{un}}$ and $v_{\mathrm{ex}}{}^{\mathrm{un}}$, respectively, and similarly define $v_{\mathrm{dir}}{}^{\mathrm{lk}}$ and $v_{\mathrm{ex}}{}^{\mathrm{lk}}$ from (3.14). From (2.39) and (3.9), we note that these definitions are consistent with the average direct and exchange forces defined above since

$$v_{\mathrm{dir}}{}^{\mathrm{av}}=\tfrac{1}{2}(v_{\mathrm{dir}}{}^{\mathrm{lk}}+v_{\mathrm{dir}}{}^{\mathrm{un}}) \tag{3.15}$$

and similarly for exchange.

In the same way as described previously for the average direct and exchange forces, we place all the short-range contribution into the repulsive short-range direct term and construct long-range direct and exchange forces for the like and unlike interactions. It will be convenient to refer to the direct short-range force as simply the short-range force and the long-range direct and exchange forces as the direct and exchange forces, respectively. These forces are graphed in Fig. 3 for $k_F=1.4$ F^{-1}. One observes from this figure that the like and unlike forces have the expected property that the force between like particles is over all much less attractive than the force between unlike particles. It is also important to note that $\frac{3}{8}v_{\mathrm{ev}}+\frac{5}{8}v_{\mathrm{odd}}$ is much less attractive than $\frac{3}{8}v_{\mathrm{ev}}-\frac{5}{8}v_{\mathrm{odd}}$ so that the exchange integrals will be quite significant.

Thus far, our discussion has pertained to any k_F but, as before, it is necessary to adopt a simple functional form of density dependence. Short-range, direct and exchange, like and unlike forces have been computed at $k_F=1.0$, 1.4, and 1.7 F^{-1}. We select the functional form

$$v_0(r)+v_1(r)k_F{}^\alpha=\frac{(1.4)^\alpha v(k_F=1.0,r)-v(k_F=1.4,r)}{(1.4)^\alpha-1}+k_F{}^\alpha\frac{v(k_F=1.4,r)-v(k_F=1.0,r)}{(1.4)^\alpha-1}, \tag{3.16}$$

which reproduces the forces at $k_F=1.0$ and 1.4 F^{-1} and select α to give reasonable results at $k_F=1.7$ F^{-1}. For numerical purposes it is advantageous to have α integral, and we find the best value for the short-range force to be $\alpha=3$ and the best value for the direct and exchange forces to be $\alpha=1$.

Rather than use separate functions of r for the like and unlike forces which would essentially double the computing time for our calculation, since the spatial dependence for like and unlike forces shown in Fig. 3 is similar to that of the average force, we define multiplicative factors of the average forces to approximate the like and unlike forces. Consistent with our nuclear-matter weighting philosophy, these factors are defined so as to reproduce the correct like and unlike contributions in nuclear matter. Since the direct contribution to nuclear-matter binding is proportional to the volume integral of the short-range and direct forces, we define

$$F_{k_F}{}^{\mathrm{lk}}=\int v^{\mathrm{lk}}(k_F,r)r^2dr/\left(\int v^{\mathrm{av}}(k_F,r)r^2dr\right) \tag{3.17}$$

for both the direct and short-range forces, and similarly for F^{un}. Since the exchange contribution to nuclear-matter energy is proportional to

$$\int \rho_{\mathrm{ex}}(k_F,r)v_{\mathrm{ex}}(r)r^2dr, \tag{3.18}$$

where

$$\rho_{\mathrm{ex}}(k_F,r)=\int dk(3/64\pi^2)W(k_F,k)\,\sin(2kr)/(2kr),$$

TABLE V. (a) Integrals in Eqs. (3.17) and (3.18), in MeV. The interactions V_S, $V_{\rm dir}$, and $V_{\rm ex}$ are as in Table IV, and av, lk, and un indicate average, like, and unlike, respectively. (b) Factors defined in Eqs. (3.17)–(3.23), with the same notation as part (a).

(a)

k_F (F^{-1})	Force	$\int v_S r^2 dr$	$\int v_{\rm dir} r^2 dr$	$\int \rho_{\rm ex}(1.0,r) v_{\rm ex}(k_F,r) r^2 dr$	$\int \rho_{\rm ex}(1.4,r) v_{\rm ex}(k_F,r) r^2 dr$
1.0	av	25.091	−39.730	−2.629	−5.415
1.0	lk	16.914	−28.658	−1.431	−3.096
1.0	un	33.268	−50.807	−3.820	−7.714
1.4	av	26.029	−33.089	−2.560	−5.311
1.4	lk	17.705	−25.259	−1.560	−3.385
1.4	un	34.353	−40.921	−3.559	−7.237

(b)

Force	$F_{1.0}$	$F_{1.4}$	R	V_0	V_1
lk, S	0.674	0.680	1.0374	0.671	0.840
un, S	1.326	1.320		1.329	1.160
lk, dir	0.721	0.763	0.8814	0.650	0.409
un, dir	1.279	1.237		1.350	1.591
lk, ex	0.547	0.637	0.9773	0.329	−3.328
un, ex	1.453	1.363		1.671	5.328

we define

$$F_{{\rm ex},k_F}{}^{\rm lk} = \frac{\int \rho_{\rm ex}(k_F,r) v_{\rm ex}{}^{\rm lk}(k_F,r) r^2 dr}{\int \rho_{\rm ex}(k_F,r) v_{\rm ex}{}^{\rm av}(k_F,r) r^2 dr} \quad (3.19)$$

for the exchange force, and similarly for $F^{\rm un}$. The indicated integrals and F factors are tabulated in Table V for $k_F=1.0$ and 1.4 F^{-1}.

Whereas the factors derived above pertain to the individual contributions at $k_F=1.0$ and 1.4 F^{-1}, it is most useful to have factors multiplying the $v_0(r)$ and $v_1(r)$ terms in (3.16). In order to obtain these factors, it is necessary to define the ratio of the average force at $k_F=1.4$ to that at 1.0 F^{-1}. For the short-range and direct forces, it is clearly consistent to define

$$R = \int v^{\rm av}(1.4,r) r^2 dr / \left(\int v^{\rm av}(1.0,r) r^2 dr\right). \quad (3.20)$$

For the exchange force, weighting by $\rho_{\rm ex}$ at the two densities yields slightly different values so we define the average

$$R = \frac{1}{2}\left[\frac{\int \rho_{\rm ex}(1.4,r) v_{\rm ex}{}^{\rm av}(1.4,r) r^2 dr}{\int \rho_{\rm ex}(1.4,r) v_{\rm ex}{}^{\rm av}(1.0,r) r^2 dr} + \frac{\int \rho_{\rm ex}(1.0,r) v_{\rm ex}{}^{\rm av}(1.4,r) r^2 dr}{\int \rho_{\rm ex}(1.0,r) v_{\rm ex}{}^{\rm av}(1.0,r) r^2 dr}\right]. \quad (3.21)$$

Then, for each of the short-range, direct, and exchange forces, defining

$$V_0{}^{\rm lk} = \left[(1.4)^\alpha F_{1.0}{}^{\rm lk} - R F_{1.4}{}^{\rm lk}\right] / \left((1.4)^\alpha - R\right) \quad (3.22)$$

and

$$V_1{}^{\rm lk} = (F_{1.0}{}^{\rm lk} - R F_{1.4}{}^{\rm lk})/(1-R), \quad (3.23)$$

we obtain the desired form for the like force

$$v_0{}^{\rm lk} + v_1{}^{\rm lk} k_F{}^\alpha = V_0{}^{\rm lk} v_0{}^{\rm av}(r) + V_1{}^{\rm lk} v_1{}^{\rm av}(r) k_F{}^\alpha \quad (3.24)$$

and the unlike force is treated analogously. These V factors are also tabulated in Table V.

The starting energy dependence of (2.45) is easily adapted to our present treatment. Since we only consider the triplet-S starting energy dependence, by (3.13) and (3.14), the only starting energy dependence is in the unlike potential. Exploiting the freedom to distribute all delta-function forces in the direct integral we obtain, using the statistical factors in (3.13),

$$\Delta v_{\rm short}{}^{\rm un} = 4\pi(\tfrac{3}{4}) v_\delta(W) \delta^3(\mathbf{r}_1 - \mathbf{r}_2),$$
$$\Delta v_{\rm dir}{}^{\rm un} = \Delta v_{\rm ex}{}^{\rm un} = \tfrac{3}{8} \Delta v_{\rm long}(W, |\mathbf{r}_1 - \mathbf{r}_2|), \quad (3.25)$$

where $v_\delta(W)$ and $\Delta v_{\rm long}(W, |\mathbf{r}_1-\mathbf{r}_2|)$ are given in (2.43) and (2.44).

Since (3.25) is independent of density, our treatment of the starting energy dependence is somewhat inconsistent and requires further explanation. The approximation we make in (3.25) for computational simplicity is that the correction at all densities is the same as for $k_F=1.4$ F^{-1}. Whereas this is obviously a good approximation in the interior of a nucleus, we now consider a state with a single-particle energy of 10 MeV in the surface of the nucleus. For this case (3.25) corrects for a change from 50 to 10 MeV, whereas the actual change from the average nuclear-matter single-particle energy at the local density to 10 MeV is much smaller, so we appear to be including too much attraction. However, at low density, Q does not exclude nearly as many low-lying states so that a given change in starting

energy produces much more attraction. Hence, at least part of our apparent excess attraction is justified, and we believe (3.25) is therefore a satisfactory approximation.

In the previous section, we discussed the need for adjusting the effective interaction to obtain the correct nuclear-matter binding energy. Having now reduced the effective interaction to essentially six functions of r, namely, $v_0^{\rm av}(r)$ and $v_1^{\rm av}(r)$ for short-range, direct, and exchange forces, and appropriate multiplicative factors for like and unlike forces, clearly the most convenient means of adjusting the interaction is to introduce additional factors. Rather than defining a large number of parameters allowing very general modification of the interaction, we use four parameters of fairly direct physical significance. The direct and exchange average potentials are multiplied by the single parameter P_L. The short-range average potentials at $k_F=1.4$ and 1.0 are multiplied, respectively, by $P_{S,1.4}$ and $P_{S,1.0}$. In order to independently vary the absolute difference between the like and unlike potentials, we define the parameter $P_{\rm sym}$ and use modified F factors,

$$F'=1+(F-1)P_{\rm sym}/P, \tag{3.26}$$

where P denotes the parameter multiplying the average potential corresponding to F. Note that varying these parameters varies the V_0 and V_1 factors both by varying $F_{1.0}$ and $F_{1.4}$ and also by varying R for the short-range force. The choice of these parameters to reproduce the properties of nuclear matter is discussed in the following section.

Bulk Properties of Nuclear Matter from the Effective Interaction

The three physical properties of nuclear matter relevant to this work are the binding energy per particle, the symmetry energy, and the saturation density. The first two properties may be extracted from the semiempirical mass formula. Since the data are not sufficient to well determine separate bulk and surface symmetry energies, we prefer the analysis of Myers and Swiatecki,[45] which assumes the form

$$BE/A=-(a_1-a_2A^{-1/3})\,(1-\kappa[(N-Z)/A]^2)+\cdots \tag{3.27}$$

and determines the parameters

$$\begin{aligned} a_1&=15.68\ \text{MeV},\\ a_2&=18.56\ \text{MeV},\\ a_1\kappa&=28.0\ \text{MeV}. \end{aligned} \tag{3.28}$$

Other analyses which have attempted to separate volume and surface contributions have yielded somewhat higher volume symmetry energies with Green[46] and Cameron[47] obtaining 31.5 MeV.

The saturation density cannot be directly obtained from the semiempirical formula. Old arguments[48] have suggested that it is roughly equal to the density in the interior of a large nucleus, but it is difficult to believe that Coulomb, symmetry, and surface effects compensate sufficiently to justify this assertion. Current prejudice tends to favor $k_F=1.36$. This value is consistent with the central density argument, is not unreasonably different from the nuclear-matter reaction matrix result of $k_F=1.44$, and seems to be supported by a Thomas-Fermi argument[49] using Bethe's differential theory.[33] However, the nuclear-matter calculation is not a strong argument since the saturation density is sensitive to the interaction in higher partial waves which has been included only in the phase-shift approximation, and since the higher-order contributions are likely to be quite density-dependent and have only been calculated at a single density. The central density and Thomas-Fermi arguments only crudely relate finite nuclei to nuclear matter whereas our present density-dependent HF theory much more directly and accurately establishes this connection. Hence, rather than select k_F by past prejudice, we feel that it is most sensible to use our present theory to determine the k_F which most nearly reproduces the properties of finite nuclei.

Writing out the lowest-order contribution to nuclear-matter energy per particle with our effective interaction in detail, we obtain, for $N=Z$,

$$\begin{aligned} E=&\Big[\sum_i T_i+\tfrac{1}{2}\sum_{\mathbf{k}_1\mathbf{k}_2,\text{spin,isospin}}(\langle\mathbf{k}_1\mathbf{k}_2\,|\,v_{\rm dir}+v_S\,|\,\mathbf{k}_1\mathbf{k}_2\rangle+\langle\mathbf{k}_1\mathbf{k}_2\,|\,v_{\rm ex}\,|\,\mathbf{k}_2\mathbf{k}_1\rangle)\Big]/A\\ &=3k_F^2/(10m)+4k_F^3(3\pi)^{-1}\{[(2.744-k_F^3)/1.744]P_{S,1.0}\int r^2v_S^{\rm av}(1.0,r)\,dr\\ &\quad+[(k_F^3-1)/1.744]P_{S,1.4}\int r^2v_S^{\rm av}(1.4,r)\,dr-2.20-53.4I_W+(0.989+29.9I_W)W\\ &\quad-(0.0302+3.20I_W)W^2+[(1.4-k_F)/0.4]P_L\int r^2v_{\rm dir}^{\rm av}(1.0,r)\,dr+[(k_F-1)/0.4]P_L\int r^2v_{\rm dir}^{\rm av}(1.4,r)\,dr\}\\ &+(16/\pi)\Big[(-53.4+29.9W-3.20W^2)\iint(2+(k/k_F)^3-3(k/k_F))k^2[\sin(2kr)/2kr][(r-0.7)^2/(0.69+r^{8.6})]r^2dk\,dr\\ &+\iint(2+(k/k_F)^3-3(k/k_F))k^2[\sin(2kr)/2kr]r^2\{[(1.4-k_F)/0.4]P_Lv_{\rm ex}^{\rm av}(1.0,r)+[(k_F-1)/0.4]P_Lv_{\rm ex}^{\rm av}(1.4,r)\}dk\,dr\Big], \end{aligned} \tag{3.29}$$

[45] W. D. Myers and W. J. Swiatecki, Nucl. Phys. **81**, 1 (1966).
[46] A. E. S. Green, Rev. Mod. Phys. **30**, 569 (1955); Phys. Rev. **95**, 1006 (1954).
[47] A. G. W. Cameron, Can. J. Phys. **35**, 1021 (1957).
[48] B. H. Brandow, thesis, Cornell University (unpublished).
[49] H. A. Bethe and P. J. Siemens (private communication).

where

$$I_W=\int[(r-0.7)^2/(0.69+r^{8.6})]r^2dr,$$

obtained from (2.43), and W is the average starting energy. W may be written in terms of E, using

$$AE=\tfrac{1}{2}\sum_i(\epsilon_i+T_i), \tag{3.30}$$

so that

$$\bar{\epsilon}=2E-3k_F^2/10m, \tag{3.31}$$

and thus

$$W=-[4E-3k_F^2/5m](41.467)^{-1}\ \mathrm{F}^{-2}. \tag{3.32}$$

At any specific k_F, (3.29) may be written in the form

$$E=C_0+C_{S,1.0}(P_{S,1.0}-1)+C_{S,1.4}(P_{S,1.4}-1)+C_L(P_L-1)+C_1E+C_2E^2, \tag{3.33}$$

where the C's are simple numerical constants obtained from the integrals indicated in (3.29). Since C_0 is the dominant term and the C_2 term is quite small, we may write

$$E=(C_0+C_{S,1.0}(P_{S,1.0}-1)+C_{S,1.4}(P_{S,1.4}-1)+C_L(P_L-1))/D, \tag{3.34}$$

where $D=1-C_1-C_2C_0$. The constants in (3.34) are tabulated in Table VI for k_F from 1.1 through 1.5 F^{-1} and trivially yield the nuclear-matter saturation curve for any values of the adjustable parameters.

The cumulative error in our approximate effective interaction may be checked by comparing our nuclear-matter binding of 11.4 MeV at $k_F=1.4$ with the actual reaction matrix result of 11.1 MeV obtained by Siemens.[20] This small discrepancy results from a combination of the simplified starting energy dependence in (3.25), using the average starting energy indicated in (3.32), cutting off our integrals at 7 F, and the fact that Siemens uses the phase-shift approximation in partial waves above $l=2$, whereas we use OPEP. The fact that our effective interaction saturates at $k_F=1.35$, whereas Siemens's calculation saturates at $k_F=1.44$ is due to the fact that the phase-shift approximation is more attractive than OPEP, tending to give more attraction at high densities and due to the approximate density dependence we assume. We note in passing that recent calculations by Reid[50] indicate that OPEP now appears to be more reasonable than the phase-shift approximation for higher partial waves.

Symmetry Energy

We now derive the contribution to nuclear-matter symmetry energy at $k_F=1.4$ F^{-1} from our effective interaction, neglecting at present the contributions of terms involving the derivatives of G with respect to proton and neutron densities. The contribution of the kinetic energy to the symmetry energy is obtained trivially by noting that the total kinetic energy is proportional to $N^{5/3}+Z^{5/3}$. Expanding about $(N+Z)/2$,

$$N^{5/3}+Z^{5/3}=2[(N+Z)/2]^{5/3}\times(1+\tfrac{5}{9}[(N-Z)/(N+Z)]^2+\mathcal{O}[(N-Z)/(N+Z)]^4), \tag{3.35}$$

so that the general kinetic contribution to the binding energy per particle is

$$E_{\mathrm{kin}}=(3k_F^2/10m)(1-\tfrac{5}{9}[(N-Z)/(N+Z)]^2). \tag{3.36}$$

Throughout this symmetry energy discussion k_F is the Fermi momentum corresponding to $N+Z$ particles per unit volume. Evaluating (3.36) at $k_F=1.4$ F^{-1}, the kinetic term is

$$E_{\mathrm{kin}}=24.4(1-\tfrac{5}{9}[(N-Z)/(N+Z)]^2)\ \mathrm{MeV}. \tag{3.37}$$

The symmetry energy of the short-range and direct interactions are equally simple since the direct integrals contain no momentum dependence and the difference between like and unlike forces is contained in the multiplicative factors. Noting

$$(F^{\mathrm{un}}-1)=(1-F^{\mathrm{lk}})=(F^{\mathrm{un}}-F^{\mathrm{lk}})/2, \tag{3.38}$$

the total energy from the direct integral is proportional to

$$N^2\int v^{\mathrm{lk}}r^2dr+Z^2\int v^{\mathrm{lk}}r^2dr+2NZ\int v^{\mathrm{un}}r^2dr=(N+Z)^2\int v^{\mathrm{av}}r^2dr\times(1-\tfrac{1}{2}(F^{\mathrm{un}}-F^{\mathrm{lk}})[(N-Z)/(N+Z)]^2). \tag{3.39}$$

Using the normalization factors from (3.29), the contribution to the binding energy per particle from the short-range and direct forces at $k_F=1.4$ F^{-1} is

$$E_{S+\mathrm{dir}}=30.4(1-0.32[(N-Z)/(N+Z)]^2)-38.8(1-0.24[(N-Z)/(N+Z)]^2)\ \mathrm{MeV}. \tag{3.40}$$

In order to compute the exchange contribution for unequal N and Z, it is necessary to generalize the relative momentum weighting function (2.14) to account for unequal Fermi spheres. In general,

$$W(k_{F_1},k_{F_2},k)=\int d^3K\,\theta(k_{F_1}-|\mathbf{k}+\mathbf{K}/2|)\times\theta(k_{F_2}-|\mathbf{k}-\mathbf{K}/2|). \tag{3.41}$$

TABLE VI. Nuclear-matter saturation curve constants in Eq. (3.34). Units are such that E is in MeV.

k_F (F^{-1})	C_0	$C_{S,1.0}$	$C_{S,1.4}$	C_L	D
1.1	−11.40	11.45	2.80	−38.06	1.162
1.2	−13.08	10.68	7.99	−46.63	1.196
1.3	−14.18	7.29	16.70	−55.85	1.232
1.4	−14.42	−0.067	30.38	−65.58	1.272
1.5	−13.48	−13.09	50.89	−75.69	1.318

[50] R. V. Reid (private communication).

The resulting integrals are evaluated most simply if we consider Fermi spheres of radii k_F+x and k_F-x. Then the exchange contribution to the binding energy is proportional to

$$E(x,k_F)=\int_0^{k_F+x}k^2W(k_F+x,k_F+x,k)\times[\sin(2kr)/2kr]F_{\rm ex}^{\rm lk}v_{\rm ex}^{\rm av}(r)r^2dk\,dr+\int_0^{k_F-x}k^2W(k_F-x,k_F-x,k)\times[\sin(2kr)/2kr]F_{\rm ex}^{\rm lk}v_{\rm ex}^{\rm av}(r)r^2dk\,dr+2\int_0^{k_F}k^2W(k_F+x,k_F-x,k)\times[\sin(2kr)/2kr]F_{\rm ex}^{\rm un}v_{\rm ex}^{\rm av}(r)r^2dk\,dr. \quad (3.42)$$

Explicitly writing out the indicated integrals, one may obtain a Taylor series in x for E about $x=0$ by differentiating the integrals. The linear terms cancel as before and the resulting second-order expression for the exchange contribution to the binding energy per particle is

$$E_{\rm ex}=(16/\pi k_F^3)\{\int k^2(2k_F^3+k^3-3k_F^2k)\times[\sin(2kr)/2kr]v_{\rm ex}^{\rm av}(r)r^2dk\,dr+3x^2\int k^2(2k_F-k)[\sin(2kr)/2kr]v_{\rm ex}^{\rm av}(r)r^2dk\,dr-\tfrac{3}{2}x^2k_F^2\int k[\sin(2kr)/2kr]F_{\rm ex}^{\rm un}v_{\rm ex}^{\rm av}(r)r^2dr\,dk\}. \quad (3.43)$$

The quadratic terms in (3.43) are not the symmetry energy terms since Fermi spheres of radii k_F+x and k_F-x do not have the original number of particles. Thus, we should consider spheres of radii $(k_F+\Delta k_F\pm x)$, where to keep the number constant, $\Delta k_F=-x^2/k_F$. Adding the correction $(\Delta k_F/A)[\partial(AE_{\rm ex})/\partial k_F]$ to (3.43) and noting that

$$[(N-Z)/(N+Z)]^2=9x^2/k_F^2+\mathcal{O}(x^3),$$

we obtain

$$E_{\rm ex}=(16/\pi k_F^3)\Big(\int k^2(2k_F^3+k^3-3k_F^2k)[\sin(2kr)/2kr]\times v_{\rm ex}^{\rm av}(r)r^2dk\,dr+[(N-Z)/(N+Z)]^2(k_F^2/6)\times\{2\int k^3[\sin(2kr)/2kr]v_{\rm ex}^{\rm av}(r)r^2dk\,dr-k_F^2\int k[\sin(2kr)/2kr]F_{\rm ex}^{\rm un}v_{\rm ex}^{\rm av}(r)r^2dk\,dr\}\Big)$$
$$=-27.1+14.1[(N-Z)/(N+Z)]^2\ \text{MeV} \quad \text{for} \quad k_F=1.4\ \text{F}^{-1}. \quad (3.44)$$

It is interesting to note that the exchange contribution to the symmetry energy is physically quite different from the direct terms. Whereas the direct contribution arises solely from the difference between like and unlike forces, the exchange term is roughly proportional to the strength of the average interaction and arises primarily because the wave function weighting for exchange changes for $N\neq Z$. Thus, any enhancement of the exchange interaction automatically significantly increases the symmetry energy. In terms of the adjustable parameters discussed above,

$$E_{\rm sym}=E_{\rm kin}+E_{S+{\rm dir}}+E_{\rm ex}=13.6+6.44P_{\rm sym}+7.26P_L\ \text{MeV} \quad \text{at} \quad k_F=1.4. \quad (3.45)$$

With no adjustment of the force, $E_{\rm sym}$ is 27.3 MeV.

Several important effects must be included in order to compare $E_{\rm sym}$ with (3.28). Having emphasized the effect of the density dependence of the effective interaction, it is clear that $\partial V/\partial\rho$ terms should contribute significantly to the symmetry energy. Since our parametrization of the density dependence is based on equal sized Fermi spheres, it cannot in its present form reproduce the intricacies of the density dependence of the interaction between unlike particles with $N\neq Z$. For this reason, we use the results of the complete nuclear-matter calculation by Siemens[20] for $N\neq Z$ in which he obtains 31 MeV including $\partial V/\partial\rho$ terms and 27 MeV omitting them. This 4-MeV correction is quite significant since it should really be compared with the experimental symmetry energy minus the kinetic contribution of 13.6 MeV.

Since the volume contribution to symmetry energy is to be compared with the nuclear-matter symmetry energy, we must modify our calculation at $k_F=1.4$ to nuclear-matter density. Siemens[20] has shown that the symmetry energy varies as k_F^2 to an excellent approximation so that we should require

$$(k_F^{\rm sat}/1.4)^2(E_{\rm sym}+4.0)=28\ \text{MeV}. \quad (3.46)$$

In our subsequent density-dependent HF calculations, the force is adjusted such that saturation occurs at $k_F=1.31$, $P_L=1.0$, and $P_{\rm sym}=1.0$, with the result that (3.46) yields 27.5 MeV.

It might appear that our treatment neglects the effect of the difference between nuclear-matter starting energies and those in finite nuclei. Since the starting energy correction only appears in the unlike force, the direct contribution in (3.39) is quite significant because it depends on the difference between like and unlike forces. Using (3.25) in (3.39) and (3.44), we obtain

$$E_{\rm sym}=7.90-4.15W+3.55W^2\ \text{MeV}. \quad (3.47)$$

The average single-particle energy in Pb^{208} of 25.0 MeV obtained in our subsequent calculations yields $\Delta E_{\rm sym}=3.4$ MeV which one might be tempted to include with $E_{\rm sym}$ in (3.46). However, this would be incorrect since

the starting energy varies with A, and hence is included in the surface term. Physically, this is evident since the single-particle energies are determined in part by the surface energy, and this influence must decrease as the ratio of surface to volume decreases. To verify this quantitatively we use the result obtained in a later section that the average single-particle energy in Ca^{40} is 24.1 MeV and in Pb^{208} is 25.0. However, as discussed later, the starting energy for protons is not simply the sum of the single-particle energies of the two interacting particles, as for neutrons, but rather must be corrected for the Coulomb potential in intermediate states. These corrections modify the average single-particle contributions to starting energy in Ca^{40} and Pb^{208} to 28.3 and 32.9, respectively. Since the ratio of surface to volume contributions in (3.28) is -1.18 and since (3.47) is sufficiently linear over a range of 15 MeV, we write the average single-particle contribution as $E_0(1-1.18A^{-1/3})$ where $E_0=41$ MeV yields the best fit to Ca^{40} and Pb^{208}. Now E_0 is the average single-particle energy appropriate to the volume term and, hence, should be compared with the average single-particle energy in nuclear matter at the saturation density. Using the argument in (3.30) and noting that the binding energy at $k_F=1.3$ F^{-1} is 10.5, we find that the average single-particle energy at $k_F=1.3$ F^{-1} is 42 MeV. Hence, assuming nuclear-matter saturation at $k_F=1.31$ F^{-1}, the starting energy correction is quite adequately included in the surface term.

Angular-Momentum Reduction

Before performing the variation of the wave functions to derive the density-dependent HF radial equation, it is desirable to perform as much angular-momentum reduction as possible. Considering first the simple case of completely closed l shells with the same radial functions for protons and neutrons and using the notation in (3.5), the contribution from Fig. 2(b) is

$$\tfrac{1}{2}\sum_{MM'}\langle MM' \mid V \mid MM'-M'M\rangle=\tfrac{1}{2}\sum_{nlm,\,\mathrm{spin},\,\mathrm{isospin}}\int dr_1 d\Omega_1 \sum_{n'l'm',\,\mathrm{spin},\,\mathrm{isospin}}\int dr_2 d\Omega_2 [\mid R_{n'l'}(r_2)\,Y_{l'm'}(\Omega_2)\mid^2$$
$$\times V(\mid \mathbf{r}_1-\mathbf{r}_2\mid)\mid R_{nl}(r_1)\,Y_{lm}(\Omega_1)\mid^2+R_{n'l'}(r_2)\,Y_{l'm'}{}^*(\Omega_2)R_{nl}(r_1)\,Y_{lm}{}^*(\Omega_1)$$
$$\times\tilde{V}(\mid \mathbf{r}_1-\mathbf{r}_2\mid)R_{n'l'}(r_1)\,Y_{l'm'}(\Omega_1)R_{nl}(r_2)\,Y_{lm}(\Omega_2)], \quad (3.48)$$

where

$$V(\mid \mathbf{r}_1-\mathbf{r}_2\mid)=v_S{}^{\mathrm{av}}+v_{\mathrm{dir}}{}^{\mathrm{av}}$$

and

$$\tilde{V}(\mid \mathbf{r}_1-\mathbf{r}_2\mid)=v_{\mathrm{ex}}{}^{\mathrm{av}}.$$

It is useful to expand V and $\tilde{V}$ in Legendre polynomials,

$$V(\mid \mathbf{r}_1-\mathbf{r}_2\mid)=\sum_{k=0}^{\infty}V_k(r_1,r_2)P_k(\cos\omega_{12}),$$
$$V_k(r_1,r_2)=\tfrac{1}{2}(2k+1)\int V(\mid \mathbf{r}_1-\mathbf{r}_2\mid)P_k(\cos\omega_{12})\,d(\cos\omega_{12}). \quad (3.49)$$

Noting that V and $\tilde{V}$ already contain the appropriate spin and isospin average from (3.7), the direct term in (3.48) is

$$\tfrac{1}{2}\sum_{nln'l'}\int dr_1 dr_2 d\Omega_{12}4(2l'+1)R_{n'l'}{}^2(r_2)4(2l+1)R_{nl}{}^2(r_1)\,V(\mid \mathbf{r}_1-\mathbf{r}_2\mid)/4\pi$$
$$=\tfrac{1}{2}\sum_{nln'l'}\int dr_1 dr_2 4(2l'+1)R_{n'l'}{}^2(r_2)4(2l+1)R_{nl}{}^2(r_1)\,V_0(r_1,r_2). \quad (3.50)$$

Using the addition theorem for spherical harmonics,

$$P_k(\cos\omega_{12})=[4\pi/(2k+1)]\sum_{m''=-k}^{k}(-)^{m''}Y_{km''}(\Omega_1)\,Y_{k-m''}(\Omega_2), \quad (3.51)$$

the relations

$$\int d\Omega(-1)^{m'}Y_{l'-m'}(\Omega)\,Y_{lm}(\Omega)\,Y_{k-m''}(\Omega)$$
$$=(-1)^{m'}[(2l'+1)(2l+1)(2k+1)/4\pi]^{1/2}\begin{pmatrix} l' & l & k\\ 0 & 0 & 0\end{pmatrix}\begin{pmatrix} l' & l & k\\ -m' & m & -m''\end{pmatrix} \quad (3.52)$$

and

$$Y_{l'm'}(\Omega)\,Y_{km''}(\Omega)=\sum_{L=|l'-k|}^{l'+k}\sum_{M=-L}^{L}(-1)^M \times[(2l'+1)(2k+1)(2L+1)/4\pi]^{1/2}\begin{pmatrix} l' & k & L\\ 0 & 0 & 0\end{pmatrix}\begin{pmatrix} l' & k & L\\ m' & m'' & M\end{pmatrix}Y_{L-M}(\Omega), \quad (3.53)$$

and the symmetry relations for 3-j symbols, we obtain

$$\sum_{m'k}\int d\Omega_2 Y_{l'm'}(\Omega_2)\,Y_{l'm'}(\Omega_1)\,Y_{lm}(\Omega_2)\,\tilde{V}_k(r_1,r_2)\,P_k(\cos\omega_{12})=\sum_{m'km''LM}(-1)^{M+m''+m'}\tilde{V}_k(r_1,r_2)\,(2l'+1)$$
$$\times[(2L+1)(2l+1)]^{1/2}\begin{pmatrix} l' & l & k\\ 0 & 0 & 0\end{pmatrix}\begin{pmatrix} l' & L & k\\ 0 & 0 & 0\end{pmatrix}\begin{pmatrix} l' & k & l\\ m' & m'' & -m\end{pmatrix}\begin{pmatrix} l' & k & L\\ m' & m'' & M\end{pmatrix}Y_{L-M}(\Omega_1)$$
$$=\sum_k \tilde{V}_k(r_1,r_2)\,(2l'+1)\begin{pmatrix} l' & l & k\\ 0 & 0 & 0\end{pmatrix}^2 Y_{lm}(\Omega_1). \quad (3.54)$$

Thus, the exchange term in (3.48) is

$$\tfrac{1}{2}\sum_{nln'l'k}\iint dr_1dr_2 4(2l'+1)R_{n'l'}(r_2)R_{n'l'}(r_1)4(2l+1)R_{nl}(r_2)R_{nl}(r_1)\tilde{V}_k\begin{pmatrix} l' & l & k\\ 0 & 0 & 0\end{pmatrix}^2. \quad (3.55)$$

Proceeding to the more complicated general case of closed j shells, the wave functions must be written

$$|\,M\rangle=R_{nl}(r)\mathcal{Y}_{lj}^{m}(\Omega)\tau_s. \quad (3.56)$$

The assumption that $R_{nl}(r)$ does not depend on j is consistent with the previous development since we will only consider the average radial function for closed l shells and only the lower level of an unfilled spin-orbit doublet. The effect of the two-body spin-orbit force, which has been averaged out of our effective interaction, is not included in the present discussion, but will be approximated at a later stage. For notational simplicity, we denote the projectors appearing in (3.11) as

$$P=(1+aP_m+bP_\tau+cP_mP_\tau)/4, \quad (3.57)$$

where each of the four cases may be treated by appropriate choice of a, b, and c, and we use P_τ instead of P_σ because of the explicit τ dependence in (3.56). Then, (3.48) becomes

$$\tfrac{1}{2}\sum_{\text{SE,TE;SO,TO}}\sum_{nljs,n'l'j's'}\langle nljs\,|\,VP\,|\,n'l'j's'\rangle, \quad (3.58)$$

where

$$\langle nljs\,|\,VP\,|\,n'l'j's'\rangle=\sum_{mm'}\iint dr_1d\Omega_1dr_2d\Omega_2R_{nl}(r_1)R_{n'l'}(r_2)\mathcal{Y}_{lj}^{m*}(1)\mathcal{Y}_{l'j'}^{m'*}(2)$$
$$\times\tau_s(1)\tau_{s'}(2)\,V(r_{12})P[R_{nl}(r_1)R_{n'l'}(r_2)\mathcal{Y}_{lj}^{m}(1)\mathcal{Y}_{l'j'}^{m'}(2)\tau_s(1)\tau_{s'}(2)$$
$$-R_{nl}(r_2)R_{n'l'}(r_1)\mathcal{Y}_{lj}^{m}(2)\mathcal{Y}_{l'j'}^{m'}(1)\tau_s(2)\tau_{s'}(1)]$$
$$=\sum_{mm'm_lm_l'm_sm_s',n_ln_l'n_sn_s'}\iint dr_1d\Omega_1dr_2d\Omega_2(2j+1)(2j'+1)\begin{pmatrix}\tfrac{1}{2} & l & j\\ m_s & m_l & -m\end{pmatrix}\begin{pmatrix}\tfrac{1}{2} & l & j\\ n_s & n_l & -m\end{pmatrix}$$
$$\times\begin{pmatrix}\tfrac{1}{2} & l' & j'\\ m_s' & m_l' & -m'\end{pmatrix}\begin{pmatrix}\tfrac{1}{2} & l' & j'\\ n_s' & n_l' & -m'\end{pmatrix}R_{nl}(r_1)R_{n'l'}(r_2)\,Y_{lm_l}{}^*(\Omega_1)\,Y_{l'm_l'}(\Omega_2)\chi_{m_s}(1)$$
$$\times\chi_{m_s'}(2)\tau_s(1)\tau_{s'}(2)\,V(r_{12})P[R_{nl}(r_1)R_{n'l'}(r_2)\,Y_{ln_l}(\Omega_1)\,Y_{l'n_l'}(\Omega_2)\chi_{n_s}(1)\chi_{n_s'}(2)\tau_s(1)\tau_{s'}(2)$$
$$-R_{nl}(r_2)R_{n'l'}(r_1)\,Y_{ln_l}(\Omega_2)\,Y_{l'n_l'}(\Omega_1)\chi_{n_s}(2)\chi_{n_s}{}'(1)\tau_s(2)\tau_{s'}(1)]. \quad (3.59)$$

Explicitly inserting P from (3.57) and denoting $\delta_\tau=\delta_{ss'}$ as before, we obtain

$$\langle nljs \mid VP \mid n'l'j's'\rangle=\frac{1}{4}\iint dr_1 d\Omega_1 dr_2 d\Omega_2\Bigg[\sum_{mm'm_lm_l',m_sm_s'n_ln_l'}\Bigg\{(2j+1)(2j'+1)R_{nl}(r_1)R_{n'l'}(r_2)Y_{lm_l}{}^*(\Omega_1)Y_{l'm_l'}{}^*(\Omega_2)$$

$$\times\begin{pmatrix}\frac{1}{2} & l & j\\ m_s & m_l & -m\end{pmatrix}\begin{pmatrix}\frac{1}{2} & l & j\\ m_s & n_l & -m\end{pmatrix}\begin{pmatrix}\frac{1}{2} & l' & j'\\ m_s' & m_l' & -m'\end{pmatrix}\begin{pmatrix}\frac{1}{2} & l' & j'\\ m_s' & n_l' & -m'\end{pmatrix}V(r_{12})\big[R_{nl}(r_1)R_{n'l'}(r_2)Y_{lm_l}(\Omega_1)$$

$$\times Y_{l'n_l'}(\Omega_2)(1+b\delta_\tau)+R_{nl}(r_2)R_{n'l'}(r_1)Y_{lm_l}(\Omega_2)Y_{l'n_l'}(\Omega_1)(a+c\delta_\tau)\big]\Bigg\}$$

$$+\sum_{mm'm_lm_l',m_sm_s'n_ln_l'}\Bigg\{(2j+1)(2j'+1)R_{nl}(r_1)R_{n'l'}(r_2)Y_{lm_l}{}^*(\Omega_1)Y_{l'm_l'}{}^*(\Omega_2)\begin{pmatrix}\frac{1}{2} & l & j\\ m_s & m_l & -m\end{pmatrix}\begin{pmatrix}\frac{1}{2} & l & j\\ m_s' & n_l & -m\end{pmatrix}$$

$$\times\begin{pmatrix}\frac{1}{2} & l' & j'\\ m_s' & m_l' & -m'\end{pmatrix}\begin{pmatrix}\frac{1}{2} & l' & j'\\ m_s & n_l' & -m'\end{pmatrix}V(r_{12})\big[R_{nl}(r_1)R_{n'l'}(r_2)Y_{ln_l}(\Omega_1)Y_{l'n_l'}(\Omega_2)$$

$$\times(-c-a\delta_\tau)+R_{nl}(r_2)R_{n'l'}(r_1)Y_{ln_l}(\Omega_2)Y_{l'n_l'}(\Omega_1)(-b-\delta_\tau)\big]\Bigg\}\Bigg]. \quad (3.60)$$

The fundamental difference in structure between the two sums in (3.60) is that the four 3-j symbols in the first sum yield $\delta_{m_ln_l}\delta_{m_l'n_l'}/[(2l+1)(2l'+1)]$ when summed over m, m_s, m_s', and m', whereas no similar reduction occurs for the second sum. Thus, it is convenient to rewrite the second sum as two terms, by rewriting

$$\begin{pmatrix}\frac{1}{2} & l & j\\ m_s' & n_l & -m\end{pmatrix}\begin{pmatrix}\frac{1}{2} & l' & j'\\ m_s & n_l' & -m'\end{pmatrix}=\frac{1}{2}\begin{pmatrix}\frac{1}{2} & l & j\\ m_s & n_l & -m\end{pmatrix}\begin{pmatrix}\frac{1}{2} & l' & j'\\ m_s' & n_l' & -m'\end{pmatrix}$$

$$+\left[\begin{pmatrix}\frac{1}{2} & l & j\\ m_s' & n_l & -m\end{pmatrix}\begin{pmatrix}\frac{1}{2} & l' & j'\\ m_s & n_l' & -m'\end{pmatrix}-\frac{1}{2}\begin{pmatrix}\frac{1}{2} & l & j\\ m_s & n_l & -m\end{pmatrix}\begin{pmatrix}\frac{1}{2} & l' & j'\\ m_s' & n_l' & -m'\end{pmatrix}\right]. \quad (3.61)$$

Then, the first sum plus the first term of the second sum reduce as in (3.48), with the result

$$\langle nljs \mid VP \mid n'l'j's'\rangle=\frac{1}{4}\iint dr_1 dr_2(2j+1)(2j'+1)\big[R_{nl}{}^2(r_1)R_{n'l'}{}^2(r_2)$$

$$\times V_0(r_1,r_2)(1+b\delta_\tau-(c+a\delta_\tau)/2)+R_{nl}(r_1)R_{n'l'}(r_1)R_{nl}(r_2)R_{n'l'}(r_2)$$

$$\times\sum_k\begin{pmatrix}l & l' & k\\ 0 & 0 & 0\end{pmatrix}^2V_k(r_1,r_2)(a+c\delta_\tau-(b+\delta_\tau)/2)\big]+(VP)_{\rm dir}+(VP)_{\rm ex}, \quad (3.62)$$

where

$$(VP)_{\rm dir}=\frac{1}{4}\iint dr_1 d\Omega_1 dr_2 d\Omega_2\sum_{mm'm_lm_l',m_sm_s'n_ln_l'}(2j+1)(2j'+1)R_{nl}{}^2(r_1)R_{n'l'}{}^2(r_2)$$

$$\times Y_{lm_l}{}^*(\Omega_1)Y_{l'm_l'}{}^*(\Omega_2)\begin{pmatrix}\frac{1}{2} & l & j\\ m_s & m_l & -m\end{pmatrix}\begin{pmatrix}\frac{1}{2} & l' & j'\\ m_s' & m_l' & -m'\end{pmatrix}\Bigg[\begin{pmatrix}\frac{1}{2} & l & j\\ m_s' & n_l & -m\end{pmatrix}\begin{pmatrix}\frac{1}{2} & l' & j'\\ m_s & n_l' & -m'\end{pmatrix}$$

$$-\frac{1}{2}\begin{pmatrix}\frac{1}{2} & l & j\\ m_s & n_l & -m\end{pmatrix}\begin{pmatrix}\frac{1}{2} & l' & j'\\ m_s' & n_l' & -m'\end{pmatrix}\Bigg]V(r_{12})(-c-a\delta_\tau)Y_{ln_l}(\Omega_1)Y_{l'n_l'}(\Omega_2) \quad (3.63)$$

and

$$(VP)_{\rm ex}=\frac{1}{4}\iint dr_1 d\Omega_1 dr_2 d\Omega_2 \sum_{mm'm_lm_l',m_sm_s'n_ln_l'}(2j+1)(2j'+1)R_{nl}(r_1)R_{n'l'}(r_2)$$
$$\times Y_{lm_l}{}^*(\Omega_1)Y_{l'm_l'}{}^*(\Omega_2)\begin{pmatrix}\frac{1}{2} & l & j\\ m_s & m_l & -m\end{pmatrix}\begin{pmatrix}\frac{1}{2} & l' & j'\\ m_s' & m_l' & -m'\end{pmatrix}\Bigg[\begin{pmatrix}\frac{1}{2} & l & j\\ m_s' & n_l & -m\end{pmatrix}\begin{pmatrix}\frac{1}{2} & l' & j'\\ m_s & n_l' & -m'\end{pmatrix}$$
$$-\frac{1}{2}\begin{pmatrix}\frac{1}{2} & l & j\\ m_s & n_l & -m\end{pmatrix}\begin{pmatrix}\frac{1}{2} & l' & j'\\ m_s' & n_l' & -m'\end{pmatrix}\Bigg]V(r_{12})(-b-\delta_\tau)R_{nl}(r_2)R_{n'l'}(r_1)Y_{ln_l}(\Omega_2)Y_{l'n_l'}(\Omega_1). \quad (3.64)$$

The statistical factors weighting the interaction in (3.62) are precisely the same as in (3.13) and (3.14), since using (3.57),

$$\tfrac{1}{4}\sum_{\rm SE,TE;SO,TO}(1-c/2+[b-a/2]\delta_\tau)V=\tfrac{3}{8}(1-\delta_\tau)V_{\rm TE}+\tfrac{1}{8}(1+\delta_\tau)V_{\rm SE}+\tfrac{3}{8}(1+\delta_\tau)V_{\rm TO}+\tfrac{1}{8}(1-\delta_\tau)V_{\rm SO} \quad (3.65)$$

and

$$\tfrac{1}{4}\sum_{\rm SE,TE;SO,TO}(a-b/2+[c-1/2]\delta_\tau)V=\tfrac{3}{8}(1-\delta_\tau)V_{\rm TE}+\tfrac{1}{8}(1+\delta_\tau)V_{\rm SE}-\tfrac{3}{8}(1+\delta_\tau)V_{\rm TO}-\tfrac{1}{8}(1-\delta_\tau)V_{\rm SO}. \quad (3.66)$$

If either l or l' is a completely closed shell, then $(VP)_{\rm dir}$ and $(VP)_{\rm ex}$ in (3.62) vanish identically. To demonstrate this, we assume for definiteness that the levels $j=l\pm\frac{1}{2}$ are filled. Then,

$$\sum_{smm',m_sm_s'}(2j+1)\begin{pmatrix}\frac{1}{2} & l & j\\ m_s & m_l & -m\end{pmatrix}\begin{pmatrix}\frac{1}{2} & l' & j'\\ m_s' & m_l' & -m'\end{pmatrix}$$
$$\times\left[\begin{pmatrix}\frac{1}{2} & l & j\\ m_s' & n_l & -m\end{pmatrix}\begin{pmatrix}\frac{1}{2} & l' & j'\\ m_s & n_l' & -m'\end{pmatrix}-\frac{1}{2}\begin{pmatrix}\frac{1}{2} & l & j\\ m_s & n_l & -m\end{pmatrix}\begin{pmatrix}\frac{1}{2} & l' & j'\\ m_s' & n_l' & -m'\end{pmatrix}\right]$$
$$=\sum_{m'm_sm_s'}\Bigg[\delta_{m_sm_s'}\delta_{m_ln_l}\begin{pmatrix}\frac{1}{2} & l' & j'\\ m_s' & m_l' & -m'\end{pmatrix}\begin{pmatrix}\frac{1}{2} & l' & j'\\ m_s & n_l' & -m'\end{pmatrix}-\tfrac{1}{2}\delta_{m_sm_s}\delta_{m_ln_l}$$
$$\times\begin{pmatrix}\frac{1}{2} & l' & j'\\ m_s' & m_l' & -m'\end{pmatrix}\begin{pmatrix}\frac{1}{2} & l' & j'\\ m_s' & n_l' & -m'\end{pmatrix}\Bigg]=0. \quad (3.67)$$

Hence, the potential energy contribution from the interaction of two particles, at least one of which is in a closed l shell, retains the same simple structure as (3.50) and (3.55), with the average interaction simply being replaced by the like or unlike force. For the case of identical proton and neutron wave functions, (3.62) and (3.58) reduce identically to (3.50) and (3.55), since $2V^{\rm lk}+2V^{\rm un}=4V^{\rm av}$ and

$$\sum_{j=l-1/2}^{l+1/2}(2j+1)=2(2l+1).$$

In order to compute the potential energy contribution of two particles in the closed j shells, $j=l+\frac{1}{2}$ and $j'=l'+\frac{1}{2}$, with the levels $l-\frac{1}{2}$ and $l'-\frac{1}{2}$ completely empty, it is necessary to evaluate $(VP)_{\rm dir}$ and $(VP)_{\rm ex}$ in (3.62). To show that $(VP)_{\rm dir}=0$, it is convenient to define

$$G(m_lm_l';n_ln_l')=\sum_{mm'm_sm_s'}\begin{pmatrix}\frac{1}{2} & l & j\\ m_s & m_l & -m\end{pmatrix}\begin{pmatrix}\frac{1}{2} & l' & j'\\ m_s' & m_l' & -m'\end{pmatrix}$$
$$\times\left[\begin{pmatrix}\frac{1}{2} & l & j\\ m_s' & n_l & -m\end{pmatrix}\begin{pmatrix}\frac{1}{2} & l' & j'\\ m_s & n_l' & -m'\end{pmatrix}-\frac{1}{2}\begin{pmatrix}\frac{1}{2} & l & j\\ m_s & n_l & -m\end{pmatrix}\begin{pmatrix}\frac{1}{2} & l' & j'\\ m_s' & n_l' & -m'\end{pmatrix}\right]. \quad (3.68)$$

Then,

$$G(m_l-n_l';n_l-m_l')=\sum_{mm'm_sm_s'}\begin{pmatrix}\frac{1}{2} & l & j\\ m_s & m_l & -m\end{pmatrix}\begin{pmatrix}\frac{1}{2} & l' & j'\\ m_s' & -n_l' & -m'\end{pmatrix}$$
$$\times\left[\begin{pmatrix}\frac{1}{2} & l & j\\ m_s' & n_l & -m\end{pmatrix}\begin{pmatrix}\frac{1}{2} & l' & j'\\ m_s & -m_l' & -m'\end{pmatrix}-\frac{1}{2}\begin{pmatrix}\frac{1}{2} & l & j\\ m_s & n_l & -m\end{pmatrix}\begin{pmatrix}\frac{1}{2} & l' & j'\\ m_s' & -m_l' & -m'\end{pmatrix}\right], \quad (3.69)$$

and in both cases, the second term is

$$\delta_{n_l m_l}\delta_{n_l' m_l'}/\left(2(2l+1)(2l'+1)\right). \tag{3.70}$$

Since we only consider the lower level in a spin-orbit doublet, the only 3-j symbols which are required are

$$\begin{pmatrix} \frac{1}{2} & l & (l+\frac{1}{2}) \\ \frac{1}{2} & n & (-\frac{1}{2}-n) \end{pmatrix} = (-1)^{l+n+1}\left[(l+n+1)/(2l+2)(2l+1)\right]^{1/2} \tag{3.71}$$

and

$$\begin{pmatrix} \frac{1}{2} & l & (l+\frac{1}{2}) \\ -\frac{1}{2} & n & (\frac{1}{2}-n) \end{pmatrix} = (-1)^{l+n}\,|\,(l-n+1)/(2l+2)(2l+1)\,|^{1/2}. \tag{3.72}$$

We first consider the case $m' \neq n'$. Then,

$$G(m_l m_l'; n_l n_l') - G(m_l - n_l'; n_l - m_l') = \sum_{mm' m_s m_s'} \begin{pmatrix} \frac{1}{2} & l & j \\ m_s & m_l & -m \end{pmatrix}\begin{pmatrix} \frac{1}{2} & l & j \\ m_s' & n_l & -m \end{pmatrix}$$
$$\times\left[\begin{pmatrix} \frac{1}{2} & l' & j' \\ m_s' & m_l' & -m' \end{pmatrix}\begin{pmatrix} \frac{1}{2} & l' & j' \\ m_s & n_l' & -m' \end{pmatrix} - \begin{pmatrix} \frac{1}{2} & l' & j' \\ m_s' & -n_l' & -m' \end{pmatrix}\begin{pmatrix} \frac{1}{2} & l' & j' \\ m_s & -m_l' & -m' \end{pmatrix}\right]. \tag{3.73}$$

From the fact that the m's in each 3-j symbol must sum to zero, it is clear that for nonzero contributions to (3.73), $m_s' \neq m_s$ and $m_l' = n_l' \pm 1$. Using (3.71) and (3.72),

$$G(m_l m_l'; n_l n_l') - G(m_l - n_l'; n_l - m_l') = 0. \tag{3.74}$$

Defining

$$f(m_l m_l'; n_l n_l') = Y_{lm_l}^*(\Omega_1)\, Y_{l'm_l'}^*(\Omega_2)\, Y_{ln_l}(\Omega_1)\, Y_{l'n_l'}(\Omega_2), \tag{3.75}$$

it follows from the properties of the spherical harmonics and the fact that $m_l' = n_l' \pm 1$ that

$$\begin{aligned} f(m_l m_l'; n_l n_l') &= (-1)^{n_l' + m_l'} f(m_l - n_l'; n_l - m_l') \\ &= -f(m_l - n_l'; n_l - m_l'). \end{aligned} \tag{3.76}$$

Thus, we obtain

$$f(m_l m_l'; n_l n_l') G(m_l m_l'; n_l n_l') + f(m_l - n_l'; n_l - m_l') G(m_l - n_l'; n_l - m_l') = 0. \tag{3.77}$$

Now consider $m_l' = n_l'$ which requires $m_s' = m_s$ and $n_l = m_l$ for nonzero contributions to G. Then,

$$G(m_l m_l'; m_l m_l') = \sum_{mm' m_s} \begin{pmatrix} \frac{1}{2} & l & j \\ m_s & m_l & -m \end{pmatrix}\begin{pmatrix} \frac{1}{2} & l' & j' \\ m_s & m_l' & -m' \end{pmatrix}\begin{pmatrix} \frac{1}{2} & l & j \\ m_s & m_l & -m \end{pmatrix}\begin{pmatrix} \frac{1}{2} & l' & j' \\ m_s & m_l' & -m' \end{pmatrix}$$
$$-\left[2(2l+1)(2l'+1)\right]^{-1}$$
$$= \frac{2(l+1)(l'+1) + 2m_l m_l'}{(2l+1)(2l+2)(2l'+1)(2l'+2)} - \left[2(2l+1)(2l'+1)\right]^{-1}, \tag{3.78}$$

so that

$$G(m_l m_l'; m_l m_l') + G(m_l - m_l'; m_l - m_l') = 0. \tag{3.79}$$

Noting that $f(m_l m_l'; m_l m_l') = f(m_l - m_l'; m_l - m_l')$, we again obtain

$$f(m_l m_l'; m_l m_l') G(m_l m_l'; m_l m_l') + f(m_l - m_l'; m_l - m_l') G(m_l - m_l'; m_l - m_l') = 0. \tag{3.80}$$

Thus, we have demonstrated that (3.76) is true, in general, so that the sum over m_l, m_l', n_l, and n_l' in (3.63) yields identically zero.

It is indeed fortunate that $(VP)_{\text{dir}}$ gives zero contribution since otherwise it would have been necessary to Legendre-expand the direct interaction. However, it has already been necessary to expand the exchange interaction so it is no further complication to evaluate $(VP)_{\text{ex}}$ in general. Using (3.51), (3.52), and (3.53) as before, we may rewrite $(VP)_{\text{ex}}$ as

$$(VP)_{\text{ex}} = \frac{1}{4}\int dr_1 \int dr_2 (2j+1)(2j'+1) R_{nl}(r_1) R_{n'l'}(r_1) R_{nl}(r_2) R_{n'l'}(r_2)$$
$$\times \sum_k \begin{pmatrix} l & l' & k \\ 0 & 0 & 0 \end{pmatrix}^2 V_k(r_1, r_2)(-b-\delta_\tau) X(ljl'j'k), \tag{3.81}$$

where

$$X(ljl'j'k)=\sum_{mm'm_lm_l'm_s,m_s'n_ln_l'm''}(-1)^{m_l+m_l'+m''}(2l+1)(2l'+1)$$
$$\times\begin{pmatrix} l' & l & k\\ -m_l' & n_l & m''\end{pmatrix}\begin{pmatrix} l & l' & k\\ -m_l & n_l' & -m''\end{pmatrix}\begin{pmatrix} \frac{1}{2} & l & j\\ m_s & m_l & -m\end{pmatrix}\begin{pmatrix} \frac{1}{2} & l' & j'\\ m_s' & m_l' & -m'\end{pmatrix}$$
$$\times\left[\begin{pmatrix} \frac{1}{2} & l & j\\ m_s' & n_l & -m\end{pmatrix}\begin{pmatrix} \frac{1}{2} & l' & j'\\ m_s & n_l' & -m'\end{pmatrix}-\frac{1}{2}\begin{pmatrix} \frac{1}{2} & l & j\\ m_s & n_l & -m\end{pmatrix}\begin{pmatrix} \frac{1}{2} & l' & j'\\ m_s' & n_l' & -m'\end{pmatrix}\right].$$

$X(ljl'j'k)$ may be most easily evaluated using identities involving 6-j and 9-j symbols.[51] Simplifying the first term in X, we obtain

$$\sum_{mm'm_lm_l'm_s,m_s'n_ln_l'm''}(-1)^{m_l+m_l'+m''}\begin{pmatrix} l' & l & k\\ -m_l' & n_l & m''\end{pmatrix}\begin{pmatrix} l & l' & k\\ -m_l & n_l' & -m''\end{pmatrix}\begin{pmatrix} \frac{1}{2} & l & j\\ m_s & m_l & -m\end{pmatrix}$$
$$\times\begin{pmatrix} \frac{1}{2} & l' & j'\\ m_s' & m_l' & -m'\end{pmatrix}\begin{pmatrix} \frac{1}{2} & l & j\\ m_s' & n_l & -m\end{pmatrix}\begin{pmatrix} \frac{1}{2} & l' & j'\\ m_s & n_l' & -m'\end{pmatrix}$$
$$=\sum_{m_lm_l',n_ln_l'm''}(-1)^{m_l+m_l'+m''}\begin{pmatrix} l' & l & k\\ -m_l' & n_l & m''\end{pmatrix}\begin{pmatrix} l & l' & k\\ -m_l & n_l' & -m''\end{pmatrix}\left[\sum_{mm',m_sm_s'}\begin{pmatrix} l & j & \frac{1}{2}\\ m_l & -m & m_s\end{pmatrix}\right.$$
$$\left.\times\begin{pmatrix} l' & \frac{1}{2} & j'\\ m_l' & m_s' & -m'\end{pmatrix}\begin{pmatrix} j & \frac{1}{2} & l\\ -m & m_s' & n_l\end{pmatrix}\begin{pmatrix} \frac{1}{2} & j' & l'\\ m_s & -m' & n_l'\end{pmatrix}\right]$$
$$=\sum_{m_lm_l'n_ln_l',m''X\gamma}(-1)^{m_l+m_l'+m''}\begin{pmatrix} l' & l & k\\ -m_l' & n_l & m''\end{pmatrix}\begin{pmatrix} l & l' & k\\ -m_l & n_l' & -m''\end{pmatrix}(2X+1)$$
$$\times\begin{pmatrix} l & l' & X\\ m_l & m_l' & \gamma\end{pmatrix}\begin{pmatrix} X & l & l'\\ \gamma & n_l & n_l'\end{pmatrix}\begin{Bmatrix} l & l' & X\\ j & \frac{1}{2} & l\\ \frac{1}{2} & j' & l'\end{Bmatrix}$$
$$=\sum_X(2X+1)\left[\sum_{m_lm_l'\gamma,n_ln_l'm''}(-1)^{m_l+m_l'+m''+l+l'+k}\begin{pmatrix} l & X & l'\\ n_l & \gamma & n_l'\end{pmatrix}\begin{pmatrix} l & k & l'\\ n_l & m'' & -m_l'\end{pmatrix}\right.$$
$$\left.\times\begin{pmatrix} l & X & l'\\ m_l & \gamma & m_l'\end{pmatrix}\begin{pmatrix} l & k & l'\\ -m_l & -m'' & n_l'\end{pmatrix}\right]\begin{Bmatrix} l & l' & X\\ j & \frac{1}{2} & l\\ \frac{1}{2} & j' & l'\end{Bmatrix}$$
$$=\sum_X(2X+1)\begin{Bmatrix} l & X & l'\\ l & k & l'\end{Bmatrix}\begin{Bmatrix} l & l' & X\\ j & \frac{1}{2} & l\\ \frac{1}{2} & j' & l'\end{Bmatrix}$$
$$=(-1)^{2k}\begin{Bmatrix} j & \frac{1}{2} & l\\ l' & k & j'\end{Bmatrix}\begin{Bmatrix} \frac{1}{2} & j' & l'\\ k & l & j\end{Bmatrix}=\begin{Bmatrix} k & l & l'\\ \frac{1}{2} & j' & j\end{Bmatrix}^2. \tag{3.82}$$

[51] M. Rotenberg, R. Bivins, N. Metropolis, and J. Wooten, *The 3-j and 6-j Symbols* (Technology Press, Cambridge, Mass., 1959), Eqs. (3.21), (2.18), (3.22), and (2.16).

Since we consider only the case $j'=l'+\frac{1}{2}$, $j=l+\frac{1}{2}$, we may evaluate this explicitly,

$$\begin{Bmatrix} k & l & l' \\ \frac{1}{2} & (l'+\frac{1}{2}) & (l+\frac{1}{2}) \end{Bmatrix}^2 = \frac{(k+l+l'+2)(l+l'-k+1)}{(2l+1)(2l'+1)(2l+2)(2l'+2)}. \tag{3.83}$$

The second term in X is trivial since the 3-j symbols immediately reduce by orthogonality,

$$\sum_{mm'm_lm_l'm_s,m_s'n_ln_l'm''} \tfrac{1}{2}(-1)^{m_l+m_l'+m''} \begin{pmatrix} l' & l & k \\ -m_l' & n_l & m'' \end{pmatrix} \begin{pmatrix} l & l' & k \\ -m_l & n_l' & -m'' \end{pmatrix} \begin{pmatrix} \frac{1}{2} & l & j \\ m_s & m_l & -m \end{pmatrix}$$
$$\begin{pmatrix} \frac{1}{2} & l' & j' \\ m_s' & m_l' & -m' \end{pmatrix} \begin{pmatrix} \frac{1}{2} & l & j \\ m_s & n_l & -m \end{pmatrix} \begin{pmatrix} \frac{1}{2} & l' & j' \\ m_s' & n_l' & -m' \end{pmatrix}$$
$$= \sum_{m_lm_l',n_ln_l'm''} -\tfrac{1}{2}(-1)^{m_l+m_l'+m''} \begin{pmatrix} l' & l & k \\ -m_l' & n_l & m'' \end{pmatrix} \begin{pmatrix} l & l' & k \\ -m_l & n_l' & -m'' \end{pmatrix} \delta_{m_ln_l}\delta_{m_l'n_l'}/[(2l+1)(2l'+1)]$$
$$= -1/[2(2l+1)(2l'+1)]. \tag{3.84}$$

Thus,

$$X(ljl'j'k) = (k+l+l'+2)(l+l'-k+1)/[(2+2)(2l'+2)]-\tfrac{1}{2}$$
$$= [l(l+1)+l'(l'+1)-k(k+1)]/[4(l+1)(l'+1)]. \tag{3.85}$$

Hence, the contributions from particles in the closed j shells $j=l+\frac{1}{2}$ and $j'=l'+\frac{1}{2}$ may be treated exactly by replacing each term in the Legendre expansion of (3.66) by

$$\tfrac{3}{8}(1-\delta_r)V_{\mathrm{TE}}+\tfrac{1}{8}(1+\delta_r)V_{\mathrm{SE}}-\tfrac{3}{8}(1+\delta_r)V_{\mathrm{TO}}-\tfrac{1}{8}(1-\delta_r)V_{\mathrm{SO}}+X(ljl'j'k)$$
$$\times[\tfrac{1}{4}(1-\delta_r)V_{\mathrm{TE}}+\tfrac{1}{4}(-1-\delta_r)V_{\mathrm{SE}}+\tfrac{1}{4}(-1-\delta_r)V_{\mathrm{TO}}+\tfrac{1}{4}(1-\delta_r)V_{\mathrm{SO}}]. \tag{3.86}$$

Since we have shown that $(VP)_{\mathrm{dir}}=0$ and that the short-range part of the exchange force is equivalent to a short-range direct force, the additional term in (3.86) must not contribute at short range. This fact may be explicitly verified by noting that the kth term in the Legendre expansion of a δ-function force is proportional to $(2k+1)$, and explicit evaluation yields

$$\sum_k (2k+1) \begin{pmatrix} l & l' & k \\ 0 & 0 & 0 \end{pmatrix}^2 X(ljl'j'k)=0. \tag{3.87}$$

For computational convenience, since only the long-range part of the second factor contributes and the spin-unsaturated contribution is only a small part of the total potential, it is reasonable to approximate the force in the second term of (3.86) by a multiplicative constant times the first term. For the case of like particles, since V_{SE} is much greater than V_{TO} beyond 1 F, the constant is approximately -2. For unlike particles, it is necessary to compute an average over the region from 0.75 to 2 F, with the result being -0.4. Thus, our final result for the effective exchange contribution is to multiply each term in the Legendre expansion of (3.66) by

$$1-(0.4+1.6\delta_r)X(ljl'j'k). \tag{3.88}$$

Spin-Orbit Force

The effect of the two-body spin-orbit force is approximated by a one-body spin-orbit potential. Following the approach of Blin-Stoyle,[52] as recently elaborated upon by Scheerbaum,[53] the first term in the expansion of the contribution of the two-body force from a spin-saturated core may be written

$$V_{\mathrm{SO}}(r)=F4\pi(1/r)(d\rho/dr)\mathbf{l}\cdot\boldsymbol{\sigma}, \tag{3.89}$$

where F is a constant to be determined. This expression may be roughly related to the usual Thomas term $(1/r)(dV/dr)$ by noting that the effective single-particle potential described in the next chapter has approximately the same shape as the density and that in the interior of a nucleus, where the density is about 0.17 F^{-3}, the single-particle potential is roughly 50 MeV. Then, various determinations[54–59] of the coeffi-

[52] R. J. Blin-Stoyle, Phil. Mag. **46**, 973 (1955).
[53] R. Scheerbaum, thesis, Cornell University (unpublished).
[54] L. A. Sliv and B. A. Volchok, Zh. Eksperim. i Teor. Fiz. **36**, 539 (1959) [English transl.: Soviet Phys—JETP **9**, 374 (1959)].
[55] A. A. Ross, H. Mark, and R. D. Lawson, Phys. Rev. **102**, 1613 (1956).
[56] I. I. Levintov, Zh. Eksperim. i Teor. Fiz. **30**, 987 (1956) [English transl.: Soviet Phys.—JETP **3**, 796 (1956)].
[57] S. Fernbach, Rev. Mod. Phys. **30**, 414 (1958).
[58] J. Blomqvist and S. Wahlborn, Arkiv Fysik **16**, 545 (1960).
[59] A. E. S. Green, Phys. Rev. **99**, 1410 (1955).

cient of the Thomas term specify that F is approximately 6–9 MeV·F[5].

For the present application we shall select F to reproduce the correct spin-orbit splitting for the d and f states in calcium. From the reaction data cited by Elton and Swift,[60] the $d_{3/2}$-$d_{5/2}$ splitting in Ca^{40} is 7.2 MeV for protons and 6.3 MeV for neutrons. Requiring that (3.89) reproduce the average splitting of 6.75 with our self-consistent Ca^{40} wave functions yields $F=5.9$. Since the central force contribution to the spin-orbit splitting of unsaturated shells is included in (3.88), it is clear that (3.89) should only reproduce the spin-orbit contribution of the spin-saturated core. Hence, we should require F to reproduce the $f_{5/2}$-$f_{7/2}$ splitting in Ca^{40} rather than in Ca^{48}. The neutron data presented by Elton and Swift are unfortunate in that the $f_{7/2}$ level is obtained from binding energies whereas the $f_{5/2}$ level is obtained from (d, p), so that allowing for rearrangement energy, one may only conclude that the spin-orbit splitting is greater than 5.5 MeV. Hence, we shall use the stripping data of Cohen *et al.*,[36] which specifies the $f_{5/2}$-$f_{7/2}$ splitting in Ca^{41} to be 6.5 MeV. Using the self-consistent Ca^{40} wave functions, this splitting corresponds to $F=5.8$.

In order to check the consistency of adjusting the spin-orbit force from experimental data with our use of the effective interaction elsewhere in this calculation, it is useful to compare the spin-orbit splitting computed from matrix elements using the full effective interaction, Eqs. (2.25) and (2.33), with the experimental splitting. Considering the interaction of the $f_{5/2}$ and $f_{7/2}$ levels with the Ca^{40} core, the lowest-order contribution of the two-body effective interaction to the single-particle energy is

$$V_a=(2[2j+1])^{-1}\sum_{JTh}(2T+1)(2J+1)\times\langle ahJT\,|\,V\,|\,ahJT\rangle, \quad (3.90)$$

where a is $0f_{7/2}$ or $0f_{5/2}$ and h is summed over $0s_{1/2}$, $0p_{1/2}$, $0p_{3/2}$, $0d_{3/2}$, $0d_{5/2}$, and $1s_{1/2}$. Using $\hbar\omega=11.6$, which roughly reproduces the density distribution of the core wave functions, and using the self-consistent single-particle energies reported in Table IX in the on-energy-shell starting energies, the potential contribution to the $f_{5/2}$-$f_{7/2}$ spin-orbit splitting in Ca^{40} is 6.1 MeV. This theoretical result from the full effective interaction is in very good agreement with the experimental result of 6.5 MeV. Thus, using (3.89) with $F=6$ is not simply an *ad hoc* fit to experiment, but may be viewed as a reasonable approximation to the actual spin-orbit contribution of the effective interaction. Since the coefficient of the Thomas spin-orbit potential has been shown to be relatively constant throughout the Periodic Table,[54–59] and we have already demonstrated that (3.89) is roughly equivalent to the Thomas potential, we shall use $F=6$ for all nuclei.

Coulomb Interaction

The Coulomb interaction may be included trivially in our treatment because of the Legendre expansion

$$1/r_{12}=\sum_{l=0}^{\infty}(r_<^l/r_>^{l+1})P_l\cos(\omega_{12}). \quad (3.91)$$

It will be convenient to treat average neutron and proton wave functions for some calculations so that each particle with an average wave function has effective charge $\frac{1}{2}$. Then, using the statistical factors for the average force,

$$V_{\rm dir}^{\rm Coul}=(\tfrac{3}{8}+\tfrac{5}{8})(e/2)^2/r_{12}=0.3600/r_{12},$$
$$V_{\rm ex}^{\rm Coul}=(\tfrac{3}{8}-\tfrac{5}{8})(e/2)^2/r_{12}=-0.0900/r_{12}. \quad (3.92)$$

The Coulomb interaction between a proton and an average charge $\frac{1}{2}$ particle is twice (3.92). For the true Coulomb force between two protons, using (3.14) and (3.86),

$$V_{\rm dir}^{\rm Coul}=(\tfrac{1}{4}+\tfrac{3}{4})e^2/r_{12}=1.440/r_{12},$$
$$V_{\rm ex}^{\rm Coul}=(\tfrac{1}{4}-\tfrac{3}{4})e^2/r_{12}=-0.720/r_{12} \qquad \text{for an } l \text{ shell},$$
$$V_{\rm ex}^{\rm Coul}=\sum_k[(\tfrac{1}{4}-\tfrac{3}{4})+(-\tfrac{1}{2}-\tfrac{1}{2})X(ljl'j'k)]e^2(1/r_{12})_{(k)}$$
$$=-0.72\sum_k[1+2X(ljl'j'k)](r_<^k/r_>^{k+1}) \qquad \text{for a } j \text{ shell}. \quad (3.93)$$

Simplified Notation

Before performing the variation of the lowest-order energy expression $\langle E\rangle$, it is desirable to streamline our notation so that the above results of the angular-momentum reduction are implicitly included in simple notation. Hence, we let i represent the quantum numbers $\{n, l\}$ for closed l shells, and $\{n, l, j=l+1\}$ for closed j shells. We define

$$u_i^{(N,P)}(1)=[(2l+1)2]^{1/2}R_{nl}^{(N,P)}(r_1)/[(4\pi)^{1/2}r_1] \qquad \text{if } i \text{ is an } l \text{ shell}$$
$$=[2j+1]^{1/2}R_{nl}^{(N,P)}(r_1)/[(4\pi)^{1/2}r_1] \qquad \text{if } i \text{ is a } j \text{ shell} \quad (3.94)$$

[60] L. R. B. Elton and A. Swift, Nucl. Phys. **A94**, 52 (1967).

for both neutrons and protons. Since we will consider equivalent neutrons and protons of average charge $\frac{1}{2}$ only in closed l shells, we define

$$u_i^{\rm av}(1)=[4(2l+1)]^{1/2}R_{nl}^{\rm av}(r_1)/([4\pi]^{1/2}r_1). \tag{3.95}$$

Finally, it is useful to let I represent i and the charge state, N, P, or av, and to let q_I be 0, 1, or $\frac{1}{2}$ for each charge state, respectively. Then, we may write

$$E=\sum_I \int u_I(1)T_I(1)u_I(1)d\tau_1+\tfrac{1}{2}\sum_{II'}\int\int [u_I^2(1)u_{I'}^2(2)V(r_1,r_2)+u_I(1)u_{I'}(1)u_I(2)u_{I'}(2)\tilde{V}(r_1,r_2)]d\tau_1 d\tau_2, \tag{3.96}$$

where

$$T_I=-r_1(\hbar^2/2m)[\partial^2/\partial r_1^2-l(l+1)/r_1^2]r_1 \qquad \text{if } I \text{ is an } l \text{ shell}$$

$$=-r_1(\hbar^2/2m)[\partial^2/\partial r_1^2-l(l+1)/r_1^2]r_1+6(4\pi)(l/r_1)(d\rho/dr)(r_1) \qquad \text{if } I \text{ is a } j \text{ shell},$$

$$V=V_{S(0)}^{(\rm lk,un,av)}(r_1,r_2)+V_{{\rm dir}(0)}^{(\rm lk,un,av)}(r_1,r_2)+q_Iq_{I'}1.44/r_>,$$

$$\tilde{V}=\sum_k \begin{pmatrix} l & l' & k \\ 0 & 0 & 0 \end{pmatrix}^2 [-(\delta_{q_Iq_{I'}}\delta_{q_I1}+q_Iq_{I'})0.36r_<^k/r_>^{k+1}(1+2X(ljl'j'k))$$

$$+V_{{\rm ex}(k)}^{(\rm lk,un,av)}(r_1,r_2)\{1-(0.4+1.6\delta_\tau)X(ljl'j'k)\}],$$

$$V_{(k)}^{(\rm lk,un,av)}=v_{(k)}^{\rm lk} \qquad \text{if } I, I' \text{ are both } P \text{ or both } N$$

$$=v_{(k)}^{\rm un}+\Delta v^{\rm un}(W) \qquad \text{if one is } P \text{ and the other is } N$$

$$=v_{(k)}^{\rm av}+\Delta v^{\rm un}(W)/2 \qquad \text{otherwise},$$

$$X(ljl'j'k)=0 \quad \text{unless } I \text{ and } I' \text{ are } j \text{ shells},$$

and

$$d\tau_1=d^3r_1.$$

To further simplify notation, it is convenient to define

$$\rho^P(1)=\sum_i (u_i^P(1))^2, \qquad \rho^P(1,2)=\sum_i u_i^P(1)u_i^P(2), \tag{3.97}$$

and similarly for neutrons and average particles, bearing in mind that these are mutually exclusive categories. In addition, we define

$$\rho(1)=\rho^{\rm av}(1)+\rho^P(1)+\rho^N(1),$$

$$\rho(1,2)=\rho^{\rm av}(1,2)+\rho^P(1,2)+\rho^N(1,2), \tag{3.98}$$

and

$$\Delta\rho(1)=\rho^N(1)-\rho^P(1),$$

$$\Delta\rho(1,2)=\rho^N(1,2)-\rho^P(1,2). \tag{3.99}$$

Thus far, we have not explicitly written out the k_F dependence of the effective interaction. It is most convenient to write

$$V_0(r_1,r_2)+V_1(r_1,r_2)\rho^\alpha(R), \tag{3.100}$$

where now $\alpha=\frac{1}{3}$ times the exponent associated with k_F in (3.24), V_1 is $(\frac{3}{2}\pi^2)$ times the density-dependent term in (3.24), and $\rho(R)$ is evaluated at the c.m. point $\mathbf{R}=(\mathbf{r}_1+\mathbf{r}_2)/2$ and corresponds to the appropriate k_F. Rather than explicitly writing $\alpha=1$ for the short-range force and $\alpha=\frac{1}{3}$ for the direct and exchange forces, we shall carry out the general derivation with α.

For the case of interaction between like particles, clearly the appropriate $\rho(R)$ in (3.100) is the density corresponding to the local k_F for that particular kind of particle. Because of our normalization relating k_F to ρ, the appropriate $\rho(R)$ for two protons is twice the local proton density so that, in terms of the quantities defined in (3.98) and (3.99), this density is $\rho^{\rm av}(R)+2\rho^P(R)$ or, alternatively, $\rho(R)-\Delta\rho(R)$. Similarly, for neutrons we obtain $\rho^{\rm av}(R)+2\rho^N(R)$ or $\rho(R)+\Delta\rho(R)$.

Variation

For the interaction between unlike particles, our parametrization of the density dependence is incapable of treating the true dependence on both neutron and proton density exactly. Instead, we approximate the complicated dependence on both neutron and proton densities by setting $\rho(R)$ in (3.100) equal to the total density. This is a reasonable approximation for the density dependence arising from the Pauli operator since it approximates the exclusion of two Fermi spheres of unequal radii by that from equal Fermi spheres which exclude the same volume. It is not physically obvious that the density dependence arising from self-consistent starting energies should be accurately reproduced by this approximation, but the detailed calculations by Siemens[20] for unequal proton and neutron densities show that this approximation is quite adequate.

Thus, in general, we may write

$$\langle E\rangle=\int d\tau_1\sum_I u_I(1)T_I u_I(1)+\tfrac{1}{2}\iint d\tau_1 d\tau_2\{[\rho^{\rm av}(1)/2][\rho^{\rm av}(2)/2]$$
$$\times[V_0{}^{\rm lk}+V_1{}^{\rm lk}(\rho^{\rm av}(R)+2\rho^N(R))^\alpha+2\{V_0{}^{\rm un}+V_1{}^{\rm un}(\rho^{\rm av}(R)+\rho^P(R)+\rho^N(R))^\alpha\}+V_0{}^{\rm lk}+V_1{}^{\rm lk}(\rho^{\rm av}(R)+2\rho^P(R))^\alpha]$$
$$+2[\rho^{\rm av}(1)/2]\rho^N(2)[V_0{}^{\rm lk}+V_1{}^{\rm lk}(\rho^{\rm av}(R)+2\rho^N(R))^\alpha+V_0{}^{\rm un}+V_1{}^{\rm un}(\rho^{\rm av}(R)+\rho^P(R)+\rho^N(R))^\alpha]$$
$$+2[\rho^{\rm av}(1)/2]\rho^P(2)[V_0{}^{\rm lk}+V_1{}^{\rm lk}(\rho^{\rm av}(R)+2\rho^P(R))^\alpha+V_0{}^{\rm un}+V_1{}^{\rm un}(\rho^{\rm av}(R)+\rho^P(R)+\rho^N(R))^\alpha]$$
$$+\rho^N(1)\rho^N(2)[V_0{}^{\rm lk}+V_1{}^{\rm lk}(\rho^{\rm av}(R)+2\rho^N(R))^\alpha]+\rho^P(1)\rho^P(2)[V_0{}^{\rm lk}+V_1{}^{\rm lk}(\rho^{\rm av}(R)+2\rho^P(R))^\alpha]$$
$$+2\rho^P(1)\rho^N(2)[V_0{}^{\rm un}+V_1{}^{\rm un}(\rho^{\rm av}(R)+\rho^P(R)+\rho^N(R))^\alpha]\}+\text{exchange}, \quad (3.101)$$

where the exchange term is analogous to the direct term with $\rho(1)$ and $\rho(2)$ being replaced by $\rho(1,2)$ and V being replaced by $\tilde{V}$. Rewriting (3.101) in terms of ρ and $\Delta\rho$, expanding $(\rho\pm\Delta\rho)^\alpha$ through second order, and simplifying,

$$\langle E\rangle=\langle T\rangle+\tfrac{1}{2}\iint d\tau_1 d\tau_2\{\rho(1)\rho(2)[V_0{}^{\rm av}+V_1{}^{\rm av}\rho^\alpha(R)+(\alpha(\alpha-1)/4)V_1{}^{\rm lk}(\Delta\rho(R))^2\rho^{\alpha-2}(R)]$$
$$+\rho(1)\Delta\rho(2)V_1{}^{\rm lk}\alpha\Delta\rho(R)\rho^{\alpha-1}(R)+\tfrac{1}{2}\Delta\rho(1)\Delta\rho(2)[V_0{}^{\rm lk}-V_0{}^{\rm un}+(V_1{}^{\rm lk}-V_1{}^{\rm un})\rho^\alpha(R)]\}+\text{exchange}. \quad (3.102)$$

We now consider variation of a direct term of the form

$$\iint d\tau_1 d\tau_2\rho(1)\rho(2)V\rho^\alpha(R). \quad (3.103)$$

Varying u_i in both $\rho(1)$ and $\rho(2)$ leads to the HF contribution

$$2\int d^3r_1\delta u_i(r_1)\int d^3r_2\rho(r_2)$$
$$\times V(|\mathbf{r}_1-\mathbf{r}_2|)\rho^\alpha(\tfrac{1}{2}|\mathbf{r}_1+\mathbf{r}_2|)u_i(r_1). \quad (3.104)$$

Introducing new variables $\mathbf{R}=\mathbf{r}_1$ and $\mathbf{r}=\mathbf{r}_2-\mathbf{r}_1$, this may be written

$$2\int d^3R_1\delta u_i(R)\int d^3r\rho(|\mathbf{R}+\mathbf{r}|)$$
$$\times V(r)\rho^\alpha(|\mathbf{R}+\tfrac{1}{2}\mathbf{r}|)u_i(R). \quad (3.105)$$

To vary u_i in ρ^α, we write (3.103) in terms of the variables $\mathbf{r}=\mathbf{r}_1-\mathbf{r}_2$ and $\mathbf{R}=(\mathbf{r}_1+\mathbf{r}_2)/2$. Then, (3.103) becomes

$$\iint d^3r d^3R\rho(|\mathbf{R}+\tfrac{1}{2}\mathbf{r}|)\rho(|\mathbf{R}-\tfrac{1}{2}\mathbf{r}|)V(r)\rho^\alpha(R) \quad (3.106)$$

and variation of u_i in ρ^α yields the rearrangement contribution

$$\int d^3R\delta u_i(R)\int d^3r\rho(|\mathbf{R}+\tfrac{1}{2}\mathbf{r}|)\rho(|\mathbf{R}-\tfrac{1}{2}\mathbf{r}|)$$
$$\times V(r)\alpha\rho^{\alpha-1}(R)u_i(R). \quad (3.107)$$

Because of the similarity of the integrals in (3.105) and (3.107), we approximate the rearrangement contribution by $\alpha/2$ times the HF contribution. This approximation may be justified quantitatively by considering a plane surface with the density varying only in the z direction, and expanding the densities in (3.105) and (3.107) in powers of z about R. For the most significant contributions from V_S, r is 0.5 F, and for $V_{\rm dir}$, r is roughly 1.5 F. Integrating over angles, the terms linear in z do not contribute, and $\int(d\Omega/4\pi)z^2=r^2/3$, so that the most significant contributions from V_S occur for $z^2=0.21$ and those from $V_{\rm dir}$ occur for $z^2=0.75$. The difference in values for z^2 roughly compensates the fact that $\alpha=1$ for the short-range force and $\frac{1}{3}$ for the direct force. Explicitly evaluating the error in this approximation to the rearrangement term at the half-density point of the one-dimensional surface, taking $d\rho/dz$ from electron scattering, we find that the error is less than 1% of the HF contribution from the density-independent component of the force V_0.

This approximation serves as a prototype of the approximation we shall make in the rearrangement contribution obtained from varying each direct term in (3.102). To simplify notation, we shall indicate this approximation by

$$\iint d\tau_1 d\tau_2\delta u_i(R)\rho(1)\rho(2)V\alpha\rho^{\alpha-1}(R)u_i(R)$$
$$\sim$$
$$=\iint du_i(1)\rho(2)V\alpha\rho^\alpha(R)u_i(1)d\tau_1 d\tau_2. \quad (3.108)$$

Then, varying u_i in $\rho^{\rm av}$, which contributes to ρ, but not to $\Delta\rho$, we obtain

$$\delta\langle E\rangle=\int d\tau_1\delta u_i(1)\{T_i(1)+\int\rho(2)\{V_0{}^{\rm av}+[V_1{}^{\rm av}+V_1{}^{\rm lk}\tfrac{1}{4}(\alpha(\alpha-1))(\Delta\rho(R)/\rho(R))^2]\rho^\alpha(R)\}d\tau_2$$
$$+\int\Delta\rho(2)V_1{}^{\rm lk}\tfrac{1}{2}\alpha(\Delta\rho(R)/\rho(R))\rho^\alpha(R)d\tau_2+\sim\int\rho(2)\tfrac{1}{2}\alpha V_1{}^{\rm av}\rho^\alpha(R)d\tau_2$$
$$+\sim\int\Delta\rho(2)\{V_1{}^{\rm lk}\tfrac{1}{8}(\alpha(\alpha-1)(\alpha-2))(\Delta\rho(R)/\rho(R))\rho^\alpha(R)+V_1{}^{\rm lk}\tfrac{1}{2}(\alpha(\alpha-1))(\Delta\rho(R)/\rho(R))\rho^\alpha(R)$$
$$+(V_1{}^{\rm lk}-V_1{}^{\rm un})\tfrac{1}{4}\alpha(\Delta\rho(R)/\rho(R))\rho^\alpha(R)\}d\tau_2\}u_i(1)+\text{exchange}. \quad (3.109)$$

Since ρ^N contributes to both ρ and $\Delta\rho$, from (3.98) and (3,99), varying $u_i{}^N$ yields all the terms in (3.109) plus the

additional terms

$$\int d\tau_1 \delta u_i(1) \Big[\int \rho(2) V_1^{\mathrm{lk}} \tfrac{1}{2}\alpha \big(\Delta\rho(R)/\rho(R)\big)\rho^\alpha(R) d\tau_2 + \tfrac{1}{2}\Delta\rho(2)\{V_0^{\mathrm{lk}} - V_0^{\mathrm{un}} + (V_1^{\mathrm{lk}} - V_1^{\mathrm{un}})\rho^\alpha(R)\} d\tau_2$$
$$+ \int \Delta\rho(2)\{V_1^{\mathrm{lk}} \tfrac{1}{4}(\alpha(\alpha-1))\rho^\alpha(R) + V_1^{\mathrm{lk}} \tfrac{1}{2}\alpha\rho^\alpha(R)\} d\tau_2 \Big] u_i(1) + \text{exchange}. \quad (3.110)$$

Similarly, varying u_{ip}, we obtain the terms in (3.109) minus the terms in (3.110).

Finally, the direct term is further simplified by defining f_I as 1 for neutrons, -1 for protons, and zero for average particles. Then, we may treat the three cases above simultaneously by multiplying (3.110) by f_I, and we may write $\rho(2) = \sum_J u_J^2(2)$ and $\Delta\rho(2) = \sum_J f_J u_J^2(2)$. Thus,

$$\delta\langle E\rangle = \int d\tau_1 \delta u_I(1) \Big[T_i(1) + \sum_J \int d\tau_2 u_J^2(2)\{V_0^{\mathrm{av}} + \tfrac{1}{2}(f_I f_J)(V_0^{\mathrm{lk}} - V_0^{\mathrm{un}})$$
$$+ \rho^\alpha(R)\big[V_1^{\mathrm{av}} + \tfrac{1}{2}\alpha V_1^{\mathrm{av}} + \tfrac{1}{2}(f_I f_J)\{(V_1^{\mathrm{lk}} - V_1^{\mathrm{un}}) + V_1^{\mathrm{lk}} \tfrac{1}{2}(\alpha(\alpha+1))\}\big]$$
$$+ \rho^\alpha(R)\big(\Delta\rho(R)/\rho(R)\big)\big[V_1^{\mathrm{lk}} \tfrac{1}{4}(\alpha(\alpha-1))\big(\Delta\rho(R)/\rho(R)\big) + f_J V_1^{\mathrm{lk}}\{\tfrac{1}{2}\alpha + \tfrac{1}{8}(\alpha(\alpha-1)(\alpha+2))\}$$
$$+ f_J(V_1^{\mathrm{lk}} - V_1^{\mathrm{un}})\tfrac{1}{4}\alpha + f_I V_1^{\mathrm{lk}} \tfrac{1}{2}\alpha\big]\Big] u_I(1) + \text{exchange}. \quad (3.111)$$

Recognizing that the single term involving

$$\left(\frac{\Delta\rho(R)}{\rho(R)}\right)^2$$

is very small, we substitute

$$\frac{\Delta\rho(R)}{\rho(R)}\,\frac{(N-Z)}{(N+Z)}.$$

Then, using our effective interaction, all the direct contributions in (3.111) may be written as multiplicative factors times integrals of $u_J^2(2)$ times $V_0^{\mathrm{av}}(r_{12})$, $\Delta V^{\mathrm{un}}(W, r_{12})$, $\rho^\alpha(R) V_1^{\mathrm{av}}(r_{12})$, and

$$\rho^\alpha(R)\,\frac{\Delta\rho(R)}{\rho(R)}\,V_1^{\mathrm{av}}(r_{12}).$$

We now consider variation of an exchange term of the form

$$\tfrac{1}{2}\iint d\tau_1 d\tau_2 \rho^2(1,2)\big(\tilde{V}_0 + \tilde{V}_1\rho^\alpha(R)\big). \quad (3.112)$$

Variation of u_i in the mixed density yields

$$\int d\tau_1 \delta u_i(1) \int d\tau_2 \rho(1,2)\big(\tilde{V}_0 + \tilde{V}_1\rho^\alpha(R)\big) u_i(2). \quad (3.113)$$

Since this is the major contribution of the exchange force, and we have already noted that the exchange interaction is stronger than the direct interaction, we shall use the exact mixed density in (3.113). Varying u_i in $\rho^\alpha(R)$ in (3.112) yields

$$\iint d\tau_1 d\tau_2 \delta u_i(R)\rho^2(1,2)\tfrac{1}{2}\alpha\tilde{V}_1\rho^{\alpha-1}(R) u_i(R). \quad (3.114)$$

Since (3.114) is much smaller than (3.113), and since Lin[39] has shown the Slater approximation to the mixed density to be roughly correct, we shall use the Slater approximation

$$\rho_{\mathrm{SL}}(1,2) = (2/\pi^2)(1/r_{12}^3)(\sin k_F r_{12} - k_F r_{12}\cos k_F r_{12}), \quad (3.115)$$

where

$$k_F = k_F(\rho(R)).$$

Since all the angular-momentum structure of the wave functions has been averaged in ρ_{SL}, only the first term in the Legendre expansion in V_1 contributes. Then, (3.114) has the same structure as the direct contributions to $\delta\langle E\rangle$ and changing integration variables reduces to

$$\int d^3\tau_1 \delta u_i(1)\tfrac{1}{2}\alpha \int d^3\tau_2 \rho_{\mathrm{SL}}^2(r_2, k_F(\rho(r_1)))\tilde{V}_1(r_2) u_i(1). \quad (3.116)$$

For the case in which $\rho^2(1,2)$ in (3.112) is replaced by $\Delta\rho(1,2)\rho(1,2)$ or $\Delta\rho^2(1,2)$, it is no additional difficulty to treat the HF contribution exactly, as above. However, since for realistic neutron excesses, $\Delta\rho(1,2)$ is much smaller than $\rho(1,2)$, we shall introduce an additional simplifying approximation in the rearrangement contribution from these terms. Using the expansion for spherical Bessel functions, we may write

$$\Delta\rho_{\mathrm{SL}}(1,2) = (1/\pi^2)\{{}^N k_F^3\big[1 - \tfrac{1}{10}({}^N k_F r)^2 + \tfrac{1}{280}({}^N k_F r)^4 - \cdots\big] - {}^P k_F^3\big[1 - \tfrac{1}{10}({}^P k_F r)^2 + \tfrac{1}{280}({}^P k_F r)^4 - \cdots\big]\}. \quad (3.117)$$

Requiring that ${}^P k_F^3 + {}^N k_F^3 = 2k_F^3$ as before, we substitute $k_F = k_F \pm x - x^2/k_F + \mathcal{O}(x^3)$ in (3.117) and obtain

$$\Delta\rho_{\mathrm{SL}}(1,2) = \big[({}^N k_F^3 - {}^P k_F^3)/2k_F^3\big](2/\pi^2)k_F^3\big[1 - \tfrac{1}{10}(k_F r)^2\big(\tfrac{5}{3} + \mathcal{O}(x^2)\big) + \tfrac{1}{280}(k_F r)^4\big(\tfrac{7}{3} + \mathcal{O}(x^2)\big) - \cdots\big]$$
$$\approx \big[\Delta\rho(R)/\rho(R)\big]\rho_{\mathrm{SL}}(1,2). \quad (3.118)$$

From Fig. 3, the most significant contribution from V_{ex} occurs around 0.8 F, so that for $k_F = 1.4$ F^{-1}, this approximation underestimates $\Delta\rho(1,2)$ by roughly 10%. Recognizing that rearrangement terms involving $\Delta\rho(1,2)$ or $\Delta\rho^2(1,2)$ are smaller than (3.114) by $(N-Z)/(N+Z)$ or $[(N-Z)/(N+Z)]^2$, and (3.114) is already small compared with (3.112), the absolute error introduced by this approximation is negligible.

Hence, writing the general expression for the variation of any u_I in the exchange contribution to $\langle E\rangle$, using the f_I notation in (3.111), we obtain

$$\begin{aligned}\delta\{\tfrac{1}{2}\int\int d\tau_1 d\tau_2\{\rho^2(1,2)[\tilde V_0^{\rm av}+\tilde V_1^{\rm av}\rho^\alpha(R)+\tfrac{1}{4}(\alpha(\alpha-1))\tilde V_1^{\rm lk}(\Delta\rho(R))^2\rho^{\alpha-2}(R)]\\ +\rho(1,2)\Delta\rho(1,2)\tilde V_1^{\rm lk}\alpha\Delta\rho(R)\rho^{\alpha-1}(R)+\Delta\rho^2(1,2)[\tilde V_0^{\rm lk}-\tilde V_0^{\rm un}+(\tilde V_1^{\rm lk}-\tilde V_1^{\rm un})\rho^\alpha(R)]\}\}\\ =\int d\tau_1\delta u_I(1)\int d\tau_2\sum_J u_J(1)u_J(2)\{\tilde V_0^{\rm av}+\tfrac{1}{2}(f_If_J)(\tilde V_0^{\rm lk}-\tilde V_0^{\rm un})+\rho^\alpha(R)[\tilde V_1^{\rm av}+\tfrac{1}{2}(f_If_J)(\tilde V_1^{\rm lk}-\tilde V_1^{\rm un})]\\ +\rho^\alpha(R)(\Delta\rho(R)/\rho(R))[\tilde V_1^{\rm lk}\tfrac{1}{4}(\alpha(\alpha-1))(\Delta\rho(R)/\rho(R))+(f_J+f_I)\tilde V_1^{\rm lk}\tfrac{1}{2}\alpha]\}u_I(2)\\ +\int d\tau_1\delta u_I(r_1)\int d\tau_2\rho_{\rm SL}^2(r_2,k_F(\rho(r_1)))\tfrac{1}{2}\alpha\rho^{\alpha-1}(r_1)\{\tilde V_1^{\rm av}(r_2)+\tfrac{1}{2}[\tilde V_1^{\rm lk}(r_2)-\tilde V_1^{\rm un}(r_2)](\Delta\rho(r_1)/\rho(r_1))^2\\ +\tilde V_1^{\rm lk}(r_2)[(\alpha-1)\tfrac{1}{4}(\alpha+2)(\Delta\rho(r_1)/\rho(r_1))^2+f_I\tfrac{1}{2}(\alpha+1)(\Delta\rho(r_1)/\rho(r_1))]\}u_I(r_1).\end{aligned}\tag{3.119}$$

Again approximating

$$\left(\frac{\Delta\rho(R)}{\rho(R)}\right)^2$$

by

$$\frac{\Delta\rho(R)}{\rho(R)}\left(\frac{N-Z}{N+Z}\right),$$

the terms in (3.119) involving the true mixed density have structure analogous to (3.111), since they may all be written as multiplicative factors times integrals of $u_I(2)u_J(2)$ times $\tilde V_0^{\rm av}(r_1,r_2)$, $\Delta V^{\rm un}(W,r_1,r_2)$, $\rho^\alpha(R)\tilde V_1^{\rm av}(r_1,r_2)$, and $\rho^\alpha(R)[\Delta\rho(R)/\rho(R)]\tilde V_1^{\rm av}(r_1,r_2)$, where the coefficients of the Legendre expension of the potentials depend on I and J. The additional direct term in (3.119) involving the Slater mixed density may be written as a multiplicative factor times a function of $k_F(\rho(r_1))$.

Finally, the radial equation is obtained in the usual way by introducing Lagrange multipliers times normalization constraint terms and requiring stationarity of $\langle E\rangle$ plus the constraint terms. We write $\delta\langle E\rangle$ as

$$\begin{aligned}\delta\langle E\rangle=&\int d\tau_1\delta u_I(1)\\ &\times\{r_1[(-\hbar^2/2m)(\partial^2/\partial r_1^2)]r_1+\mathfrak{F}_I^D(r_1)\}u_I(1)\\ &+\int d\tau_1\delta u_I(1)\int d\tau_2\mathfrak{F}_I^E(r_1,r_2)(4\pi r_1r_2)^{-1}u_I(2),\end{aligned}\tag{3.120}$$

where $\mathfrak{F}_I^D(r_1)$ and $\mathfrak{F}_I^E(r_1,r_2)$ are defined by (3.111) and (3.119) and the I dependence of $\mathfrak{F}_I^D$ is due to the starting energy dependence, and that of $\mathfrak{F}_I^E$ is due both to the starting energy dependence and the l,j dependence of the coefficients of the Legendre expansion. Rewriting u_I in terms of R_I, we obtain the radial equation,

$$\begin{aligned}&-(\hbar^2/2m)(d^2R_I/dr_2)+\mathfrak{F}_I^D(r_1)R_I(r_1)\\ &\quad+\int dr_2\mathfrak{F}_I^E(r_1,r_2)R_I(r_2)=E_IR_I(r_1).\end{aligned}\tag{3.121}$$

Starting Energy

Thus far, we have not explicitly specified the starting energies which appear in $\mathfrak{F}^D$ and $\mathfrak{F}^E$ through the $\Delta V^{\rm un}(W)$ interaction in (3.96). The argument we have used previously that zero potential energy for excited states cancels the three-body contributions was motivated by nuclear-matter results, where there is no Coulomb interaction. Hence, the proper extension to finite nuclei is to specify zero nuclear potential energy in excited states, but to include the appropriate Coulomb potential energy. Since the reaction matrix calculations on which the effective interaction is based use only kinetic energy in excited states, one obtains the correct energy difference between occupied and excited states if the Coulomb energy is removed from all proton single-particle energies. At first this procedure seems to treat neutrons and protons quite inconsistently since in Pb^{208}, for example, the single-particle energies for the last neutron and last proton are roughly -8 MeV, and yet the energies used in W are 8 and 32 MeV, respectively. However, the apparent added attraction of neutrons in comparison to protons is compensated by the fact that the greater local neutron density excludes more low-lying intermediate states for neutrons than for protons.

The second aspect of starting energy dependence we must consider is its effect on orthogonality of radial functions. Orthogonality between unlike particles or states of different l is automatic, but we must assure that states of like particles with the same l are also orthogonal. Writing the energy from particle I to be used in W as ϵ_I, the explicit starting energy dependence of (3.120) may be indicated as

$$\begin{aligned}&-(\hbar^2/2m)[d^2R_I(r_1)/dr_1^2]\\ &\quad+\sum_J\mathfrak{F}_{J,I}^D(r_1,|\epsilon_J+\epsilon_I|)R_I(r_1)\\ &\quad+\int dr_2\sum_J\mathfrak{F}_{J,I}^E(r_1,r_2,|\epsilon_J+\epsilon_I|)R_I(r_2)=E_IR_I(r_1).\end{aligned}\tag{3.122}$$

Then the usual orthogonality argument for the radial functions of like particles R_{nl} and $R_{n'l}$ becomes

$$\begin{aligned}&\int dr_1R_{n'l}(r_1)\sum_J[\mathfrak{F}_{J,nl}^D(r_1,|\epsilon_J+\epsilon_{nl}|)\\ &\quad-\mathfrak{F}_{J,n'l}^D(r_1,|\epsilon_J+\epsilon_{n'l}|)]R_{nl}(r_1)\\ &\quad+\int dr_1dr_2R_{n'l}(r_1)\\ &\quad\times\sum_J[\mathfrak{F}_{J,n}^E(r_1,r_2,|\epsilon_J+\epsilon_{nl}|)\\ &\quad-\mathfrak{F}_{J,n'}^E(r_1,r_2,|\epsilon_J+\epsilon_{n'l}|)]R_{nl}(r_2)\\ &=(E_{nl}-E_{n'l})\int R_{nl}(r_1)R_{n'l}(r_1)dr_1,\end{aligned}\tag{3.123}$$

where we have used the fact that $\mathfrak{F}^E$ is symmetrical in r_1 and r_2 from (3.119) and the reality of R_{nl} and have eliminated the kinetic contributions by integration by parts. Evidently, the only way to ensure orthogonality is to make $\mathfrak{F}^D$ and $\mathfrak{F}^E$ Hermitian by requiring $\epsilon_{nl}=\epsilon_{n'l}$. We note that this argument would not work for the orthogonality of a radial function in a spin-unsaturated shell to one in a spin-saturated shell because of the dependence of $\mathfrak{F}_{J,I}{}^E$ on the j of the Ith particle if it is spin unsaturated. However, this case never arises in practice since the unsaturated shell always has the highest l for a given kind of particle. Thus, the energy to be used in the starting energy is defined by the following average, where $\bar{E}^C$ is the average Coulomb energy per proton:

$$\epsilon_l{}^P=(n_{\max}+1)^{-1}\sum_{n'=0}^{n_{\max}}(E_{nl}{}^P-\bar{E}^C) \quad \text{for protons,}$$

$$\epsilon_l{}^N=(n_{\max}+1)^{-1}\sum_{n'=0}^{n_{\max}}E_{nl}{}^N \quad \text{for neutrons.} \tag{3.124}$$

For the case in which we have some average particles in a given l state, all neutron and proton wave functions of the same l must be orthogonal. Hence, for that l,

$$\epsilon_l=\Big[\sum_{n=n_{\min}}^{n_{\max}}(2E_{nl}{}^{\mathrm{av}}-\bar{E}^C)+\sum_{n'=n_{\min}'}^{n_{\max}'}(E_{n'l}{}^P-\bar{E}^C)+\sum_{n''=n_{\min}''}^{n_{\max}''}E_{n''l}{}^N\Big]/(n_{\max}-n_{\min}+n_{\max}'-n_{\min}'+n_{\max}''-n_{\min}''). \tag{3.125}$$

An alternative method of treating starting energies, which is not used in this work, has recently been suggested by Brandow,[42] in which one does not use the same energy for all radial functions of the same l, but rather allows nonorthogonal radial functions and computes observables such as the density using biorthogonal complements.

The definition of starting energies in (3.124) and (3.125), together with (3.96), (3.111), and (3.119), completely specifies the radial equation (3.120). Given a set of eigenvalues and radial equations, one may construct $\mathfrak{F}^D$ and $\mathfrak{F}^E$ and solve for a new set of eigenvalues and radial functions, and iterate until self-consistency is achieved. The details of the numerical computation are described in Appendix A.

IV. COMPARISON OF DENSITY-DEPENDENT HF RESULTS WITH EXPERIMENT

c.m. Correction

The two main experimental quantities we wish to compare with our calculations, the binding energy and ground-state density distribution, both pertain to a reference frame in which the c.m. of the nucleus is fixed. Our density-dependent HF calculation, on the other hand, is performed in the rest frame of the self-consistent potential, with respect to which the c.m. is certainly not stationary. Hence, we must consider the relation of energy and density in the potential frame, in which we assume $3A$ degrees of freedom, to the energy and density in the c.m. frame, with $3(A-1)$ degrees of freedom.

In general, Lipkin[61] has shown that the transformation of observables from the potential frame to the c.m. frame is not unique. However, in the simple case of a harmonic oscillator, the various methods agree, and may be understood most simply in terms of the argument of Elliott and Skyrme.[62] This argument shows that the product wave function of harmonic-oscillator functions in the ground state may be rewritten so that the c.m. motion explicitly appears as a $0s$ wave function in which the size parameter is $(\hbar/Am\omega)^{1/2}$ and that the energy from the c.m. motion is $\frac{3}{4}\hbar\omega$. Since our calculations corroborate the validity of the harmonic-oscillator approximation for nuclei up to and including calcium, these c.m. corrections should be quite adequate for these nuclei. Although the harmonic-oscillator approximation breaks down for heavy nuclei, the corrections become very small for large A, so that the discrepancy between the harmonic-oscillator correction and the true correction is expected to be negligible.

Using this harmonic-oscillator c.m. correction, the proton density in the c.m. system $\rho_{\mathrm{c.m.}}{}^P$ is related to the density in the HF self-consistent potential frame $\rho_{\mathrm{HF}}{}^P$ by

$$\begin{aligned}\rho_{\mathrm{c.m.}}{}^P(r)&=\int d^3r_1(B\sqrt{\pi})^{-3}\exp(r_1{}^2/B^2)\rho_{\mathrm{HF}}{}^P(|\,\mathbf{r}-\mathbf{r}_1\,|)\\&=\int d^3r_1(B\sqrt{\pi})^{-3}\exp[(\mathbf{r}-\mathbf{r}_1)^2/B^2]\rho_{\mathrm{HF}}{}^P(r_1),\end{aligned} \tag{4.1}$$

where $B=b/\sqrt{A}=|\,\hbar/m\omega A\,|^{1/2}$. Since the charge density $\rho_{\mathrm{ch}}(r)$ is the experimental observable, it is necessary to fold the proton charge distribution with $\rho_{\mathrm{c.m.}}{}^P$. Measurements of the proton form factor[63–66] indicate that the proton charge distribution is very accurately represented by an exponential. However, smearing a proton distribution with either a Gaussian or an ex-

[61] H. J. Lipkin, Phys. Rev. **110**, 1395 (1958).

[62] J. P. Elliott and T. H. R. Skyrme, Proc. Roy. Soc. (London) **A232**, 561 (1955).

[63] R. Hofstadter, F. Bumiller, and M. R. Yearian, Rev. Mod. Phys. **30**, 482 (1958).

[64] F. Bumiller, M. Croissiaux, E. Dally, and R. Hofstadter, Phys. Rev. **124**, 1623 (1961).

[65] E. E. Chambers and R. Hofstadter, Phys. Rev. **103**, 1454 (1956).

[66] S. D. Drell, in *Proceedings of the Thirteenth International Conference on High Energy Physics, Berkeley, California, 1966* (University of California Press, Berkeley, Calif., 1967).

ponential of the proton rms radius yields very similar results, so for the present we shall consider a Gaussian proton distribution. Then

$$\rho_{\rm ch}(r) = \int d^3r_2 (P\sqrt{\pi})^{-3} \exp[-(\mathbf{r}-\mathbf{r}_2)^2/P^2]\rho_{\rm c.m.}{}^P(r)$$
$$= \int d^3r_1 d^3r_2 (P\sqrt{\pi})^{-3}(B\sqrt{\pi})^{-3}$$
$$\times \exp[-(\mathbf{r}-\mathbf{r}_2)^2/P^2+(\mathbf{r}_2-\mathbf{r}_1)^2/B^2]\rho_{\rm HF}{}^P(r_1)$$
$$= \int d^3r_1 ([P^2-B^2]\pi)^{-3/2}$$
$$\times \exp[-(\mathbf{r}-\mathbf{r}_1)^2/(P^2-B^2)]\rho_{\rm HF}{}^P(r_1), \quad (4.2)$$

where $P=(\frac{2}{3})^{1/2}\langle r^P\rangle_{\rm rms}$. Thus, it is convenient to include the c.m. correction and proton smearing simultaneously, by defining an effective rms radius for the proton

$$\langle r^{\rm eff}\rangle_{\rm rms} = [\langle r^P\rangle_{\rm rms}{}^2 - \tfrac{3}{2}(b^2/A)]^{1/2}. \quad (4.3)$$

Since for all nuclei of interest the proton radius correction is much larger than the c.m. correction, it is more accurate to use an exponential distribution of rms radius $\langle r^{\rm eff}\rangle_{\rm rms}$ for the combined correction. The value of $\langle r^P\rangle_{\rm rms}=0.8$ F is obtained from proton form factor measurements.[63–66] For oxygen and calcium, we use $b=1.76$ and 1.90 F, respectively, and for zirconium and lead, the values of b are obtained from (2.30).

Binding Energy and Single-Particle Energies

The total energy in the rest frame of the self-consistent potential $\langle E\rangle$ is given by (3.96), and is corrected for c.m. motion by subtracting $\frac{3}{4}\hbar\omega$. To relate $\langle E\rangle$ to the single-particle eigenvalues, it is convenient to explicitly separate the HF terms in the variation of $\langle E\rangle$ from the rearrangement terms. Thus, varying u_I, we obtain

$$\delta\langle E\rangle = \int d\tau_1 \delta u_I(r_1) T u_I(r_1) + \tfrac{1}{2}\sum_J \int d\tau_1 \int d\tau_2 \delta u_I(r_1) 2u_J{}^2(r_2) V u_I(r_1)$$
$$+\tfrac{1}{2}\int d\tau_1 \int d\tau_2 \delta u_I(r_1) \sum_{JK} u_J{}^2(|\mathbf{r}_1+\tfrac{1}{2}\mathbf{r}_2|) u_K{}^2(|\mathbf{r}_1-\tfrac{1}{2}\mathbf{r}_2|)(\partial V/\partial\rho) u_I(r_1) + \tfrac{1}{2}\sum_J \int d\tau_1 \int d\tau_2 \delta u_I(r_1) 2u_J(1) u_J(2) \tilde{V} u_I(2)$$
$$+\tfrac{1}{2}\int d\tau_1 \int d\tau_2 \delta u_I(r_1) \sum_{JK} u_J(|\mathbf{r}_1+\tfrac{1}{2}\mathbf{r}_2|) u_J(|\mathbf{r}_1-\tfrac{1}{2}\mathbf{r}_2|) u_K(|\mathbf{r}_1+\tfrac{1}{2}\mathbf{r}_2|) u_K(|\mathbf{r}_1-\tfrac{1}{2}\mathbf{r}_2|)(\partial\tilde{V}/\partial\rho) u_I(r_1). \quad (4.4)$$

Multiplying the resulting eigenvalue equation for u_I by $\frac{1}{2}u_I(r_1)$, integrating over r_1, and summing over I, we obtain

$$\tfrac{1}{2}\sum_I \int d\tau_1 u_I(r_1)(E_I+T) u_I(r_1) = \sum_I \int d\tau_1 u_I(r_1) T_I u_I(r_1) + \tfrac{1}{2}\sum_{IJ} \iint d\tau_1 d\tau_2 u_I{}^2(r_1) u_I{}^2(r_2) V$$
$$+\tfrac{1}{2}\sum_{IJ} \iint d\tau_1 d\tau_2 u_I(r_2) u_J(r_1) u_J(r_2) \tilde{V} + \sum_I \tfrac{1}{2}\iint d\tau_1 d\tau_2 \sum_{JK} u_J{}^2(|\mathbf{r}_1+\tfrac{1}{2}\mathbf{r}_2|) u_K{}^2(|\mathbf{r}_1-\tfrac{1}{2}\mathbf{r}_2|)(\partial V/\partial\rho) u_I{}^2(r_1)$$
$$+\sum_I \tfrac{1}{2}\iint d\tau_1 d\tau_2 \sum_{JK} u_J(|\mathbf{r}_1+\tfrac{1}{2}\mathbf{r}_2|) u_J(|\mathbf{r}_1-\tfrac{1}{2}\mathbf{r}_2|) u_K(|\mathbf{r}_1+\tfrac{1}{2}\mathbf{r}_2|) u_K(|\mathbf{r}_1-\tfrac{1}{2}\mathbf{r}_2|)(\partial\tilde{V}/\partial\rho) u_I{}^2(r_1)$$
$$= \langle E\rangle - \sum_I \tfrac{1}{2}\Delta E_I \int d\tau_1 u_I{}^2(r_1), \quad (4.5)$$

where

$$\Delta E_I = -[\iint d\tau_1 d\tau_2 \sum_{JK} u_J{}^2(|\mathbf{r}_1+\tfrac{1}{2}\mathbf{r}_2|) u_K{}^2(|\mathbf{r}_1-\tfrac{1}{2}\mathbf{r}_2|)(\partial V/\partial\rho) u_I{}^2(r_1)$$
$$+\iint d\tau_1 d\tau_2 \sum_{JK} u_J(|\mathbf{r}_1+\tfrac{1}{2}\mathbf{r}_2|) u_J(|\mathbf{r}_1-\tfrac{1}{2}\mathbf{r}_2|) u_K(|\mathbf{r}_1+\tfrac{1}{2}\mathbf{r}|) u_K(|\mathbf{r}_1-\tfrac{1}{2}\mathbf{r}|)(\partial\tilde{V}/\partial\rho) u_I{}^2(r_1)]/[\int d\tau_1 u_I{}^2(r_1)].$$

Then, defining N_I equal to $2(2l+1)$, $(2j+1)$, or $4(2l+1)$ for neutron or proton l shells, neutron or proton j shells, or average particles, respectively, we may write

$$\langle E\rangle = \tfrac{1}{2}\sum_I N_I[E_I+T_I+\Delta E_I]. \quad (4.6)$$

The E_I and T_I terms in (4.6) are the usual terms appearing in the HF expression for $\langle E\rangle$, except for the case of j shells, in which case T_I contains the single-particle spin-orbit potential, Eq. (3.96), in addition to the usual kinetic energy. The ΔE_I terms are corrections arising from the density-dependent theory, and since the density dependence contributes to saturation, it is clear that the over-all sign of ΔE_I must be negative.

The presence of the ΔE_I terms resolves a troublesome defect of the simple HF theory. In the light nuclei, where the wave functions are quite well described by harmonic-oscillator functions, the kinetic energy is approximately determined by the experimental charge radius from electron scattering. With $\Delta E_I=0$, Eq. (4.6) then provides a constraint relating single-particle energies to the total energy. Using the single-particle energies quoted by Elton and Swift[60] for the $1s_{1/2}$, $0d_{1/2}$, and $0d_{3/2}$ levels in Ca^{40}, the recent proton single-particle energies for the $0s$ and $0p$ states by James *et al.*,[67] and assuming the proton–neutron energy difference for the $0s$ and $0p$ states is the same as for the $0d$ difference, one obtains $(1/2A)\sum_I E_I=-12.9$ MeV. Taking the value $\hbar\omega=11.47$ obtained from electron scattering, $(1/2A)\sum_I T_I=8.6$ MeV. Including a cor-

[67] A. N. James, P. T. Andrews, P. Kirkby, and B. G. Lowe, Nucl. Phys. **A138**, 145 (1969).

rection of -0.2 MeV for c.m. motion, Eq. (4.6) with $\Delta E_I=0$ yields a binding energy per particle of 4.5 MeV instead of 8.6. Thus, the experimental data are incompatible with the simple HF relation between single-particle energies and binding energy, and require corrections ΔE_I which average roughly -8.2 MeV. It will be shown below that corrections of this magnitude do result from our theory, and yield satisfactory agreement with binding energies and single-particle energies.

The corrections ΔE_I are most easily evaluated by taking the full eigenvalue equation for u_I arising from (3.111) and (3.119), multiplying by $\frac{1}{2}u_I(r_1)$, integrating over r_1, summing over I, and subtracting $\langle E\rangle$ as given in (3.102). In this way, one obtains

$$-\tfrac{1}{2}\sum_I N_I\Delta E_I=\tfrac{1}{2}\sum_{IJ}\int\int d\tau_1 d\tau_2 u_I^2(r_1)u_J^2(r_2)\{\rho^\alpha(R)[\tfrac{1}{2}\alpha V_1^{\rm av}+\tfrac{1}{2}(F_IF_J)V_1^{\rm lk}\tfrac{1}{2}(\alpha(\alpha+1))]+\rho^\alpha(R)(\Delta\rho(R)/\rho(R))$$
$$\times[F_JV^{\rm lk}\tfrac{1}{8}(\alpha(\alpha-1)(\alpha+2))+F_J(V_1^{\rm lk}-V_1^{\rm un})\tfrac{1}{4}\alpha]\}+\tfrac{1}{2}\sum_I\int\int d\tau_1 d\tau_2 u_I^2(r_1)\tfrac{1}{2}\alpha\rho_{\rm SL}^2(r_2,k_{\rm F}(\rho(r_1)))\rho^{\alpha-1}(r_1)$$
$$\times[V_1^{\rm av}+\tfrac{1}{2}(V_1^{\rm lk}-V_1^{\rm un})(\Delta\rho(R)/\rho(R))^2+V_1^L\{(\alpha-1)\tfrac{1}{4}(\alpha+2)(\Delta\rho(R)/\rho(R))^2+F_I(\alpha+1)(\Delta\rho(R)/\rho(R))\}]. \quad (4.7)$$

Since only the sum $\sum_I N_IE_I$ enters into the theory, the definition of the individual ΔE_I terms is not unique. However, for computational purposes, removing the sum over I from both sides of Eq. (4.7) is the most convenient definition since the quantities contributing to ΔE_I are then a subset of the quantities required for the Ith radial equation.

The relation between the eigenvalues E_I and the experimental removal energy is established by a simple generalization of the Koopman theorem. Noting that $u_I(r)$ is normalized to N_I, the variation in $\langle E\rangle$ due to varying N_I is obtained from (4.4) by replacing $\delta u_I(r_a)u_I(r_b)$ by $(\delta N_I/N_I)u_I(r_a)u_I(r_b)$. Thus, comparing the resulting equation with the eigenvalue equation for u_I multiplied by $u_I(r_1)$ and integrated over r_1, one obtains

$$\delta\langle E\rangle/\delta N_I=E_I. \quad (4.8)$$

Whereas in the simple HF case (4.8) is exact for the removal of one particle, in the density-dependent theory, (4.8) is strictly true only for an infinitesimal change in N_I. For our purposes, the second derivative terms are sufficiently small that we shall use (4.8) for the removal of one particle, and thus conclude that if a particle is removed from the Ith orbit and the wave functions of the remaining particles are not allowed to change, the change in energy is $-E_I$. Physically, the wave functions will change somewhat to lower the energy of the resulting system, giving rise to an additional rearrangement energy (not to be confused with the Brueckner rearrangement energy associated with $\partial V/\partial\rho$). Thus, the eigenvalues of the last particles may be compared with experimental binding energies by the following inequality:

$$BE(A)-BE(A-1)\leq|E_I|. \quad (4.9)$$

In Appendix A, the computational details are discussed and the limitation on the number of radial wave functions is explained. For O^{16}, Ca^{40}, Ca^{48}, and Zr^{90}, it is possible to include separate wave functions for neutrons and protons. In the interest of economy, it is most efficient to perform early iterations with average wave functions for states which are equally occupied by neutrons and protons until self-consistency is achieved, and then to compute the proton and neutron wave functions due to this average nucleon distribution. The entire set of neutron and proton wave functions may then be used to obtain fully self-consistent neutron and proton wave functions. One finds, even in Zr^{90}, that there is very little change from the proton and neutron wave functions calculated from the potential due to the average wave functions to the fully self-consistent proton and neutron wave functions.

Physically, the only difference in the potential arising from orbitals with average particles and the potential from the corresponding orbitals of neutrons and protons is that in the former case the like and unlike contributions are exactly superimposed, whereas in the latter case, the two contributions are slightly displaced due to the slightly different proton and neutron radial functions. Considering the potential for a proton, for example, there are slightly fewer protons near the center than indicated by the average wave functions and slightly more neutrons, so that the like force contributes slightly less than in the average case, and the unlike force contributes correspondingly more. Since the unlike force is more attractive than the like force, the over-all effect is to increase the attraction in the interior, and similarly, to decrease the attraction in the surface. Hence, in the fully self-consistent case, the protons see a small additional potential tending to decrease the radii of the wave functions, and by an analogous argument, the neutron wave-function radii become slightly larger. Thus, in the fully self-consistent case, the additional corrections tend to reduce the difference between proton and neutron wave functions, but by a very small amount which is proportional to the difference between the neutron and proton wave functions in the levels which were approximated by average particles.

For the case of Pb^{208}, the computer program cannot handle the fully self-consistent case, so we have treated

TABLE VII. Single-particle energies and binding energies for Ca^{40}, in MeV. Single-particle energies represent barycenters for spin-orbit doublets, and binding energies contain the c.m. correction. DDHF indicates density-dependent Hartree-Fock and adjusted refers to the parameters (4.10). Experimental energies are from Refs. 60, 67, and 37.

	$0s$	$0p$	$0d$	$1s$	B.E.
HF, bare	−58.2	−37.3	−16.5	−14.4	3.0
DDHF, bare	−43.6	−25.3	−9.7	−8.0	3.2
DDHF, adjusted	−46.9	−30.2	−15.2	−11.9	7.5
Expt	−53±11	−37±6	−16.2	−15.7	8.55

orbitals up through the $2s$ levels as average particles, and use separate neutron and proton wave functions for the $0h$ level and above. Having obtained the self-consistent average orbitals, two additional iterations were performed in which the neutron and proton radial functions arising from the potential due to the self-consistent average particles below the $0h$ levels and the protons and neutrons in the $0h$ and higher levels were obtained. By the preceding argument, we expect that the true self-consistent proton orbitals below $0h$ will have radial functions of slightly smaller radii and the true neutron radial functions below $0h$ will have slightly larger radii. Based on the experience with Zr^{90} in which we could compare this approximation with the fully self-consistent case, we expect the corrections to our results to be extremely small.

The motivation for adjusting the effective interaction to reproduce nuclear-matter properties has been discussed previously. From the structure of the exchange contribution to the symmetry energy, we have seen that increasing the long-range effective interaction significantly increases the symmetry energy. For this reason and because we feel that the long-range part of the interaction is the most accurately determined, we shall set the parameter P_L equal to unity. Then, as discussed in connection with (3.46), using $P_{\rm sym}=1$ results in a nuclear-matter symmetry energy which is in satisfactory agreement with the semiempirical value. Having specified P_L and $P_{\rm sym}$, selecting the nuclear-matter binding energy and saturation density uniquely specify $P_{S,1.0}$ and $P_{S,1.4}$. Requiring nuclear-matter binding energy of 15.68 MeV, the saturation density is the only free parameter which is varied to fit the experimental data, and we have previously argued that there is no reliable theory to specify it *a priori*. The optimal fit is obtained with saturation at $k_F=1.31$, so that using (3.34), the values of all the adjustable parameters are

$$\begin{aligned} P_{S,1.0}&=0.66903,\\ P_{S,1.4}&=0.83702,\\ P_L&=1.0,\\ P_{\rm sym}&=1.0. \end{aligned} \tag{4.10}$$

To obtain the appropriate binding and saturation, we note that the short-range repulsion has been reduced and made more density-dependent.

Calculated Energies

Because several numerical simplifications in the construction of the effective interaction have slightly altered the saturation point of nuclear matter, the most significant simplifications being the ρ^α density dependence and the omission of the density dependence of the starting energy correction, it is evidently desirable to distinguish these effects from the deliberate modifications to obtain nuclear-matter binding. Hence, we shall define the bare interaction as the interaction resulting from setting $P_L=1.0$, $P_{\rm sym}=1.0$, and requiring saturation at $k_F=1.40$ F^{-1} and 11.0 MeV. This interaction differs only slightly from the case in which all adjustable parameters are set to unity, and should be regarded as the most accurate representation of the true two-body effective interaction.

The effects of the rearrangement terms in the density-dependent HF theory and of the adjustment of the interaction using (4.10) are demonstrated for Ca^{40} in Table VII. For the simple HF theory, which omits the rearrangement terms, and using the bare interaction defined above, it is evident that the single-particle energies are reasonable, but that the nucleus is grossly underbound. Using the bare effective interaction, but including the rearrangement terms of the density-dependent theory slightly improves the binding, but tends to increase the single-particle energies. Finally, adjusting the interaction according to (4.10) brings the binding energy and single-particle energies into satisfactory agreement with experiment.

Theoretical and experimental binding energies and rms radii using the adjusted interaction and the density-dependent theory are presented in Table VIII for the five closed-shell nuclei studied in this work. The over-all binding energy agreement is quite satisfactory, with the theory tending to slightly underbind

TABLE VIII. Binding energies, in MeV, and rms radii, in F, for closed-shell nuclei.

Nucleus	O^{16}	Ca^{40}	Ca^{48}	Zr^{90}	Pb^{208}
E	−6.08	−7.28	−7.30	−7.77	−7.50
c.m. correction	−0.67	−0.21	−0.18	−0.08	−0.03
Theoretical B.E.	6.75	7.49	7.48	7.85	7.53
Experimental B.E.	7.98	8.55	8.67	8.71	7.87
Point proton rms radius	2.71	3.41	3.45	4.18	5.37
Point neutron rms radius	2.69	3.37	3.68	4.30	5.60

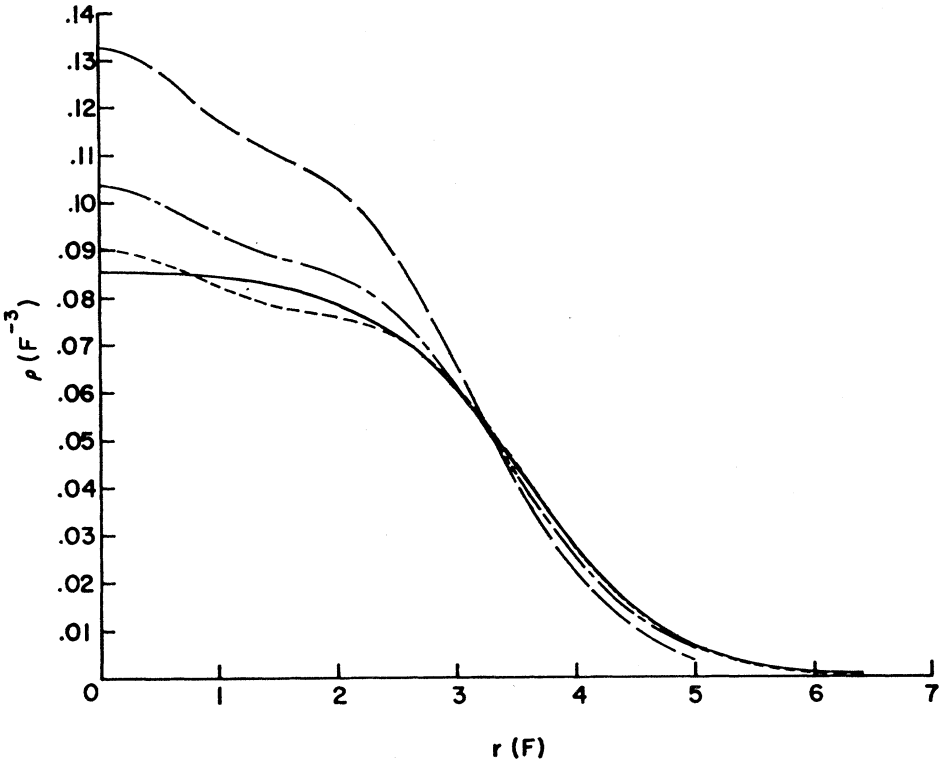

FIG. 4. Ca^{40} charge-density distributions for ordinary HF theory without rearrangement using the bare effective interaction (long dashes), for the density-dependent HF theory with the bare effective interaction (dot-dash), and for the density-dependent HF theory with the interaction adjusted by the parameters in (4.10) (short dashes). The theoretical charge densities include the proton size and c.m. motion corrections described in the text. The solid line indicates the empirical dastribution of Ref. 69.

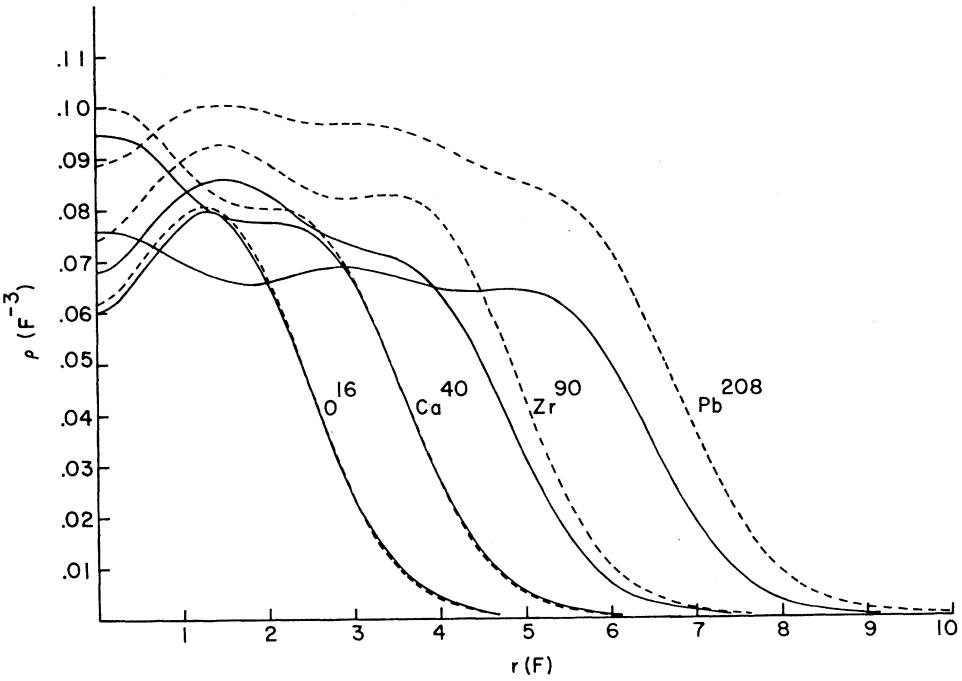

FIG. 5. Neutron (dashed lines) and proton (solid lines) density distributions, with no nucleon size or c.m. motion corrections.

TABLE IX. Energies, optimal harmonic-oscillator size parameters, and expansion coefficients for doubly closed-shell nuclei. Expt indicates the experimental single particle energy, and E denotes the theoretical eigenvalue. The first eight expansion coefficients are numbered 0–7. Harmonic-oscillator phases are defined such that radial functions are always positive near the origin.

State	Expt	E (MeV)	ΔE (MeV)	KE (MeV)	$b(F)$	0	1	2	3	4	5	6	7
O^{16}													
$0s(P)$	-40 ± 8[a]	−32.81	−8.48	9.65	1.78477	0.99984	0.00044	−0.01008	−0.01354	0.00072	0.00314	0.00389	0.00270
$0p(P)$	−16.8[b]	−14.23	−5.37	15.86	1.80320	0.99914	0.00060	0.03294	−0.02428	0.00284	−0.00229	0.00435	0.00241
$0s(N)$		−36.00	−8.66	9.87	1.76484	0.99986	0.00021	−0.00940	−0.01205	0.00135	0.00345	0.00389	0.00264
$0p(N)$		−17.34	−5.46	16.07	1.79166	0.99925	0.00057	0.03034	−0.02306	0.00249	−0.00167	0.00425	0.00247
Ca^{40}													
$0s(P)$	-50 ± 11[a]	−43.16	−11.87	7.40	2.04429	0.99910	0.00038	−0.03940	−0.01533	−0.00010	0.00204	0.00031	−0.00140
$0p(P)$	-34 ± 6[a]	−26.85	−9.19	13.34	1.96893	0.99942	0.00049	−0.02747	−0.01969	−0.00022	0.00242	0.00148	−0.00035
$0d(P)$	−12.6[b]	−11.83	−6.73	19.11	1.94576	0.99959	0.00064	0.00606	−0.02744	0.00171	0.00086	0.00288	0.00208
$1s(P)$	−11.6[b]	−8.55	−6.90	17.68	2.02831	0.01044	0.99836	0.00645	0.03316	−0.04301	0.00044	−0.00361	−0.00103
$0f_{7/2}(P)$	−1.1[b]	−0.25	−4.87	24.00	1.96745	0.99625	0.00064	0.05311	−0.05424	0.00796	−0.00979	0.00046	0.00923
$0s(N)$		−50.57	−12.31	7.73	2.00085	0.99933	0.00166	−0.03422	−0.01187	0.00070	0.00158	−0.00039	−0.00190
$0p(N)$		−33.94	−9.49	13.68	1.94369	0.99950	0.00057	−0.02632	−0.01711	0.00053	0.00247	0.00114	−0.00073
$0d(N)$	−19.8[b]	−18.68	−6.91	19.47	1.92787	0.99968	0.00056	0.00265	−0.02477	0.00168	0.00157	0.00287	0.00165
$1s(N)$	−18.2[b]	−15.30	−7.14	18.24	1.99256	0.00540	0.99897	0.00324	0.02169	−0.03839	−0.00072	−0.00266	−0.00027
$0f_{7/2}(N)$	−8.4[b]	−6.93	−4.91	24.65	1.94366	0.99807	0.00072	0.03838	−0.04581	0.00198	−0.00562	0.00170	0.00662
$1p_{3/2}(N)$	−6.3[b]	−3.70	−6.05	17.90	2.05457	−0.11257	0.97436	−0.06633	0.13733	−0.08537	0.02584	−0.00250	−0.01465
Ca^{48}													
$0s(P)$	-55 ± 9[a]	−47.58	−11.60	6.87	2.12500	0.99872	0.00019	−0.04719	−0.01731	−0.00012	0.00257	0.00060	−0.00135
$0p(P)$	-35 ± 7[a]	−32.66	−9.39	12.67	2.02220	0.99902	0.00038	−0.03910	−0.01992	0.00000	0.00317	0.00142	−0.00066
$0d(P)$	-18 ± 8	−18.70	−7.30	18.72	1.96691	0.99956	0.00058	−0.01637	−0.02421	0.00079	0.00313	0.00274	0.00121
$1s(P)$		−14.26	−7.41	18.23	2.05032	0.04875	0.99772	0.02764	−0.00022	−0.03666	−0.00415	−0.00029	−0.00010
$0f_{7/2}(P)$	−9.6[b]	−7.15	−5.63	24.45	1.95321	0.99910	0.00076	0.00483	−0.04074	−0.00121	−0.00015	0.00371	0.00569
$0s(N)$		−51.03	−12.62	7.43	2.03655	0.99956	0.00039	−0.02827	−0.00612	0.00245	0.00071	−0.00203	−0.00320
$0p(N)$		−34.86	−10.38	13.12	1.98327	0.99964	0.00035	−0.02379	−0.01099	0.00336	0.00267	−0.00019	−0.00214
$0d(N)$		−19.79	−8.00	18.72	1.96581	0.99981	0.00060	0.00056	−0.01804	0.00516	0.00371	0.00230	0.00061
$1s(N)$		−17.10	−7.75	18.08	2.02028	0.01460	0.99924	0.00854	0.01295	−0.03128	0.00080	−0.00065	−0.00160
$0f_{7/2}(N)$	−9.9[b]	−7.87	−5.48	23.45	1.99785	0.99850	0.00280	0.02941	−0.04323	0.00247	0.00042	0.00228	0.00711
$1p_{3/2}(N)$	−6.1[b]	−4.88	−6.51	18.79	2.06504	−0.08488	0.98470	−0.04988	0.10986	−0.06797	0.02001	0.00359	−0.01018
Zr^{90}													
$0s(P)$	-54 ± 8[a]	−48.06	−13.45	5.18	2.45790	0.99751	−0.00064	−0.06656	−0.02202	0.00180	−0.00561	0.00282	0.00038
$0p(P)$	-43 ± 8[a]	−38.10	−11.65	10.01	2.28198	0.99749	0.00025	−0.06667	−0.02267	0.00264	0.00606	0.00237	−0.00023
$0d(P)$	-27 ± 8[a]	−25.30	−9.86	15.27	2.18386	0.99797	0.00035	−0.05796	−0.02548	0.00099	0.00535	0.00135	−0.00098
$1s(P)$		−21.08	−10.22	16.07	2.27156	0.11259	0.98906	0.06234	−0.05795	−0.04132	−0.00698	0.00631	0.00425
$0f(P)$		−13.44	−8.16	20.85	2.11664	0.99884	0.00043	−0.03777	−0.02877	0.00011	0.00565	0.00071	−0.00069
$1p(P)$		−8.15	−8.31	20.61	2.20846	0.06053	0.99600	0.03644	−0.01921	−0.04593	−0.00899	0.00855	0.00133
$0s(N)$		−58.19	−14.83	5.74	2.31911	0.99901	−0.00044	−0.04329	−0.00899	0.00274	0.00163	−0.00072	−0.00105

TABLE IX. (*Continued*).

State	Expt	E (MeV)	ΔE (MeV)	KE (MeV)	$b(F)$	0	1	2	3	4	5	6	7
$0p(N)$		−46.74	−12.95	10.64	2.20772	0.99882	0.00176	−0.04691	−0.01123	0.00403	0.00283	−0.00081	−0.00177
$0d(N)$		−32.99	−10.99	15.78	2.14432	0.99897	0.00056	−0.04201	−0.01559	0.00344	0.00348	−0.00110	−0.00250
$1s(N)$		−29.79	−11.02	16.24	2.20325	0.06862	0.99525	0.04098	−0.04743	−0.02802	−0.00046	0.00553	0.00128
$0f(N)$		−20.18	−8.98	20.99	2.10968	0.99946	0.00322	−0.02348	−0.02097	0.00301	0.00544	−0.00070	−0.00194
$1p(N)$		−16.52	−8.87	20.72	2.16344	0.03329	0.99841	0.02087	−0.01195	−0.03528	−0.00277	0.00779	−0.00091
$0g_{9/2}(N)$		−10.55	−6.81	25.87	2.09958	0.99897	0.00018	−0.01463	−0.03813	−0.00032	0.01150	0.00274	0.00122
Pb^{208}													
$0s(P)$		−48.50	−14.40	3.33	3.11129	0.99427	0.00008	−0.09923	−0.03811	0.00049	0.00911	0.00563	0.00092
$0p(P)$		−42.66	−13.36	6.68	2.81262	0.99453	−0.00038	−0.09911	−0.03040	0.00590	0.01006	0.00427	−0.00058
$0d(P)$		−34.21	−12.28	10.57	2.63741	0.99480	0.00024	−0.09721	−0.02712	0.00685	0.00978	0.00357	−0.00148
$1s(P)$		−30.20	−12.39	11.58	2.76529	0.16929	0.97293	0.09248	−0.11152	−0.05886	−0.00723	0.00972	0.00825
$0f(P)$		−26.13	−11.19	14.97	2.50751	0.99522	−0.00017	−0.09320	−0.02526	0.00599	0.00961	0.00377	−0.00198
$1p(P)$		−20.92	−11.22	16.29	2.60624	0.13880	0.97891	0.08298	−0.11097	−0.05239	−0.00533	0.01068	0.01014
$0g(P)$		−15.83	−9.85	19.55	2.42296	0.99587	0.00039	−0.08519	−0.02449	0.00213	0.00908	0.00520	−0.00218
$1d(P)$	−9.2[c]	−10.18	−9.84	20.67	2.51088	0.10825	0.98426	0.07113	−0.10154	−0.04503	−0.01161	0.00648	0.01303
$2s(P)$	−8.0[c]	−7.46	−9.74	20.50	2.54178	0.06823	0.11083	0.97850	0.07611	−0.11090	−0.04976	−0.01883	0.00096
$0h_{11/2}(P)$	−9.4[c]	−8.02	−7.67	23.96	2.37870	0.99493	0.00046	−0.08915	−0.02687	0.00093	0.01265	0.01013	−0.00186
$0s(N)$		−62.53	−14.40	3.70	2.90120	0.99779	−0.00026	−0.06442	−0.01511	0.00441	0.00435	0.00084	−0.00084
$0p(N)$		−54.98	−13.36	7.16	2.69790	0.99713	−0.00035	−0.07359	−0.01573	0.00614	0.00516	0.00060	−0.00141
$0d(N)$		−45.44	−12.28	11.08	2.56626	0.99680	−0.00020	−0.07759	−0.01672	0.00641	0.00613	0.00132	−0.00130
$1s(N)$		−42.39	−12.39	12.07	2.64632	0.13172	0.98410	0.07206	−0.08790	−0.03358	0.00233	0.00903	0.00485
$0f(N)$		−36.11	−11.19	15.46	2.46232	0.99688	0.00046	−0.07615	−0.01818	0.00396	0.00587	0.00180	−0.00156
$1p(N)$		−31.86	−11.22	16.81	2.53570	0.12210	0.98490	0.07295	−0.09012	−0.03712	−0.00319	0.00708	0.00566
$0g(N)$		−25.23	−9.95	19.90	2.39874	0.99746	0.00233	−0.06718	−0.01727	−0.00019	0.00525	0.00303	−0.00223
$1d(N)$		−20.49	−9.84	21.00	2.46312	0.09341	0.98976	0.05921	−0.07813	−0.02813	−0.00868	0.00432	0.00917
$2s(N)$		−18.39	−9.74	21.05	2.48058	0.04737	0.09631	0.98719	0.06708	−0.07968	−0.02684	−0.01168	0.00250
$0h(N)$		−15.99	−9.49	24.58	2.34169	0.99793	0.00064	−0.05416	−0.01449	−0.00580	0.00475	0.00597	−0.00246
$1f(N)$	−8.9[c]	−11.30	−8.98	24.35	2.40477	0.04574	0.99287	0.02939	−0.06480	−0.01420	−0.01893	−0.00223	0.01629
$2p(N)$	−8.0[c]	−8.80	−8.37	22.65	2.43755	0.05615	0.02159	0.98560	0.01674	−0.07468	−0.00200	−0.02507	−0.01475
$0i_{13/2}(N)$	−9.0[c]	−8.79	−7.72	28.65	2.32680	0.99592	0.00061	−0.06269	−0.01598	−0.00869	0.00703	0.01419	0.00138

[a] Reference 67.
[b] Reference 60.
[c] Reference 68.

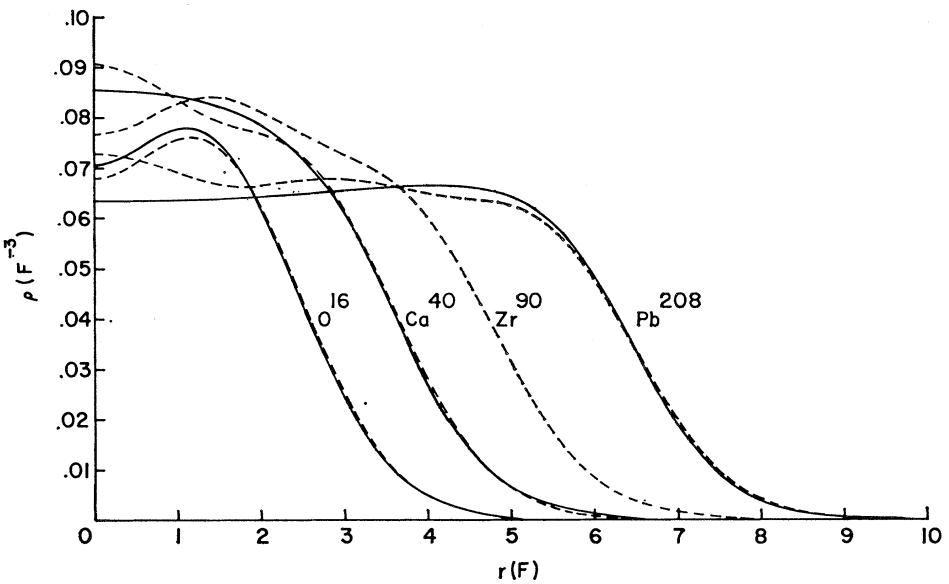

FIG. 6. Theoretical (dashed lines) and empirical (solid lines) charge-density distributions, including proton size and c.m. motion corrections. The empirical distributions for O^{16}, Ca^{40}, and Pb^{208} are from Refs. 72, 69, and 73, respectively.

by at most 1.2 MeV. Since the binding energy discrepancy increases smoothly as one progresses to light nuclei, it is reasonable to attribute the error to the inaccuracy of the LDA in the surface. Quantitatively, the relative error in the potential energy is still quite small, since the error in binding energy per particle should be compared with the average potential energy which is of the order of 50 MeV.

The eigenvalues, density-dependent corrections, and kinetic energies for each state in the five nuclei are tabulated in Table IX. We have not attempted systematic comparison of eigenvalues with the experimental single-particle energies, but the data cited in Refs. 60, 67, and 68 have been included in Table IX, and they generally agree with our eigenvalues within several MeV. One should note that the average starting energies introduced in (3.124) for purposes of orthogonality have the undesirable effect of raising the energy

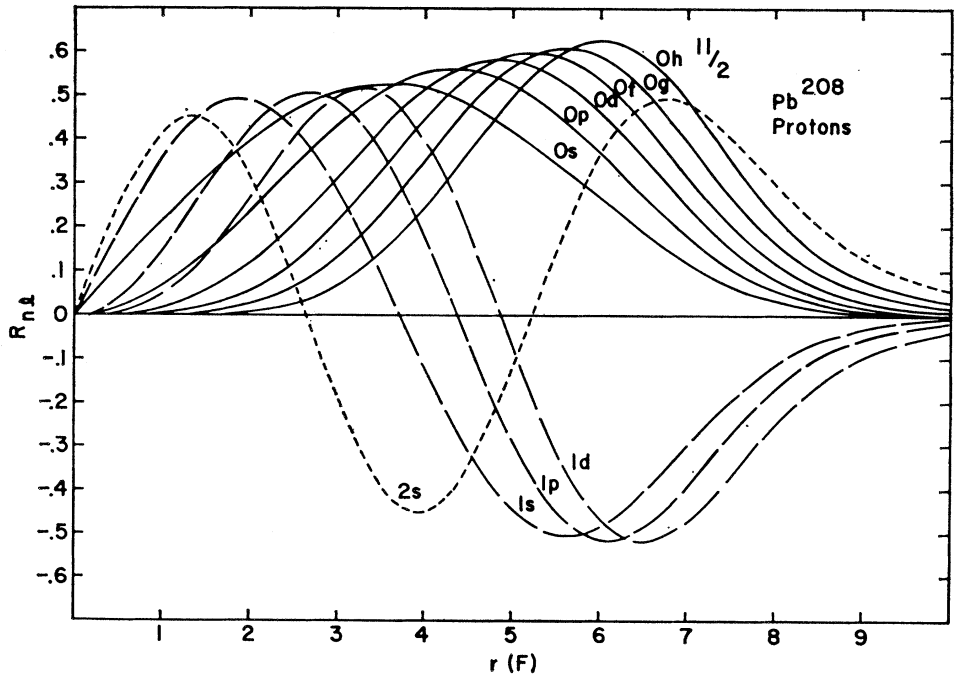

FIG. 7. Single-particle radial functions R_{nl} for protons in Pb^{208}.

[68] E. Rost, Phys. Letters 26B, 184 (1968).

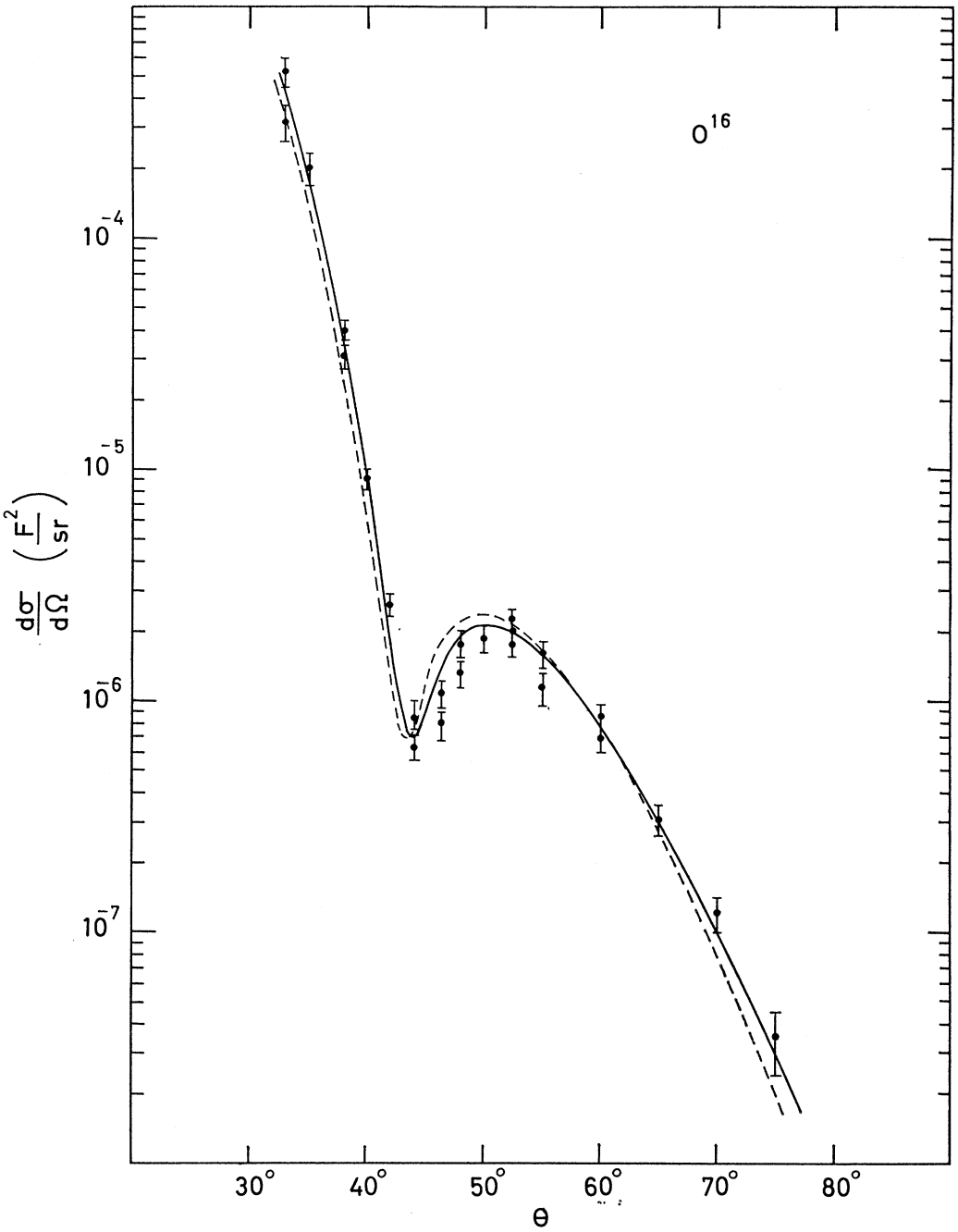

FIG. 8. Electron scattering in DWBA from the theoretical charge distribution (dashed line) and empirical distribution (solid line) for O^{16} at 420 MeV. The experimental data and empirical distribution are from Ref. 72.

of states with high n for a given l and lowering the energy of states with low n. The correction can be estimated in perturbation theory by multiplying the difference between the eigenvalue and average starting energy by an average κ for the appropriate orbital, and is usually of the order of 1 MeV. It appears that in general this theory is able to simultaneously produce the correct binding energy and reasonable single-particle energies primarily because of the sizeable density dependent corrections ΔE_I indicated in Table IX.

Also tabulated in Table IX are the harmonic-oscillator expansion coefficients for the self-consistent radial functions. The size parameter $b=[h/m\omega]^{1/2}$ for each orbital is obtained by maximizing the overlap $\int R_{nl}(r)R_{nl}^{\text{H.O.}}(r)dr$, and the first eight expansion coefficients are calculated using this size parameter. Although an expansion coefficient greater than 0.99 does not necessarily imply that a given radial function is accurately approximated in detail by an harmonic-oscillator function, it is still interesting to observe the

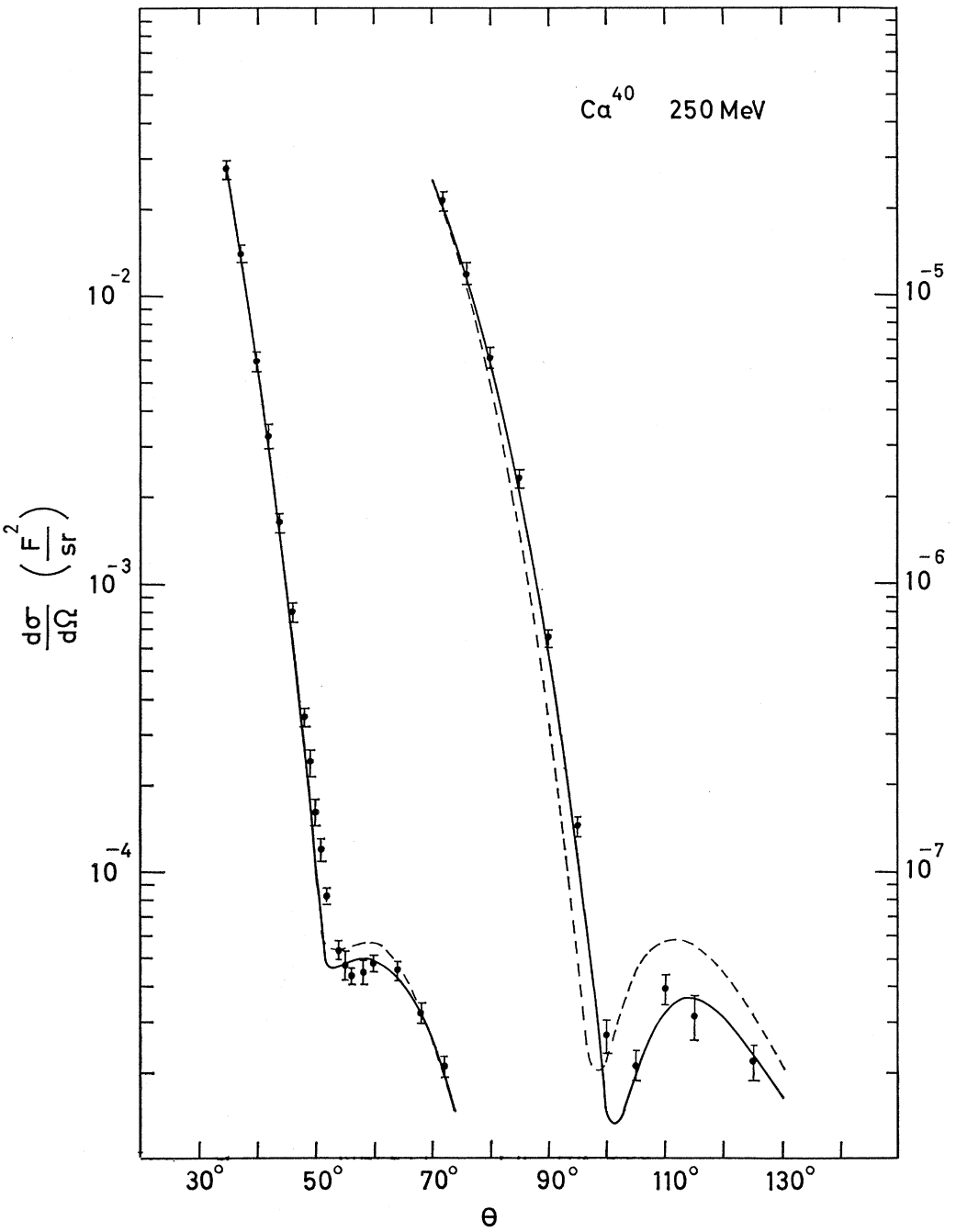

FIG. 9. Electron scattering in DWBA from the theoretical charge distribution (dashed line) and empirical distribution (solid line) for Ca^{40} at 250 MeV. The experimental data and empirical distribution are from Ref. 69.

large overlaps obtained even in Pb^{208}, and that the overlaps generally are highest for states with the lowest number of nodes. One should note that the expansion coefficients do not fall off particularly rapidly with n, and that even higher terms are non-negligible, as may be seen by comparing the sum of the squares of the coefficients with unity. The eight terms tabulated give a reasonable approximation to the wave functions for all practical purposes. The eight term expansion generally agrees with the radial functions to within 0.5%, except in the extreme tail, and of course oscillates about the true radial functions so that the average agreement is much better. The error in the extreme tail may easily be corrected by attaching an exponential tail using the tabulated eigenvalues.

Electron Scattering and Density Distributions

A crude evaluation of the validity of calculated radial functions may be obtained by comparing the resulting charge distribution, corrected for c.m. motion and

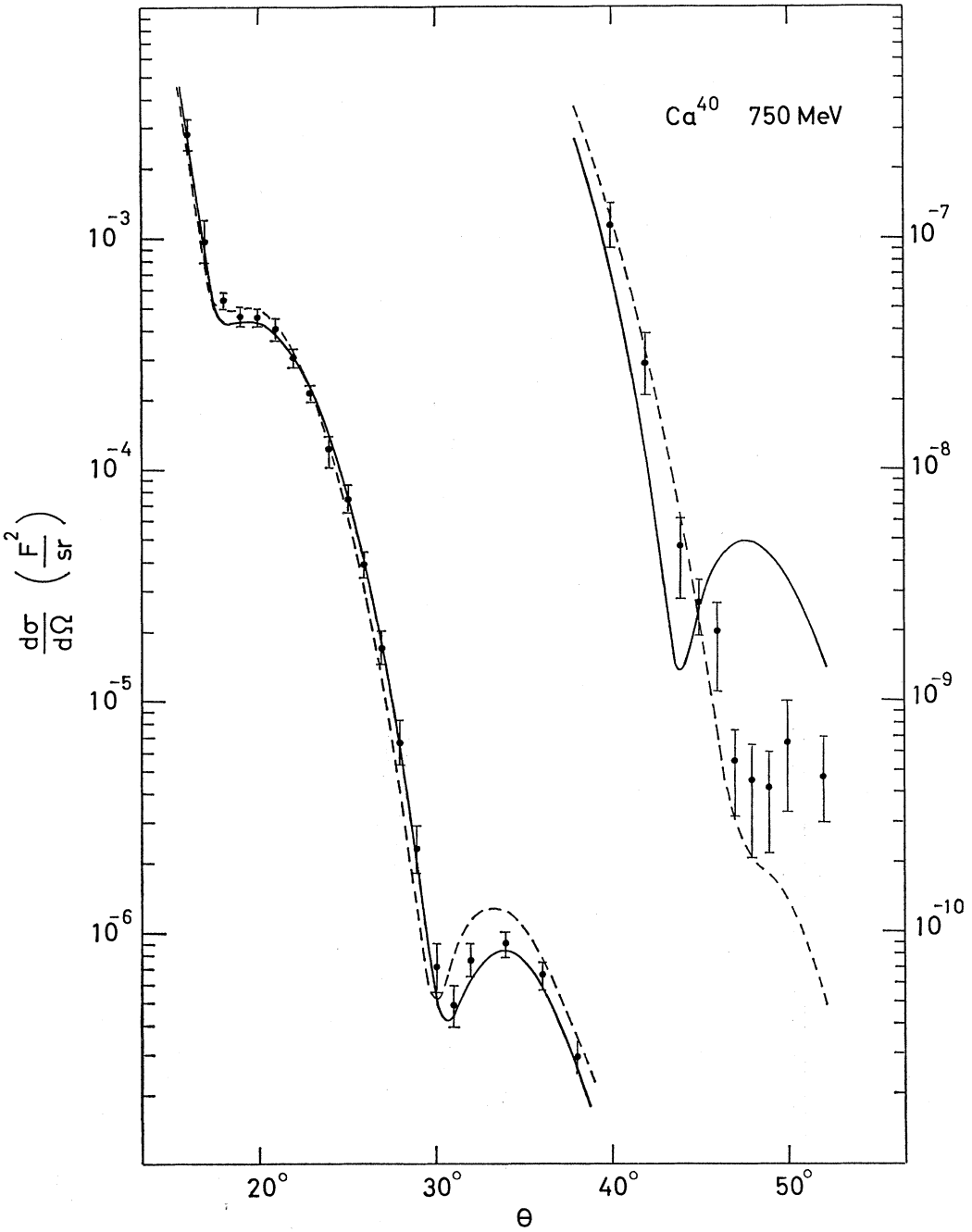

FIG. 10. Electron scattering in DWBA from the theoretical charge distribution (dashed line) and empirical distribution (solid line) for Ca^{40} at 750 MeV. The experimental data and empirical distribution are from Ref. 69.

proton size, with the empirical distribution derived from electron scattering. In Figure 4, several distributions for Ca^{40} are compared with the three-parameter distribution of Bellicard *et al.*[69] The simple HF calculation, which omits the $\partial V/\partial\rho$ rearrangement terms in the radial equation and uses the bare effective interaction, clearly yields far too much central density. It is reassuring to note that this density distribution is very similar to that obtained in a HF calculation by Davies[70] using Kuo's matrix elements. Using the bare interaction, but performing the full density-dependent HF calculation by including the $\partial V/\partial\rho$ terms, the curve in Fig. 4 indicates very significant improvement. Finally, the theoretical and empirical distributions virtually

[69] J. B. Bellicard, P. Bounin, R. F. Frosch, R. Hofstadter, J. S. McCarthy, F. J. Uhrhane, M. R. Yearian, B. C. Clark, R. Herman, and D. G. Ravenhall, Phys. Rev. Letters **19**, 527 (1967); R. F. Frosch, R. Hofstadter, J. S. McCarthy, G. K. Nöldeke, K. J. van Oostrum, and M. R. Yearian, Phys. Rev. **174**, 1380 (1968).

[70] K. T. R. Davies (private communication).

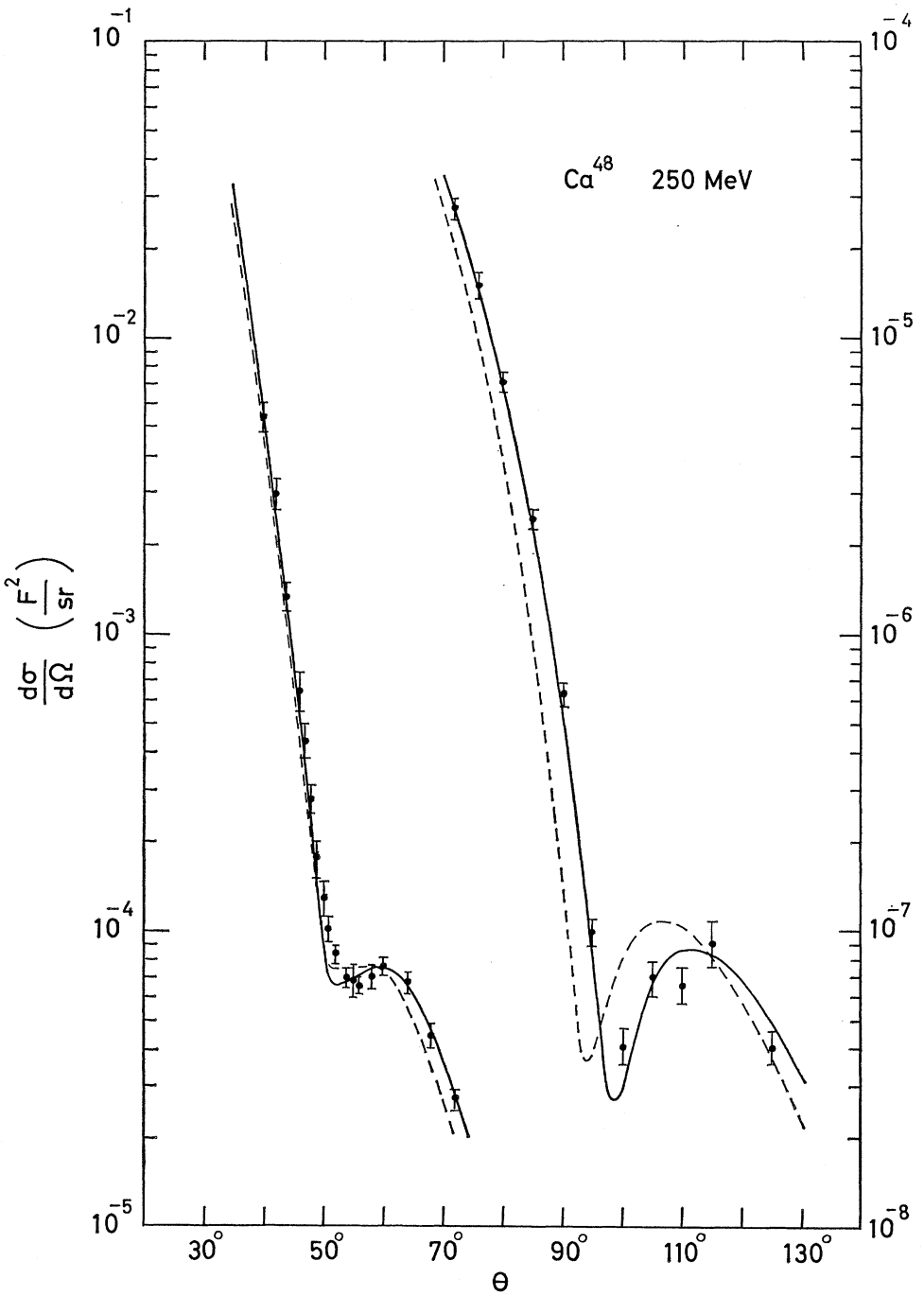

FIG. 11. Electron scattering in DWBA from the theoretical charge distribution (dashed line) and empirical distribution (solid line) for Ca^{48} at 250 MeV. The experimental data and empirical distribution are from Ref. 69.

coincide in the surface when the parameters given in (4.10) are used in the effective interaction. The subsequent results discussed in this section all refer to the full density-dependent theory with this set of parameters.

The proton and neutron densities with no c.m. or size corrections for O^{16}, Ca^{40}, Zr^{90}, and Pb^{208} are shown in Fig. 5. Ignoring the interior oscillations, it is interesting to note the similarity in shape of proton and neutron densities and that the surface has essentially the same slope for all the nuclei. The similarity of proton and neutron distributions is in disagreement with the recent optical potential analysis of Greenlees,[71] and we attribute the discrepancy to his omission of density dependence. In Fig. 6, the charge distributions

[71] G. W. Greenlees, G. J. Pyle, and Y. C. Tang, Phys. Rev. 171, 1115 (1968).

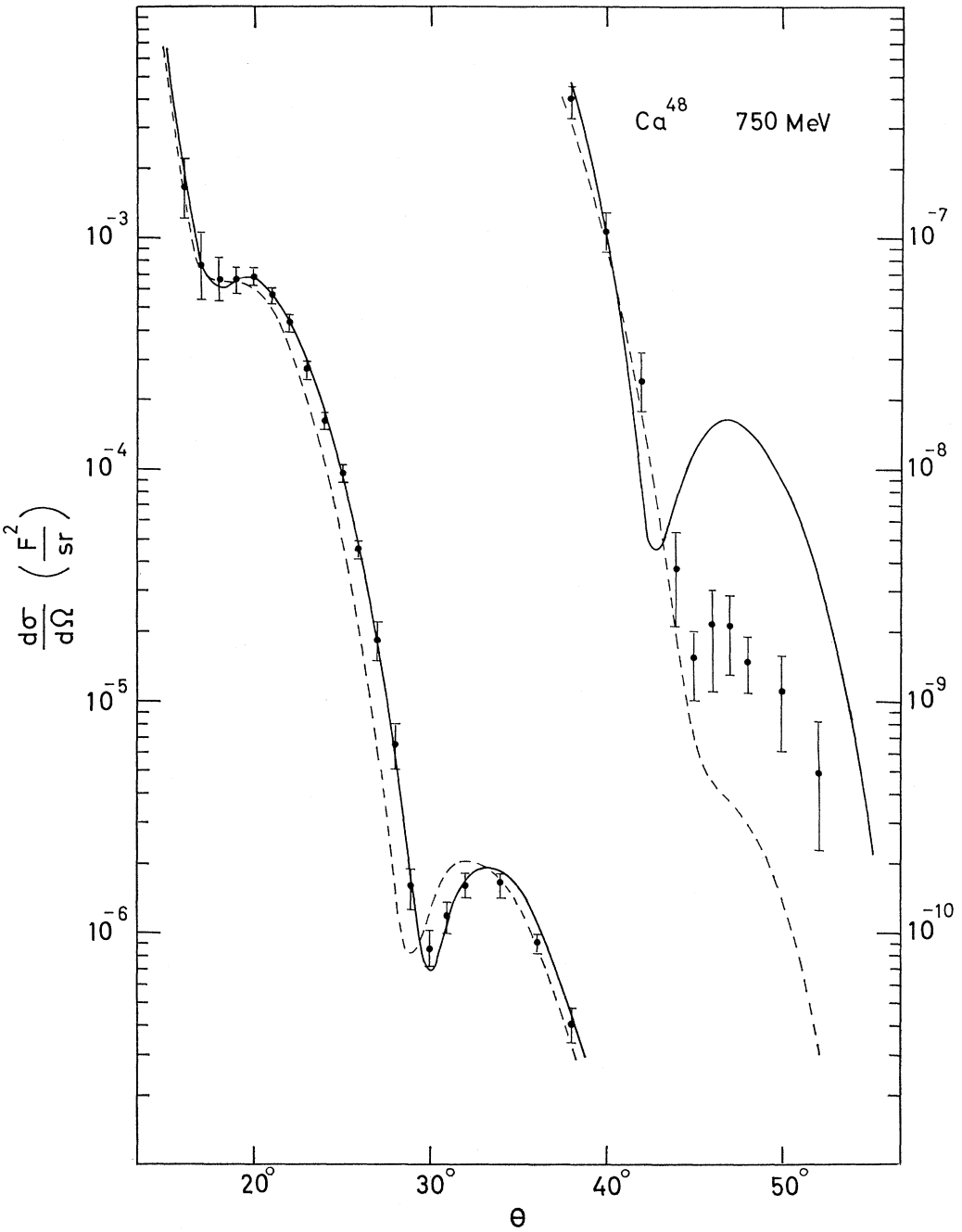

FIG. 12. Electron scattering in DWBA from the theoretical charge distribution (dashed line) and empirical distribution (solid line) for Ca^{48} at 750 MeV. The experimental data and empirical distribution are from Ref. 69.

for these nuclei, including c.m. and proton size corrections, are compared with empirical distributions.[69,72,73] It is evident that the oscillations in the interior are significantly reduced by the finite proton size, and the agreement in the surface already demonstrated for Ca^{40} is seen to be equally satisfactory for the other nuclei. Individual proton radial functions for Pb^{208} are shown in Fig. 7.

From Figs. 4 and 6, it is evident that comparison with empirical distributions provides only a qualitative test of the validity of the theoretical distributions. Since electron scattering is most sensitive to the position and magnitude of the maximum slope, it is clear that one should strive to reproduce the empirical distributions in the surface, but it is impossible to determine the quantitative significance of discrepancies without

[72] H. F. Ehrenberg, R. Hofstadter, U. Meyer-Berkhout, D. G. Ravenhall, and S. E. Sobottka, Phys. Rev. **113**, 666 (1959).
[73] J. B. Bellicard and K. J. van Oostrum, Phys. Rev. Letters **19**, 242 (1967).

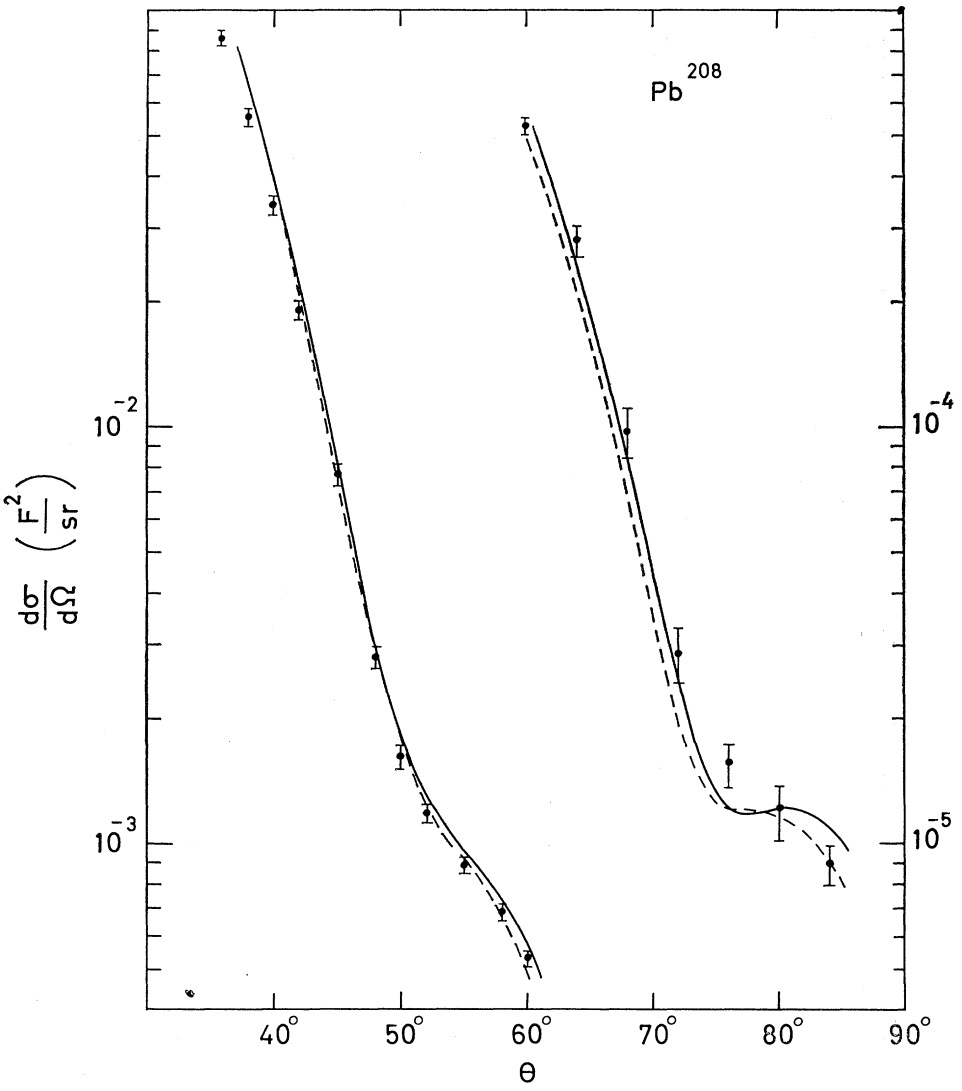

FIG. 13. Electron scattering in DWBA from the theoretical charge distribution (dashed line) and empirical distribution (solid line) for Pb^{208} at 250 MeV. The experimental data and the empirical distribution are from Ref. 73, and we have used the distribution which was fit to both the 175- and 250-MeV data.

calculating the electron scattering predicted for the theoretical distributions. In addition, one obtains complementary information about the charge distribution from the analysis of muonic x rays, and this provides in some respects a far more sensitive test of charge distributions.

Although ideally, it would be desirable to calculate electron scattering using the full partial wave analysis, such calculations would be rather lengthy for the large number of distributions we wish to study in this work. Hence, we have used the approximate distorted-wave Born approximation of Yennie, Boos, and Ravenhall.[74] In this approximation, all orders of contributions by soft photons are approximately included by using eikonal wave functions for the incoming and outgoing waves, and the single exchange of a hard photon is included by using these wave functions in first Born approximation. Thus, the approximate scattering amplitude is

$$f=(k/2\pi)\int \phi_{k_F}^{(-)\dagger} V(r)\phi_{k_I}^{(+)} d^3r. \qquad (4.11)$$

Details of the calculation of electron scattering are presented in Appendix B.

Recognizing that there exist non-negligible discrepancies between the full partial-wave analysis and the approximate distorted wave analysis of the same charge distribution, our electron scattering results should not be compared directly with the experimental cross sections. The most consistent procedure would be to shift the experimental data by the discrepancy between the partial-wave and distorted-wave results for the empirical distribution fit by the experimenters,

[74] D. R. Yennie, F. L. Boos, and D. G. Ravenhall, Phys. Rev. **137**, B882 (1965).

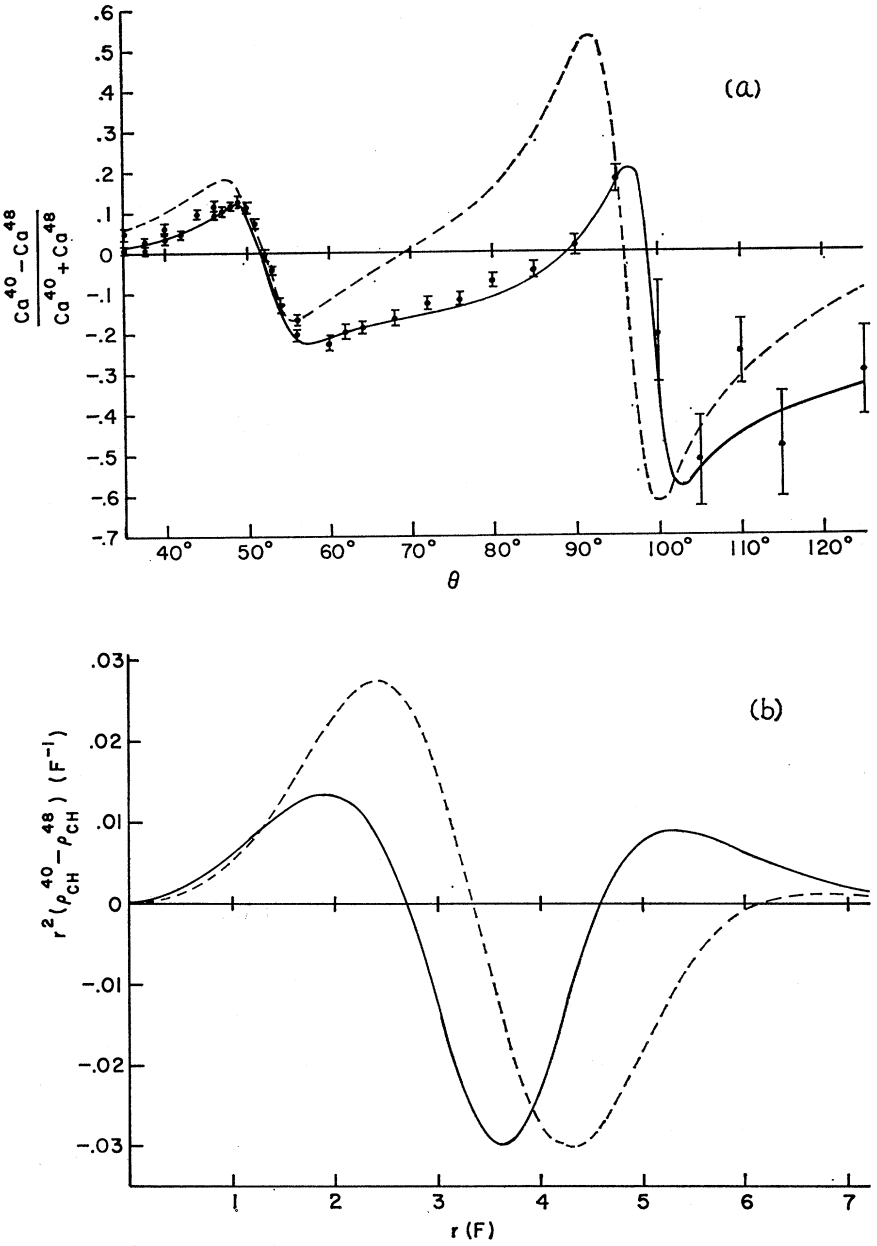

FIG. 14. Ca^{40}-Ca^{48} isotope shift for the empirical charge distributions of Ref. 69 (solid lines) and the density-dependent HF distributions (dashed lines). The experimental data for the ratio of the difference of the electron scattering cross sections to the sum of the cross sections in (a) are from Ref. 69. The theoretical charge distribution difference in (b) contains the proton size correction and the appropriate c.m. motion corrections for Ca^{48} and Ca^{40}.

yielding a set of pseudo-experimental data with which subsequent distorted-wave calculations should be compared. Since one of the distorted-wave parameters is unrealistically sensitive to density oscillations in the interior of the nucleus, as described in Appendix B, the parameters calculated for the empirical distribution are used for the analysis of all other density distributions. For the results presented in this section we have not shifted the experimental data, but rather have plotted the distorted-wave results for the empirical distributions as well as our theoretical distributions. Hence, except in regions in which the partial-wave analysis presented in the original experimental references does not fit the data, our curves should be compared with the empirical curves instead of the experimental data. In regions in which the partial-wave analysis of the empirical distributions disagrees seriously with experiment, the discrepancy is large compared with the error in the distorted-wave analysis, so that comparison with the experimental data is sufficient.

The electron scattering results from charge distributions obtained from our density-dependent HF wave functions are presented in Figs. 8–13. In general, one observes that the agreement is quite satisfactory. The 750-MeV results for the calcium isotopes in Figs. 10 and 12 are especially interesting. It is clear that our distribution is slightly in error at the second maximum (regarding the forward peak as the first maximum), but it is far superior to the three-parameter fit at the

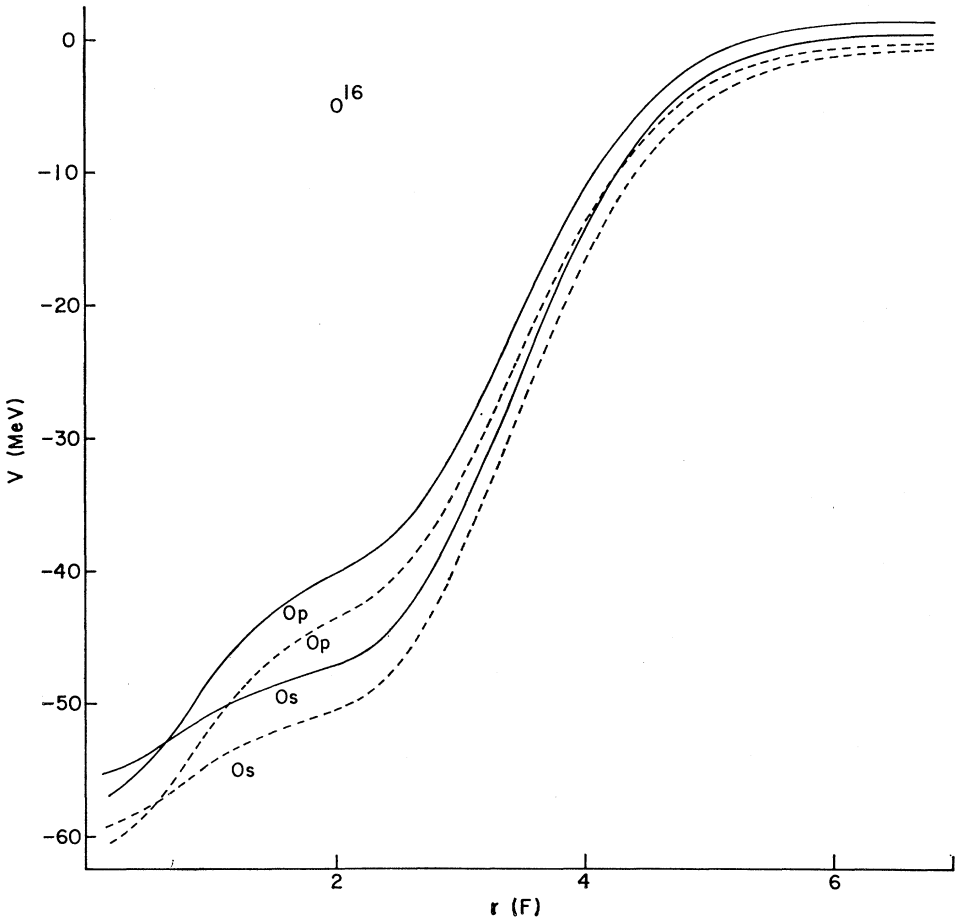

FIG. 15. Equivalent local single-particle proton (solid lines) and neutron (dashed lines) potentials for O^{16} as defined in Eq. (4.12).

third maximum. At the third maximum the scattering is sensitive to the interior oscillations arising from the s-shell wave functions, and thus it appears that our theory yields approximately the correct density oscillations. In Pb^{208} (Fig. 13) it is also evident that our density distribution reproduces the qualitative behavior of the scattering at high momentum transfer better than the best three-parameter fit.

One of the most sensitive tests of the detailed structure of our theoretical density distributions is the calcium isotope shift. Experimentally, the difference in electron scattering between Ca^{40} and Ca^{48} may be measured more accurately than the absolute cross section of either isotope alone.[75] The experimental differences in cross section and the difference in charge density between the best three-parameter fits to the 250-MeV data are shown in Fig. 14. From the shape of the density difference, one may deduce that $\langle r \rangle$ increases from Ca^{40} to Ca^{48}, whereas $\langle r^2 \rangle^{1/2}$ decreases. The shift in muonic x rays by this change in charge distribution agrees with the experimental x-ray measurements.[69] Hence, the experimental situation is quite consistent, and one might aspire to understand this isotope shift in terms of our density-dependent HF theory.

From the results shown in Fig. 14, it is clear that the present theory cannot explain the isotope shift. Whereas the experiments indicate that roughly as much charge is pulled in from the tail as is pulled out from the interior, the density-dependent HF calculation indicates that the $f_{7/2}$ neutrons primarily pull protons out from the interior and not in from the tail. Corrections due to short-range correlations, the error from approximating the $0d_{5/2}$ and $0d_{3/2}$ orbitals by a single average $0d$ orbital, and the effect of changing the $0f_{7/2}$ neutron distribution by adjusting the spin-orbit potential are discussed below in connection with Figure 24, but are too small to account for the difference.

The most plausible explanation of the isotope shift is that Ca^{40} is not a perfectly closed shell, but rather includes non-negligible admixtures of proton states in the $1p$-$0f$ shell. Gerace and Green[76] have shown that the Ca^{40} ground state contains a large deformed component, due to the fact that the energy gap for the Nilsson levels becomes small for large deformation.

[75] R. D. Ehrlich, D. Fryberger, D. A. Jensen, C. Nissim-Sabat, R. J. Powers, V. L. Telegdi, and C. K. Hargrove, Phys. Rev. Letters **18**, 959 (1967).

[76] W. J. Gerace and A. M. Green, Nucl. Phys. **A93**, 110 (1967).

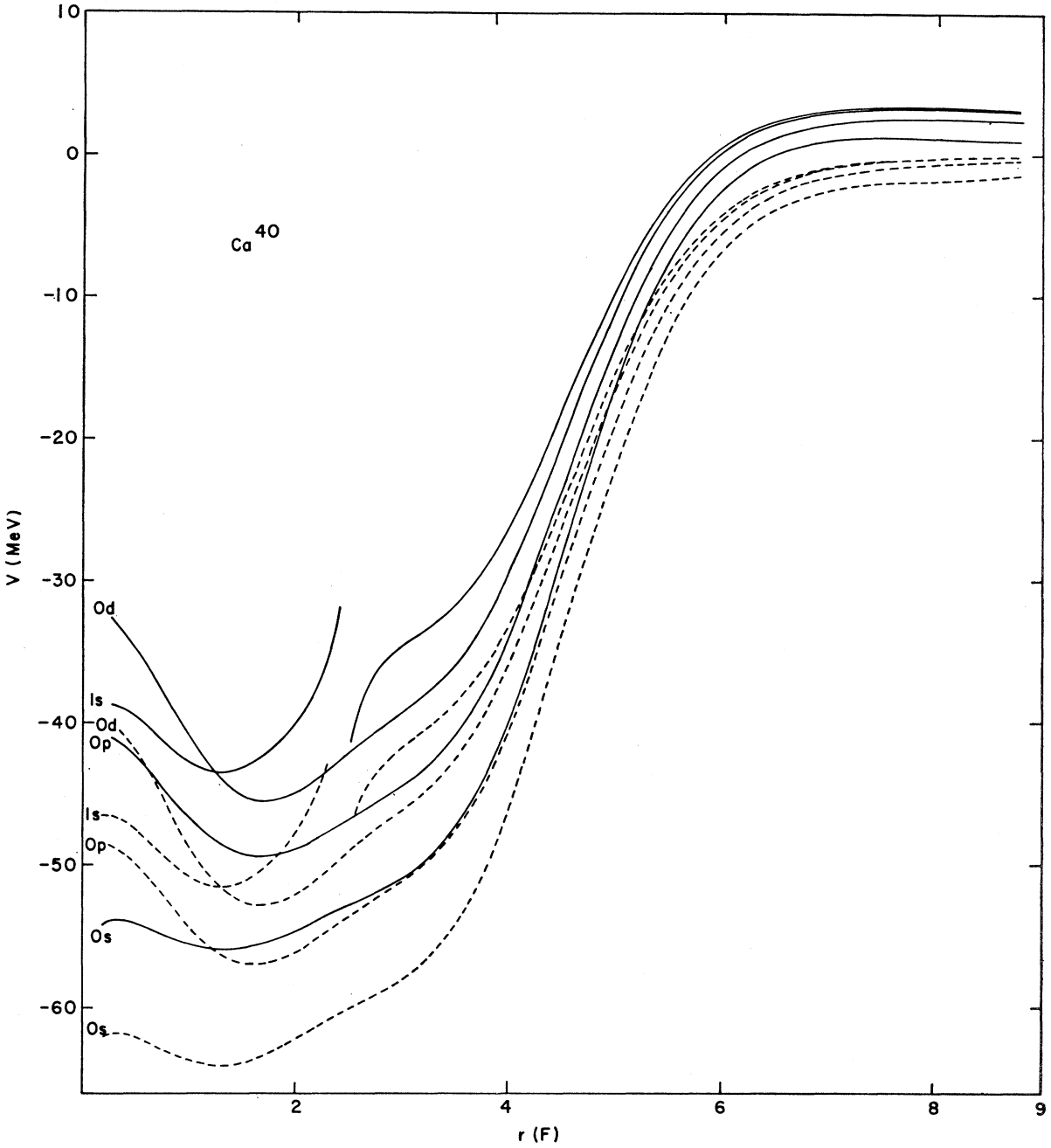

FIG. 16. Equivalent local single-particle proton (solid lines) and neutron (dashed lines) potentials for Ca^{40}.

The spherical average of their deformed-wave function is calculated in Appendix C, and is shown to differ negligibly from the spherical case. Then, the main effect of their ground state is that 20% of the time, one proton is excited into the $1p$-$0f$ shell, which is not sufficient to account for the isotope shift. Whereas this particular calculation cannot explain the effect, it is reasonable to expect that a sufficiently careful calculation of the Ca^{40} ground state, allowing admixtures of states in the $1p$-$0f$ shell, and using matrix elements of the effective interaction may yield satisfactory agreement.

Equivalent Local Single-Particle Potential

It is instructive to define an equivalent one-body local potential which reproduces the eigenvalues and radial functions of the density-dependent HF theory. Multiplying and dividing the exchange term of the radial equation (3.121) by the self-consistent radial function, we obtain the formally equivalent equation

$$\{-(\hbar^2/2m)[d^2/dr^2-l(l+1)/r^2]+V_I^{EL}(r)-E_I\}R_I(r)=0, \quad (4.12)$$

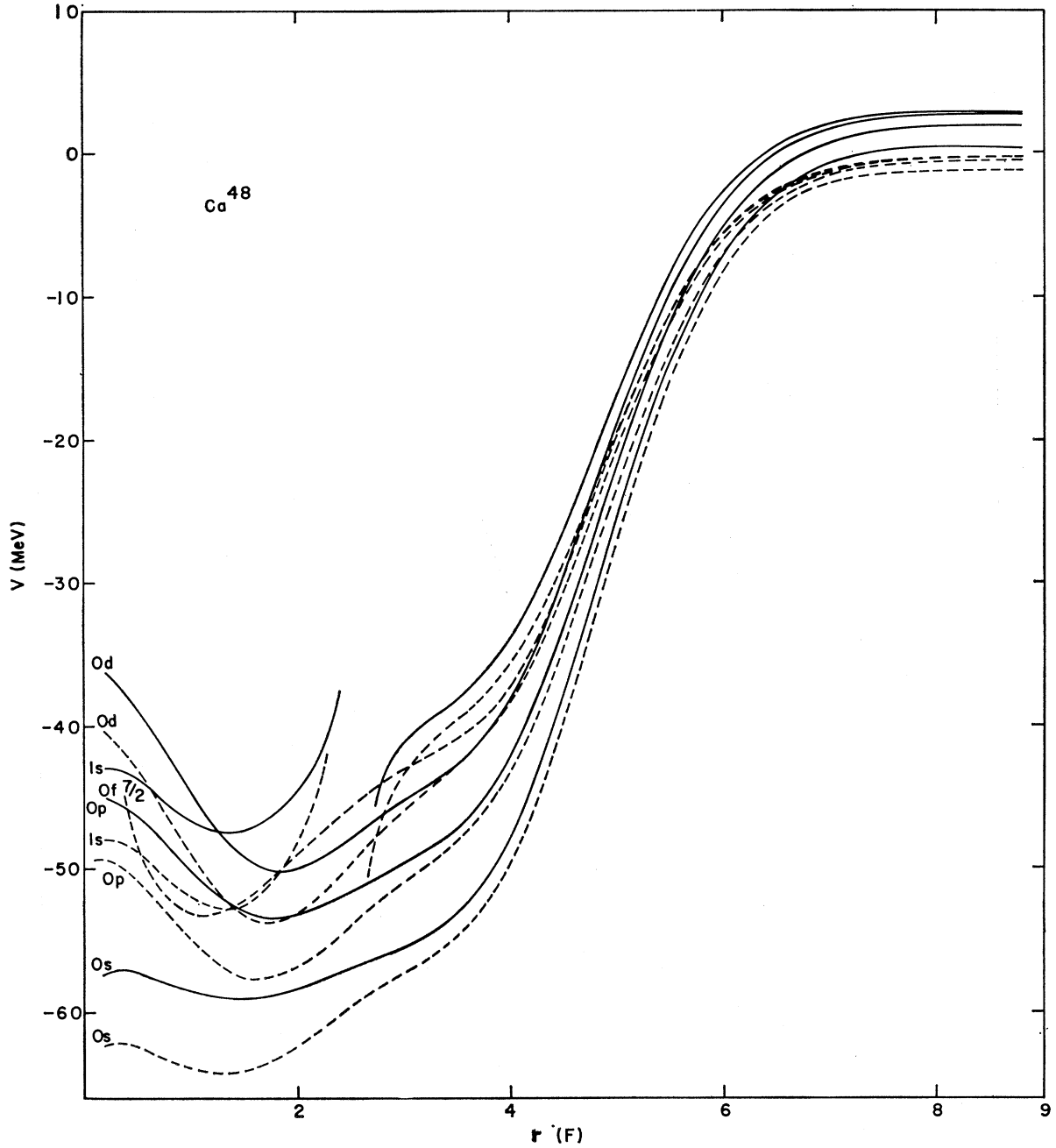

FIG. 17. Equivalent local single-particle proton (solid lines) and neutron (dashed lines) potentials for Ca^{48}.

where

$$V_I^{EL}(r) = \mathfrak{F}_I^D(r) - \hbar^2 l(l+1)/2mr^2 + \int dr' \mathfrak{F}_I^E(r, r') R_I(r')/R_I(r).$$

For states with no nodes, V_I^{EL} may be compared directly with phenomenological potentials, whereas for the remaining states, the singularities arising from the nodes should be ignored. Physically, it is clear from perturbation theory that solving the Schrödinger equation in a potential defined by smoothly joining V_I^{EL} in the region of singularities must give eigenvalues and radial functions which differ negligibly. For high angular-momentum states, since $R_{nl}(r) \sim r^{l+1}$ at the origin, V^{EL} is again badly defined, but this is unimportant physically because of the dominance of the angular-momentum barrier in this region.

The equivalent local potentials for the density-dependent HF theory are shown in Figs. 15–21. The most outstanding property is the significant state dependence, arising primarily from the exchange force. This state dependence is crucial in obtaining reasonable density distributions as may be seen by attempting to

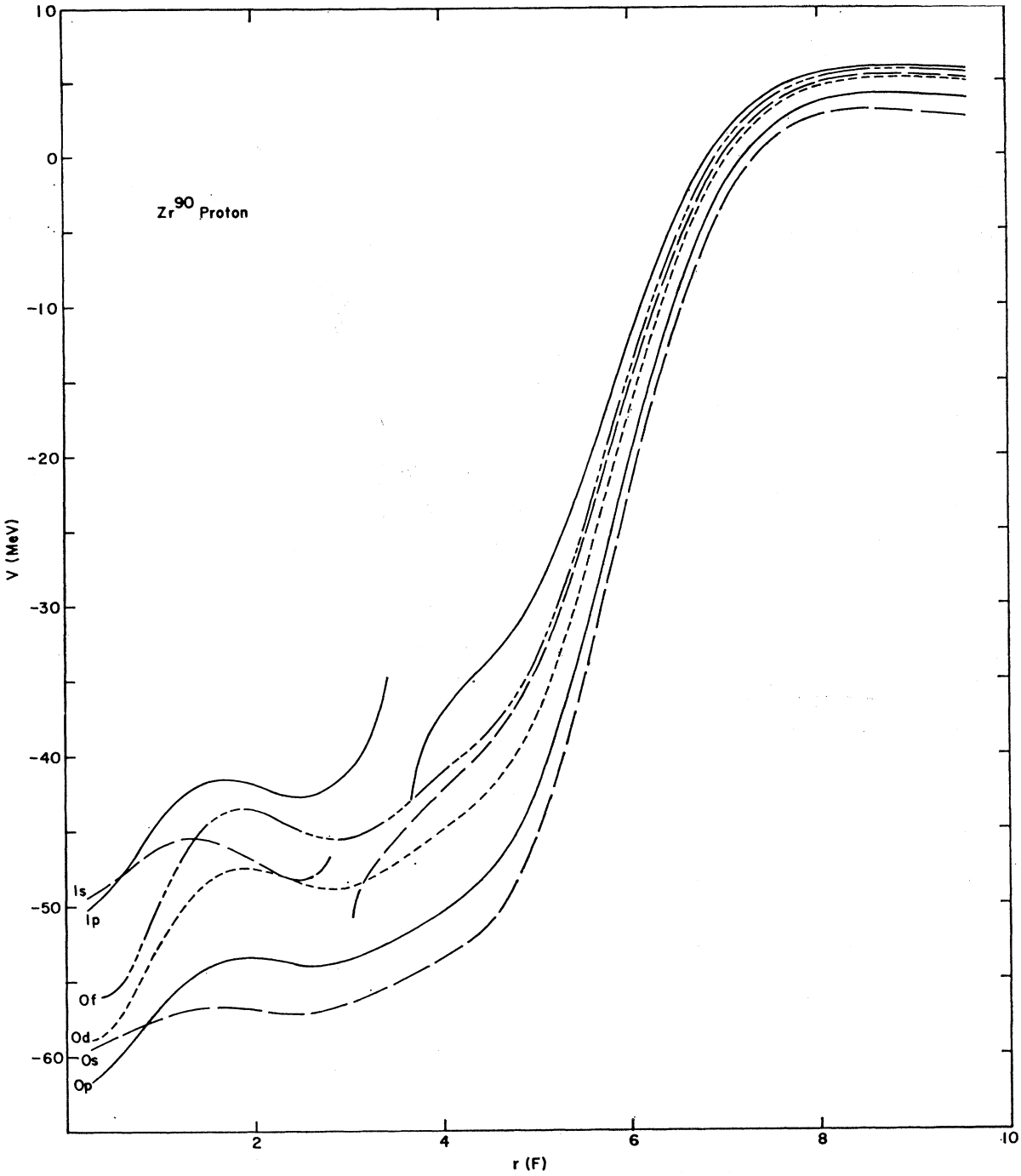

FIG. 18. Equivalent local single-particle proton potentials for Zr^{90}.

construct the density by filling a harmonic-oscillator or Woods-Saxon well. The anomalous neutron radius obtained by Rost[68] in attempting to fit single-particle energies with a state-independent potential is a further indication of the importance of state dependence.

A second important feature of these equivalent local potentials is that the depth of the 0*s* state potential in the interior is essentially the same in all nuclei, being approximately −55 MeV for protons and −65 MeV for neutrons. The saturation of this potential is unique to this density-dependent theory, and is experimentally substantiated by the 0*s* single-particle energies of James *et al.*[67]

The qualitative behavior of the individual potentials follows fairly directly from the properties of the effective interaction. The oscillations in the neutron or proton potentials reflect primarily the oscillations in the total density of the protons or neutrons, respectively,

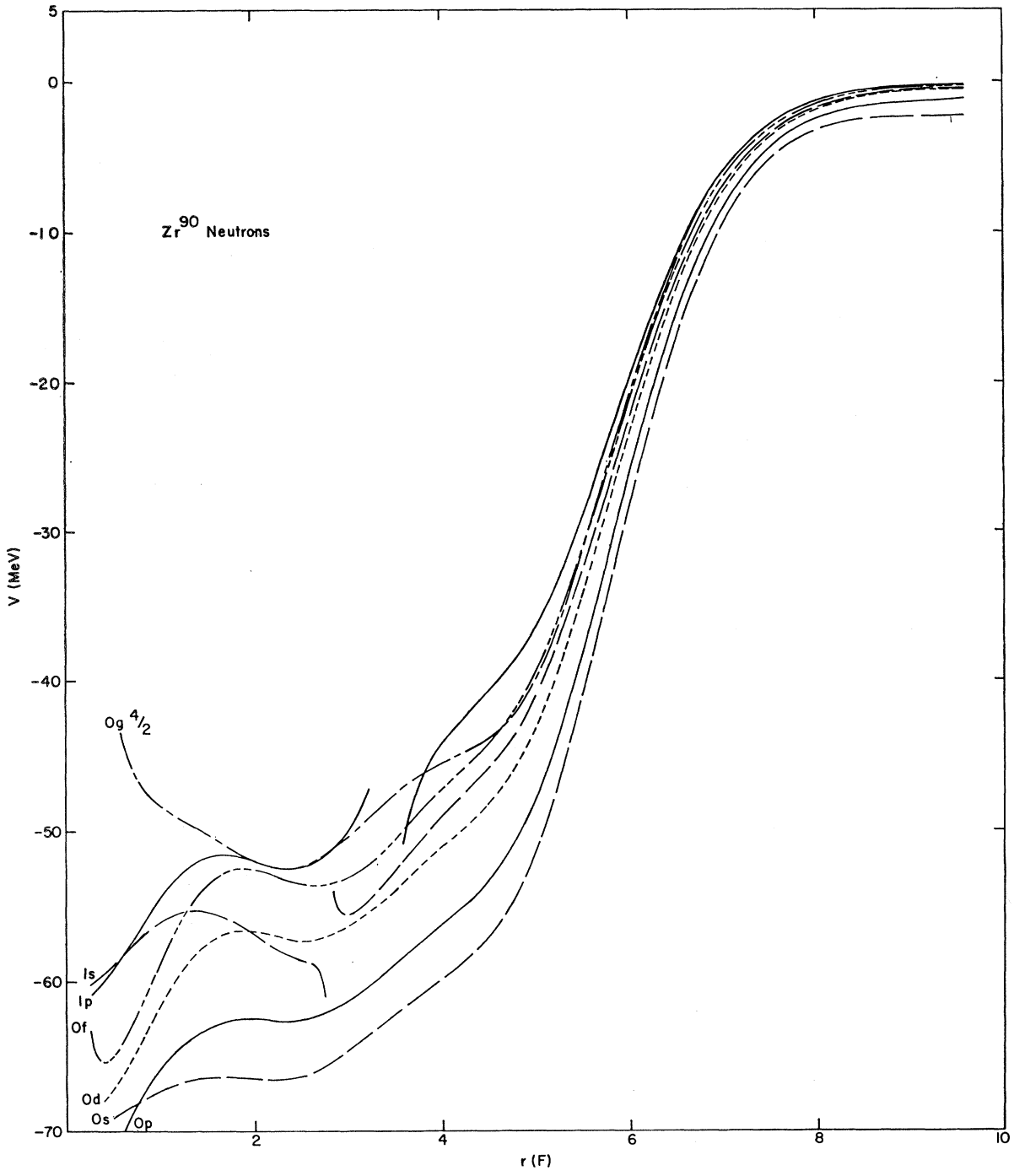

FIG. 19. Equivalent local single-particle neutron potentials for Zr^{90}.

since the unlike interaction is much stronger than the like interaction. In O^{16} and Ca^{40}, the corresponding neutron and proton potentials differ by the full Coulomb energy, whereas in the heavier nuclei, the neutron excess contributes more attraction to the protons than to the neutrons, so that the corresponding neutron and proton potentials do not differ by the full Coulomb energy until the extreme tail. Hence, in the heavy nuclei, the proton potential has a steeper surface than the neutron potential. Finally, one notes that the neutron or proton potentials do not approach zero or the Coulomb potential as rapidly as the density approaches zero. Rather,

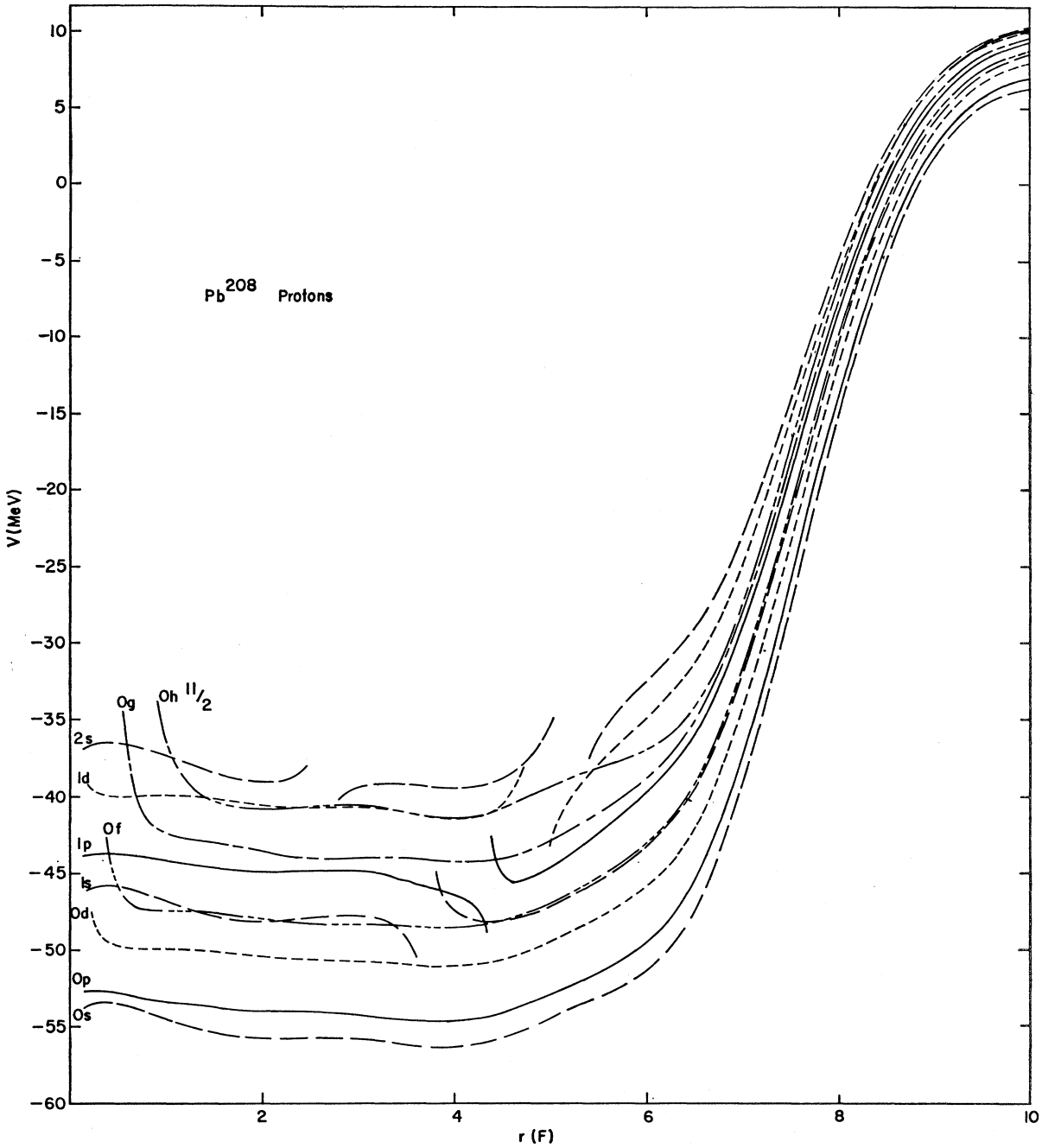

FIG. 20. Equivalent local single-particle proton potentials for Pb^{208}.

they decay to within several MeV of the appropriate limit roughly as the density, and then fall off very much more slowly, due to the long range of OPEP.

Short-Range Correlation Corrections

Thus far, we have only considered the lowest-order contribution to the density expansion, Fig. 2(A). We have previously argued that the total contribution from diagrams B–I should be small so we shall now concentrate our attention on diagrams J and K, which we shall refer to as the particle and hole corrections, respectively. Explicit calculations will be performed only for calcium.

The contribution from the hole diagram may be written

$$\Delta\rho_{\text{hole}}(\mathbf{r}) = -\tfrac{1}{2}\sum_{m'mn,ab}\langle m'n-nm' \mid G/e \mid ab\rangle \times\langle ab \mid G/e \mid mn-nm\rangle\Phi_m^*(\mathbf{r})\Phi_{m'}(\mathbf{r}), \quad (4.13)$$

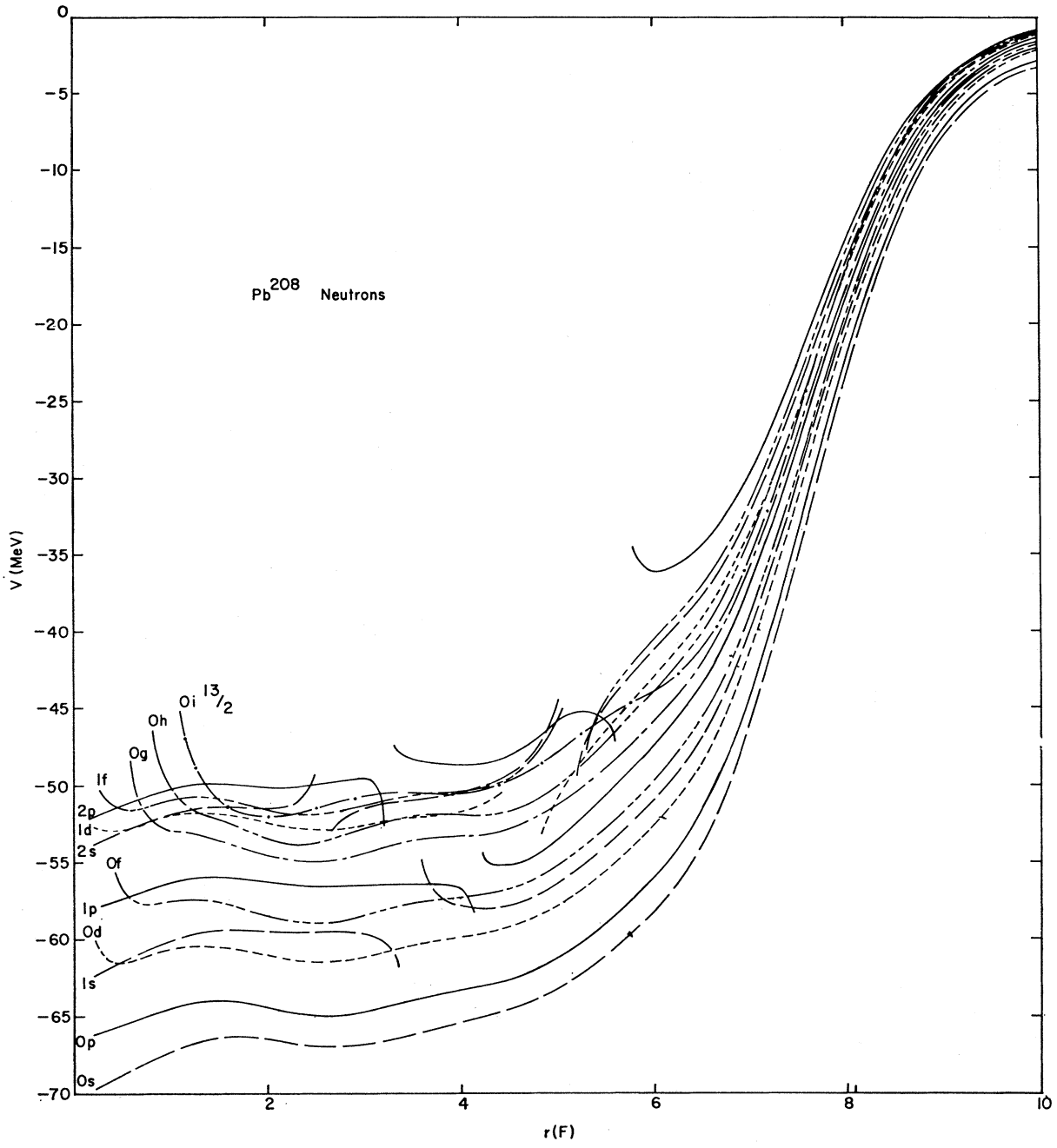

FIG. 21. Equivalent local single-particle neutron potentials for Pb^{208}.

where the factor of $\frac{1}{2}$ arises because there is one equivalent pair of lines and the sign is negative because the number of closed loops plus the number of hole lines is odd. From (2.1), it follows that $(QG/e)\Phi_{mn}=\zeta_{mn}$, so that it is convenient to denote $QG/e=\hat{\zeta}$. Noting that a and b are summed only over intermediate states, we may use closure by inserting the projector Q in both matrix elements and extending the sum on a and b over all states. Thus,

$$\begin{aligned}\Delta\rho_{\text{hole}}(\mathbf{r}) &= -\tfrac{1}{2}\sum_{m'mn}\langle m'n-nm' \mid (GQ/e)(QG/e) \mid mn \\ &\quad -nm\rangle\Phi_m(\mathbf{r})^*\Phi_{m'}(\mathbf{r}) \\ &= -\sum_{m'mn}\langle m'n \mid \hat{\zeta}^\dagger\hat{\zeta} \mid mn-nm\rangle\Phi_m^*(\mathbf{r})\Phi_{m'}(\mathbf{r}). \quad (4.14)\end{aligned}$$

The essential simplification which reduces (4.14) to a manageable form is the following approximation suggested by Brandow[77]

$$\langle \mathbf{rR} \mid \zeta \mid nm \rangle = \zeta(\mathbf{r}, \mathbf{R}, W_{mn}) \Phi_m(\mathbf{R}) \Phi_n(\mathbf{R}). \quad (4.15)$$

The physical motivation for (4.15) is that due to the wave function healing, the defect function is zero everywhere except in a small region of space about R, and, in this region, it should be approximately spherically symmetrical and represented by the nuclear-matter defect function at the local density with the starting energy W_{mn}. Using the definition of κ in (3.3), we obtain

$$\kappa(R, W) = \rho(R) [\int \zeta^*(r', R, W) \times \zeta(r', R, W)^{(\mathrm{D-E})} d^3r'] (\text{spin, isospin, average}), \quad (4.16)$$

where the R dependence indicates dependence on the local density, and (D-E) indicates direct minus exchange. For nuclei with identical neutron and proton wave functions, the spin and isospin average in (4.14) is the same as in nuclear matter, so that substituting (4.15) and (4.16) in (4.14), we obtain

$$\Delta\rho_{\mathrm{hole}}(\mathbf{r}) = -4 \sum_{\hat{m}\hat{m}'} d^3R \Phi_{m'}{}^*(R) \Phi_{m'}(r) \times \Phi_m(R) \Phi_m{}^*(r) \kappa(R, W), \quad (4.17)$$

where $W = \frac{1}{2}(\mid E_m \mid + \mid E_{m'} \mid) + (1/A) \sum_n \mid E_n \mid$, $\hat{m}$ indicates all the quantum numbers of state m except spin and isospin, and the statistical factor is 4 instead of 16 because m and m' must be in the same charge and spin state. Rather than explicitly calculating the exchange density, we note that in Ca^{40}, the integral over angles yields orthogonality between all but the $0s$ and $1s$ states, and since the $0s$ wave function is concentrated in the interior where $\kappa(R)$ is roughly constant, the radial integral of the $0s$ and $1s$ wave functions with $\kappa(R)$ is approximately zero. Thus, to a good approximation, for Ca^{40}

$$\Delta\rho_{\mathrm{hole}}(r) = -(4/4\pi) \sum_{\hat{m}} [R_m{}^2(r)/r^2] \times \int R_m{}^2(R) \kappa(R, W_m) dR, \quad (4.18)$$

where

$$W_m = \mid E_m \mid + (1/A) \textstyle\sum_n \mid E_n \mid .$$

The correction for the proton density is simply $\frac{1}{2}\Delta\rho_{\mathrm{hole}}(r)$.

The situation for Ca^{48} is more complicated, since we should define separate functions $\zeta(r, R, W_{mn})$ for like and unlike particles, in exact analogy with the definition of like and unlike forces. Then the correction to the proton density for Ca^{48} should be

$$\Delta\rho_{\mathrm{hole}}{}^{\mathrm{prot}}(r) = -(2/4\pi) \sum_{\hat{m}_{\mathrm{core}}} [R_m{}^2(r)/r^2] \int R_m{}^2(R) \times \{ \sum_{\hat{n}_{\mathrm{core}}} [R_n{}^2(R)/4\pi R^2] \int \zeta_{\mathrm{av}}{}^*(r', R, W_{mn}) \times \zeta_{\mathrm{av}}(r', R, W_{mn})^{(\mathrm{D-E})} d^3r' + \sum_{\hat{n}f} [R_n{}^2(R)/4\pi R^2] \int \zeta_{\mathrm{un}}{}^*(r', R, W_{mn}) \times \zeta_{\mathrm{un}}(r', R, W_{mn})^{(\mathrm{D-E})} d^3r' \} dR, \quad (4.19)$$

where core refers to the Ca^{40} core and f refers to the $f_{7/2}$ neutrons. For our rough calculation, we shall not evaluate ζ_{un}, but rather use ζ_{av} for the $f_{7/2}$ level as well, so that (4.19) reduces to (4.18) with the ρ appearing in κ now being the total density including the $f_{7/2}$ level. Since the unlike force contains more triplet-s and less singlet-s components than the average force, this approximation omits some of the tensor force contribution to ζ which is described below.

The particle diagram contribution, Fig. 2(J), is

$$\Delta\rho_{\mathrm{part}}(\mathbf{r}) = \tfrac{1}{2} \sum_{mnaa'b} \langle mn-nm \mid G/e \mid a'b \rangle \langle a' \mid \mathbf{r} \rangle \times \langle \mathbf{r} \mid a \rangle \langle ab \mid G/e \mid mn-nm \rangle, \quad (4.20)$$

where the sign is positive because there is one less hole line than in the hole diagram. If a and a' are proton states, it is clear that both m and n cannot be neutrons. Then inserting Q, performing closure over a and a', and approximating ζ_{un} by ζ_{av}, the correction to the proton density is

$$\begin{aligned}
\Delta\rho_{\mathrm{part}}{}^{\mathrm{prot}}(\mathbf{r}) &= \sum_{\text{all } n,m=\mathrm{prot}} \int \langle mn \mid \zeta^\dagger \mid \mathbf{rs} \rangle \langle \mathbf{rs} \mid \zeta \mid mn-nm \rangle d^3s \\
&= \sum_{\text{all } n,m=\mathrm{prot}} \int d^3s \phi_m{}^*(\tfrac{1}{2}(\mathbf{r}+\mathbf{s})) \phi_n{}^*(\tfrac{1}{2}(\mathbf{r}+\mathbf{s})) \phi_m(\tfrac{1}{2}(\mathbf{r}+\mathbf{s})) \phi_n(\tfrac{1}{2}(\mathbf{r}+\mathbf{s})) \\
&\qquad \times \zeta^*[\mathbf{r}-\mathbf{s}, \tfrac{1}{2}(\mathbf{r}+\mathbf{s}), W_{mn}] \zeta[\mathbf{r}-\mathbf{s}, \tfrac{1}{2}(\mathbf{r}+\mathbf{s}), W_{mn}]^{(\mathrm{D-E})} \\
&= \sum_{m_{\mathrm{core}}} \int d^3t [2R_m{}^2(\mathbf{r}-\tfrac{1}{2}\mathbf{t})/4\pi(\mathbf{r}-\tfrac{1}{2}\mathbf{t})^2] \rho_{\mathrm{total}}(\mathbf{r}-\tfrac{1}{2}\mathbf{t}) \zeta^*(\mathbf{t}, \mathbf{r}-\tfrac{1}{2}\mathbf{t}, W_m) \zeta(\mathbf{t}, r-\tfrac{1}{2}\mathbf{t}, W_m)^{(\mathrm{D-E})}. \quad (4.21)
\end{aligned}$$

[77] B. H. Brandow, thesis, Cornell University (unpublished); and private communication.

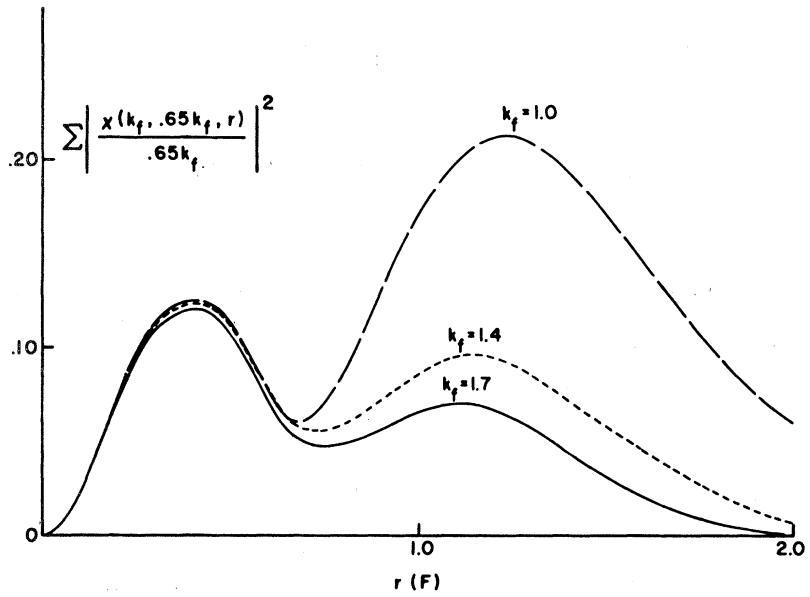

FIG. 22. Sum of the squares of the singlet-S and triplet-S defect functions in nuclear matter at $k_F=1.0$, 1.4, and 1.7 F^{-1}.

The averaged starting energy W_m is introduced to simplify the final form of (4.21) and is consistent with the approximation in (4.18).

The different structure of the particle and hole corrections is now apparent from (4.18) and (4.21). For the hole correction, there is a certain probability for depopulation of each wave function, given by an average κ for that wave function. For the particle correction, however, the distribution of extra density depends only on the local density within the range of the defect function. If we ignore for the moment the smearing in (4.21) due to the range of ζ, the particle correction at a given point is roughly proportional to the radial function times κ at that point. Since κ is larger at high densities, it is evident that the hole correction removes density uniformly from a given radial function and this density is redistributed preferentially at high densities by the particle correction. The smearing in the particle correction compensates this effect somewhat, tending to reduce the central density and increase the density in the tail, but the net effect of the sum $\Delta\rho_{\text{hole}}^{\text{prot}}+\Delta\rho_{\text{part}}^{\text{prot}}$ is still to slightly increase the central density.

In order to evaluate these corrections numerically, it is necessary to obtain an approximate function for $\zeta(r, R, W)$. From the reaction matrix calculations by Siemens,[20] it turns out that the defect function is not very sensitive to the relative momentum, so that we may evaluate it at an average momentum $k_{\text{av}}=0.65k_F$ and trivially perform the integral over relative momentum. Then, using the nuclear-matter result in (3.3), the s-wave contribution to κ is

$$\kappa_s=\tfrac{3}{8}\rho(4\pi/k_{\text{av}}^2)\int dr[\{\chi_{01}^0(k_F, k_{\text{av}}, r)\}^2+\{\chi_{21}^0(k_F, k_{\text{av}}, r)\}^2]. \quad (4.22)$$

At $k_F=1.4$ F^{-1}, the singlet-s contribution to κ is 0.0238 and the triplet-s contribution is 0.0955, whereas the total κ including all partial waves is 0.136. Thus, it is a reasonable approximation to take the dependence of the s-state contribution and enhance it by the factor 0.136/0.119. Comparing (4.22) with (4.16), we obtain

$$[\zeta^*(r, R, W)\zeta^{(\text{D}-\text{E})}(r, R, W)](\text{spin, isospin, average}) = (0.136/0.119)\tfrac{3}{8}[4\pi/(0.65k_F)^2]\times[\{\chi_{01}^0(k_F(R), 0.65k_F(R), r)\}^2+\{\chi_{21}^0(k_F(R), 0.65k_F(R), r)\}^2]. \quad (4.23)$$

The function

$$[\{\chi_{01}^0(k_F, 0.65k_F, r)\}^2+\{\chi_{21}^0(k_F, 0.65k_F, r)\}^2]/(0.65k_F)^2$$

is shown in Fig. 22 for $k_F=1.7$, $k_F=1.4$, and $k_F=1.0$ F^{-1}. The peak at 0.4 F is virtually density-independent, and has the form one expects for a simple hard core, with the defect function being essentially $\mathcal{J}_0$ inside the core and falling rapidly as the wave function heals outside the core. The peak at 1.2 F is due to the tensor force in the $^3S_1$ state, and because of its sensitivity to Q/e, becomes exceedingly important at low densities. Even though the tensor force peak grows strongly with decreasing k_F, κ still decreases with k_F because of the factor k_F^3 from ρ.

Rather than fitting the detailed spatial distribution shown in Fig. 22, we approximate each peak by a δ function with its strength fitted to yield the correct contribution in nuclear matter at $k_F=1.0$ and 1.4 F^{-1}. Although an exponential in k_F gives a better fit at $k_F=1.7$, a Gaussian interpolates roughly the same between 1.0 and 1.4, and extrapolates to much smaller values at low density. Thus we choose

$$\frac{[\chi_{01}^0(k_F, r)]^2+[\chi_{21}^0(k_F, r)]^2}{(0.65k_F)^2}\propto 1.09\delta(r-0.4)+11.7\exp(-k_F^2/0.96)\delta(r-1.2) \quad (4.24)$$

and

$$\kappa(k_F)=\frac{1.09+11.7\exp(-k_F^2/0.96)}{2.61}\left[\frac{k_F}{(1.4)}\right]^3(0.136). \quad (4.25)$$

The starting energy dependence is included by multiplying (4.24) and (4.25) by a polynomial in W which approximately reproduces the W dependence at $k_F=1.36$ F^{-1}. From nuclear-matter defect functions computed at $W=2.4$, 1.69, and 0.48 F^{-2}, the ratio of the s-state contribution to κ at $W=1.69$ F^{-2} to that at the nuclear-matter value of $W=2.4$ F^{-2} is 1.11, and at $W=0.48$ F^{-2}, the ratio is 1.41. Hence, the contributions in (4.24) and (4.25) are multiplied by

$$f(W)=1.57-0.354W+0.0482W^2. \quad (4.26)$$

Using (4.25) and (4.26) in (4.18) and using the self-consistent eigenvalues and wave functions in Table IX, one finds that the probability for excitation out of each of the occupied states in Ca^{40} is 0.129, 0.135, 0.138, and 0.127 for the $0s$, $0p$, $0d$, and $1s$ states, respectively, so that the weighted average is 0.135. This value is essentially the nuclear-matter result $\kappa=0.136$, in contradiction to the qualitative argument that κ must be much larger in finite nuclei than in nuclear matter because the defect function increases greatly in the surface. The error in this argument is the fact that the effective weighting of the defect function in (4.18) is

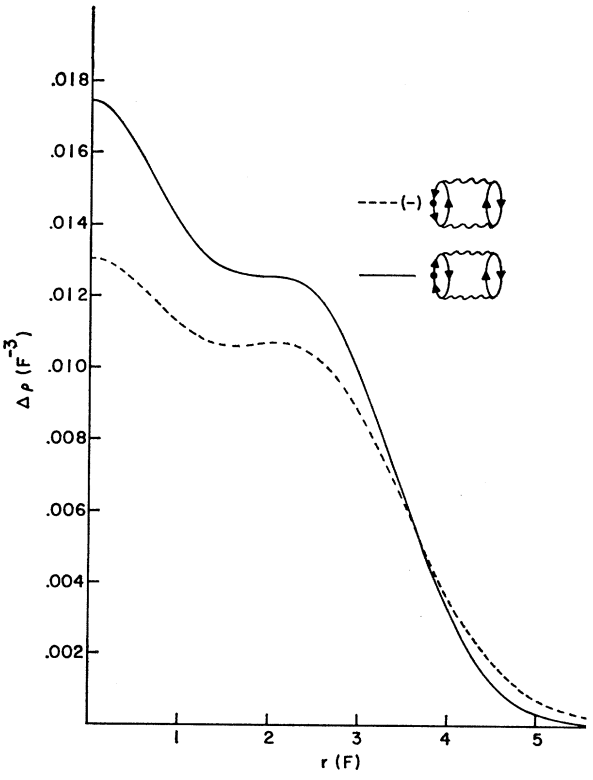

FIG. 23. Corrections to the ground-state density due to short-range correlations. Note that the dashed line corresponds to the negative of the hole correction.

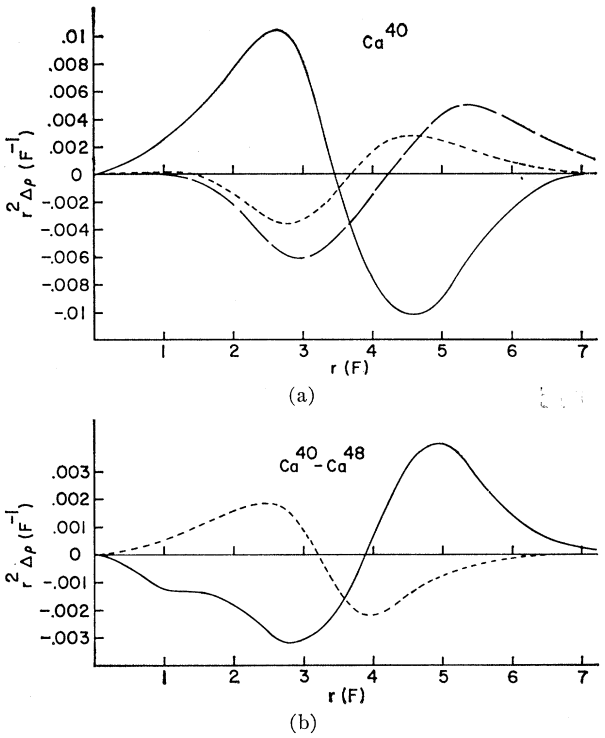

FIG. 24. Corrections to the calcium ground-state density distributions. The corrections for Ca^{40} shown in (a) are the following: short-range correlations (solid line), deformed admixtures as calculated in Appendix C (short dashes), and ten times the correction for a true $0d_{5/2}$-$0d_{3/2}$ spin-orbit doublet instead of an average $0d$ radial function (long dashes). The corrections to the Ca^{40}-Ca^{48} isotope shift in (b) are the contributions of short-range correlations (dashed line) and the effect of increasing the binding of the $0f_{7/2}$ neutron level in Ca^{48} by 5.3 MeV as described in the text (solid line).

k_F^6, generously dominating the increase in defect function at small k_F.

By particle conservation, the 13.5% of the particles removed in the hole correction must be replaced by the particle correction, which we have already noted is slightly more concentrated in the interior. The proton density corrections computed for Ca^{40} are shown in Fig. 23, and it is evident that the two 13.5% corrections largely cancel, leaving a net correction of only a few percent. Whereas there remains considerable uncertainty due to the other diagrams in Fig. 2 which have not been evaluated, this calculation indicates that the higher-order corrections to the density are likely to be of the order of a few percent, which is well within the level of theoretical ignorance concerning the saturation density of nuclear matter.

Finally, in Fig. 24, we collect for comparison several corrections to the Ca^{40} density distribution and the difference between the Ca^{40} and Ca^{48} densities. The error due to treating a single wave function for a spin-orbit doublet is indicated by calculating the difference between the density from the proper combination of $0d_{5/2}$ and $0d_{3/2}$ wave functions calculated from the potential produced by the self-consistent wave functions and the density from the single $0d$ wave func-

tion, and is seen to be negligible. The error arising from deformed admixtures, calculated in Appendix C, is somewhat smaller than the short-range correlation correction discussed above, and is of the opposite sign. With the approximation of replacing the unlike defect function by the average defect function, the Ca^{48} proton short-range correlation correction may easily be computed, and the difference between the Ca^{40} and Ca^{48} corrections is shown in Fig. 24. Comparison with the discrepancy in Fig. 14 indicates that even allowing for generous errors, the difference in correlation corrections does not significantly affect the isotope shift. To test the sensitivity of the isotope shift to the arbitrariness of our spin-orbit potential, we increased the strength so as to lower the $f_{7/2}$ neutron eigenvalue by 5.3 MeV, thereby decreasing the tail of the neutron wave function and pulling the protons inward in Ca^{48}. The negligible effect in the desired direction shown in Fig. 24 indicates that the isotope shift is insensitive to quite significant changes in the strength of the one-body spin-orbit potential.

DISCUSSION

We have shown that the fundamental features of the structure of finite nuclei may be understood in terms of a simple density-dependent HF theory. The essential simplification in this theory is the fact that the reaction matrix in all finite nuclei may be approximated by a density-dependent and energy-dependent interaction obtained from nuclear-matter theory. With slight additional approximation, the effective interaction may be cast into the form of direct and exchange interactions suitable for calculations in position space.

Even without adjusting the bare effective interaction, we have shown in Fig. 4 and Table VII that the density and energies for Ca^{40} are reasonably close to experiment, and certainly superior to any previous calculations with realistic forces. The two salient features of the rearrangement terms in the density-dependent theory are the reduction in central density and the modification of the HF relation between single-particle energies and the binding energy.

Although the adjustment of the effective interaction to reproduce nuclear-matter binding energy cannot be rigorously justified, we feel that it is the most sensible way to span the void between present nuclear-matter theory and the ultimate theory which includes the density dependence of higher-order diagrams. Our adjustable parameters are constrained by the binding energy and symmetry energy of nuclear matter, with the result that essentially only the short-range repulsion may be adjusted. Varying the one free variable, the saturation density of nuclear matter, results in an optimal fit to experimental data with $k_F=1.31$, corresponding to a reduction in strength and an increase in the density dependence of the short-range repulsion. The fact that the adjusted interaction, fit to nuclear-matter properties, simultaneously produces the correct densities, single-particle energies, and binding energies throughout the Periodic Table is a significant result, and lends credibility to the adjustment of the effective interaction.

ACKNOWLEDGMENTS

It is a great pleasure to express my deep appreciation and gratitude to my advisor, Professor Hans Bethe, for generously giving of his time, wisdom, and physical insight, and for his gentle encouragement and contagious enthusiasm. I am also most grateful to my colleague, Phil Siemens, for numerous illuminating discussions and for the use of his nuclear-matter calculations, which are fundamental to this work. My thanks are due D. R. Yennie for his advice on electron scattering, B. H. Brandow for fruitful discussions concerning formal many-body theory and short-range correlation corrections, Bob Scheerbaum for conversations relating to the effective one-body spin-orbit force, and Y. C. Lin for the use of his electron-scattering code. In addition, various phases of this work have benefited from suggestions and ideas from J. M. Irvine, G. E. Brown, K. T. R. Davies, and L. R. B. Elton. Fellowship support from the National Science Foundation during the course of this work is gratefully acknowledged.

APPENDIX A: COMPUTATIONAL DETAILS OF DENSITY-DEPENDENT HF CALCULATION

The basic equation to be solved for each radial function is

$$\tfrac{1}{2}(d^2/dr^2)R(r)=(\mathfrak{F}^D(r)-E)R(r)+\int dr'\mathfrak{F}^E(r,r')R(r'), \quad \text{(A1)}$$

where $\mathfrak{F}^D$ and $\mathfrak{F}^E$ are specified by (3.96), (3.111), and (3.119). Given a set of eigenvalues and radial functions, we shall refer to a major iteration as the construction of $\mathfrak{F}^D$ and $\mathfrak{F}^E$ and the solution of (A1) for a new set of eigenvalues and radial functions. The solution of (A1) will itself involve an iterative process, and we shall refer to successive solutions of this equation as minor iterations.

In order to treat all nuclei through Pb^{208}, the radial equation is solved out to 10 F. The short-range contribution to $\mathfrak{F}^D(r_1)$ may be written as

$$\int_0^\infty dr_2\int_{-1}^1 dx\rho((r_1^2+r_2^2-2r_1r_2x)^{1/2})V(r_2)r_2^2$$

and similarly for the density-dependent term. The integrals over x and r_2 are performed using Simpson's rule with step sizes of 0.1 and 0.05 F, respectively. For given r_1 and r_2, contributions to $\mathfrak{F}^D(r_1)$ and $\mathfrak{F}^E(r_1,r_2)$ from $V_{\rm dir}$, $V_{\rm ex}$, and $V^{\rm un}(W)$ all involve integrals of the form

$$\int_{-1}^1 I(x)dx,\ I(x)=V((r_1^2+r_2^2-2r_1r_2x)^{1/2})\times[a+bf(\tfrac{1}{2}[r_1^2+r_2^2+2r_1r_2x]^{1/2})]P_k(x). \quad \text{(A2)}$$

Although $\mathfrak{F}^E(r_1, r_2)$ varies so rapidly that it must be defined in 0.1-F steps to perform the integral

$$\int \mathfrak{F}^E(r_1,r_2)R(r_2)dr_2, \quad \text{(A3)}$$

the resulting function of r_1 is sufficiently smooth that it may be defined in steps of 0.2 F. Due to the range of the potential, we perform the integral (A3) using Simpson's rule with mesh sizes 0.1 F for $0\leq|r_1-r_2|\leq 1.8$, 0.2 F for $1.8<|r_1-r_2|\leq 3.0$, and 0.4 F for $3.0<|r_1-r_2|\leq 10$, so that utilizing the symmetry in r_1 and r_2, $\mathfrak{F}^E(r_1, r_2)$ is calculated at 2316 points. Because of the rapid variation of V for x near -1 when r_1 and r_2 are large and nearly equal and because Legendre polynomials up through P_{12} are needed for Pb^{208}, (A2) is evaluated in the form

$$\int_{\max[-1,x(1.45)]}^{\min[1,x(0.45)]} I(x)\,dx+\int_{\max[-1,x(7.0)]}^{\min[1,x(1.45)]} I(x)\,dx, \quad \text{(A4)}$$

where

$$x(r)=(r_1^2+r_2^2-r^2)/(2r_1r_2).$$

The integrals in (A4) are evaluated by 16-point and 12-point Gaussian quadrature, respectively, and the potentials are interpolated from the values in Table IV by 4-point interpolation. The Legendre polynomials up to twice the maximum l are obtained most efficiently by the recursion formula. Finally, since the same integrals (A2) are required in $\mathfrak{F}_I^D$ and $\mathfrak{F}_I^E$ for each radial equation, it is evidently most efficient to construct and store $\mathfrak{F}_I^D$ and $\mathfrak{F}_I^E$ for all orbitals at once. Since $\mathfrak{F}_I^D(r_1)$ is evaluated at 50 equally spaced values of r_1 and $\mathfrak{F}_I^E(r_1, r_2)$ is evaluated at 2316 points, the available storage allows a maximum of 16 different orbitals.

In order to solve (A1) by inserting an approximate radial function in the nonlocal term, solving the resulting inhomogeneous equation, and iterating, we decrease the over-all strength of the kernel by adding and subtracting a δ-function term. Thus, we rewrite (A1) as

$$(d^2/dr^2)R(r)=(F(r)-2E)R(r)+\int dr'K(r,r')R(r'), \quad \text{(A5)}$$

where

$$K(r,r')=2\mathfrak{F}^E(r,r')-\delta(r-r')G(r),$$
$$G(r)=A\int 2\mathfrak{F}^E(r,r')\,dr',$$
$$F(r)=2\mathfrak{F}^D(r)+G(r).$$

With the appropriate choice of A, the strength of $K(r, r')$ is sufficiently weak that a given error in the solution for the $(N-1)$th minor iteration $R^{(N-1)}$ induces a smaller error in $R^{(N)}$. The inhomogeneous equation for $R^{(N)}$ is

$$d^2R^N(r)/dr^2=(F(r)-2E)R^N(r)+H(r),$$
$$H(r)=\int dr'2\mathfrak{F}^E(r,r')R^{(N-1)}(r')-G(r)R^{(N-1)}(r). \quad \text{(A6)}$$

This equation is integrated outward from the origin in double precision using Runge-Kutta integration with a step size of 0.04 F and using 4-point interpolation for F and H. Starting one solution ${}_{(1)}R_{nl}(r)$ as ar^{l+1} at the origin and a second solution ${}_{(2)}R_{nl}(r)$ as br^{l+1}, the general solution with proper behavior at the origin is $R_{nl}(r)={}_{(1)}R_{nl}(r)+C({}_{(1)}R_{nl}(r)-{}_{(2)}R_{nl}(r))$, and C is specified by requiring that $R_{nl}'(10)/R_{nl}(10)=-(2E)^{1/2}$. Since (A6) is inhomogeneous, the normalization of $R^{(N)}$ is not arbitrary, but is dependent on the value of E. Since $R^{(N-1)}$ used in H is normalized to unity, E must be varied until $R^{(N)}$ is also normalized to unity. Minor iterations are continued until $R^{(N)}$ becomes self-consistent.

The calculations reported in this work were performed on the IBM 360/65 in Fortran G. Computing times per major iteration ranged from 3.7 min for O^{16} with 4 orbitals to 32.0 min for Pb^{208} with 14 orbitals.

APPENDIX B: ELECTRON SCATTERING IN DISTORTED-WAVE BORN APPROXIMATION

Electron scattering from a charge distribution is calculated using what is referred to as approximation I by Yennie, Boos, and Ravenhall.[74] The charge distribution is normalized such that

$$4\pi\int_0^\infty \rho(r)r^2dr=1. \quad \text{(B1)}$$

Throughout this Appendix, distances are measured in F, and energies and momenta are in F^{-1}.

The eikonal wave functions depend on four principal parameters, the local wave number k', an expansion coefficient of the potential a, the curvature of the distorted waves b, and a correction to the curvature c. For a charge distribution which has zero slope at the origin, the potential may be expanded as follows:

$$V(\lambda)=-4\pi\gamma\left[\lambda^{-1}\int_0^\lambda \rho(r)r^2dr+\int_\lambda^\infty \rho(r)r\,dr\right]$$
$$=-4\pi\gamma\left[\int_0^\infty \rho(r)r\,dr-\rho(0)\tfrac{1}{6}\lambda^2+\cdots\right], \quad \text{(B2)}$$

where $\gamma=Z/137.0388$. The local wave number is related to the incident energy k, using (B2),

$$k'=k-V(0)=k+4\pi\gamma\int_0^\infty r\rho(r)\,dr. \quad \text{(B3)}$$

The expansion coefficient a is obtained from the quadratic term in (B2), and is defined as

$$a=4\pi\gamma\rho(0)\,(k')^{-3}/3. \quad \text{(B4)}$$

The curvature parameters for the distorted waves are

$$b=\frac{4\pi\gamma}{8k'}\left[\frac{1}{k}+\frac{1}{k'}\right]\int_0^\infty \rho(r)\,dr,$$
$$c=-\frac{1}{8}\frac{\pi\gamma}{(k')^4}\int_0^\infty \frac{1}{r}\frac{\partial\rho}{\partial r}\,dr. \quad \text{(B5)}$$

Defining q' as $2k'\sin(\theta/2)$ and K' as $2k'\cos(\theta/2)$, where θ is the scattering angle, the full formula for the

scattering amplitude is

$$f=\frac{ik\gamma}{(q')^3}\exp[2iS(0)]\left(\frac{k'}{k}\right)^2 4\pi\cos\tfrac{1}{2}\theta\int_{-\infty}^{\infty}\frac{\rho(r)G(r)}{C^2(r)}e^{i\chi}r\,dr,$$

where

$$G(r)=\frac{1+3bq'r+a(q'^2-2k'^2)r^2-\frac{5}{2}cq'K'^2r^3}{1-a(\frac{3}{2}k'^2-\frac{1}{2}q'^2)r^2+b(-2k'^2+\frac{3}{2}q'^2)r/q'+c(k'^2-\frac{5}{4}q'^2)K'^2(r^3/q')},$$

$$C(r)=1-a(\tfrac{3}{2}k'^2-\tfrac{1}{4}q'^2)r^2-bK'^2(r/q')+cK'^4(r^3/2q'), \tag{B6}$$

$$\chi(r)=q'r-a[q'(k'^2/2)-(q'^3/12)]r^3-\tfrac{1}{2}bK'^2r^2+\tfrac{1}{8}cK'^4r^4.$$

The differential cross section is $d\sigma/d\Omega=|f|^2$, so that the phase factor $e^{2iS(0)}$ does not contribute.

Several practical considerations arise when using (B6) for numerical calculations. The parameter a gives the proper quadratic term near the center of the charge distribution, but the greatest accuracy is desired in the surface region. Higher-order terms in the expansion may be effectively included by varying a to give the parabola which yields the best fit in the surface. As it stands, the expression for c in (B5) is unrealistically sensitive to oscillations in the central density which must occur due to s-state orbitals. Since it is physically clear that the distortion must be specified by rather low Fourier components of the charge distribution, we calculate c using the empirical parabolic Fermi distribution for the appropriate nucleus. The integration is cut off at small r to eliminate the singularity at $r=0$ due to the fact that the empirical distributions have a small but finite slope at the origin, whereas the true distribution must have zero slope.

The radial integration in f must be cut off at large r to eliminate zeros in the denominator of $G(r)$ and in $C(r)$. It is clear that zeroes occur in both functions since they are cubic and r goes from $-\infty$ to $+\infty$. Physically, of course, this indicates that the expansion of the distorted waves breaks down at some radius, and it is evident that this radius decreases at small scattering angles since the cubic terms vary as $1/q'$. The zeroes themselves are of no practical concern since in the energy and angular ranges of interest in this work they are more than 5 F beyond the surface, but one can see that the approximation becomes rather inaccurate at small scattering angles by comparing our results with the exact partial-wave analysis in Refs. 69 and 72–73. In practice, the calculations are quite insensitive to the cutoff, with Pb^{208} yielding essentially identical results for cutoffs of 10 and 12 F.

The numerical computations were performed using a somewhat modified version of a computer code written by Lin, to whom the author is indebted for the use of this program.

APPENDIX C: DEFORMED ADMIXTURES IN Ca^{40}

It has been shown by Brown and Green[78] and by Gerace and Green[76] that significant admixtures of deformed states are present in the ground states of O^{16} and Ca^{40}. Whereas it is not entirely clear how to correctly treat a deformed spin-zero ground state,[79–82] the adiabatic approximation of Bohr and Mottelson[79] and the method of projected Slater determinants[81] indicate that only the spherical average of the deformed state is relevant to electron scattering. Thus, in this Appendix, the quantitative effect of the deformed admixture on the spherical average of the ground-state density distribution of Ca^{40} is evaluated and shown to be negligible. The analogous analysis of O^{16} yields similar results.

In treating the 20% deformed admixture in Ca^{40}, it is useful to consider two separate effects on the spherically averaged charge density. One effect is that one proton is removed from the $0d$ shell and distributed in the $1p$, $0f$ shell, and the second effect is that even with this proton in the $0d$ shell, the spherical average of the deformed ground state is slightly different from the spherically symmetric ground state. Actually, there is a slight error in superimposing these two effects, since the discrepancy between the spherically symmetric and spherically averaged wave functions will be slightly different for the $0d$ and $1p$ or $0f$ wave functions, but since only one proton is involved, this error is quite negligible.

For harmonic-oscillator functions, the discrepancy between the spherically symmetric density and the spherical average of the deformed density is quite different from that in the case of distributions with a sharp surface. The spherical average of an oblate spheroid with a sharp surface is a spherical distribution with a diffuse surface, which is qualitatively quite different, whereas the spherical average of an anisotropic harmonic-oscillator density distribution is very similar to an isotropic harmonic-oscillator density distribution.

We now consider an anisotropic harmonic oscillator such that

$$\omega_x=\omega_y=\omega(1+\tfrac{1}{3}\epsilon),$$
$$\omega_z=\omega(1-\tfrac{2}{3}\epsilon). \tag{C1}$$

[78] G. E. Brown and A. M. Green, Nucl. Phys. **75**, 401 (1966).

[79] A. Bohr and B. R. Mottelson, Kgl. Danske Videnskab. Selskab, Mat.-Fys. Medd. **27**, No. 16 (1953).

[80] B. W. Downs, D. G. Ravenhall, and D. R. Yennie, Phys. Rev. **106**, 1285 (1957).

[81] F. Villars, in *Proceedings of the International School of Physics "Enrico Fermi," Course XXXVI* (Academic Press Inc., New York, 1966).

[82] R. E. Peierls and D. J. Thouless, Nucl. Phys. **38**, 154 (1962).

In this notation, the deformation considered by Gerace and Green[76] corresponds to $\epsilon=+0.2$. Filling the Cartesian harmonic-oscillator states for protons in Ca^{40}, we obtain

$$\rho_{\rm prot}=(2/\pi^{3/2})[(1+\tfrac{1}{3}\epsilon)(1+\tfrac{1}{3}\epsilon)(1-\tfrac{2}{3}\epsilon)]^{1/2}\times\exp[-(x^2/b_x^2+y^2/b_y^2+z^2/b_z^2)]\times[\tfrac{5}{2}+2(x^2/b_x^2+y^2/b_y^2+z^2/b_z^2)^2]. \quad (C2)$$

Substituting (C1) in (C2), changing to spherical coordinates, and angle averaging, we obtain

$$\bar{\rho}_{\rm prot}=(4\pi)^{-1}\int\rho_{\rm prot}d\Omega=2\pi^{-3/2}(1+\tfrac{1}{3}\epsilon)(1-\tfrac{2}{3}\epsilon)^{1/2}\times\int_0^1\exp[-r^2/b^2(1+\tfrac{1}{3}\epsilon-\epsilon\cos^2\theta)]\times[\tfrac{5}{2}+2(r^4/b^4)(1+\tfrac{1}{3}\epsilon-\epsilon\cos^2\theta)^2]d\cos\theta. \quad (C3)$$

Equation (C3) may be cast into a form convenient for comparison with spherical harmonic-oscillator densities by expanding the quantities of order ϵ out of the exponential and integrating. Retaining terms of order ϵ^2, we obtain

$$\bar{\rho}_{\rm prot}=2\pi^{-3/2}[1-\tfrac{1}{6}\epsilon^2]\exp(-r^2/b^2)\times[\tfrac{5}{2}+2r^4/b^4+\tfrac{18}{45}(r^4/b^4)\epsilon^2-\tfrac{16}{45}(r^6/b^6)\epsilon^2+\tfrac{4}{45}(r^8/b^8)\epsilon^2]. \quad (C4)$$

Recognizing $2\pi^{-3/2}(\frac{5}{2}+2r^4/b^4)$ as the Ca^{40} ground state in a spherical basis, it is evident that (C4) represents the removal of $\epsilon^2/6$ or 0.67% of the protons from the spherical ground state and redistribution of them in higher states. One may verify that the normalization of (C4) is correct to order ϵ^2.

To simplify the inclusion of the single proton in an excited Nilsson state, it is most convenient to rewrite (C4) in terms of spherical harmonic-oscillator radial functions $R_{nl}(r)$. Clearly, there is no unique way of doing so, but the following form has the advantage of a small number of radial functions with roughly comparable coefficients.

$$\bar{\rho}_{\rm prot}=\rho_s+(2\pi r^2)^{-1}[-\tfrac{1}{6}\epsilon^2R_{00}^2-\tfrac{1}{2}\epsilon^2R_{01}^2-\tfrac{25}{12}\epsilon^2R_{02}^2-\tfrac{1}{6}\epsilon^2R_{10}^2+\tfrac{2}{3}\epsilon^2R_{12}^2+\tfrac{9}{4}\epsilon^2R_{04}^2], \quad (C5)$$

where ρ_s is the density of the Ca^{40} ground state for a spherical harmonic oscillator. Using Nilsson's tabulated wave functions,[83] removing a single proton from orbit 8 and placing it in orbit 14 with $\epsilon=0.2$ corresponds to a change in density of

$$\delta_\rho=(2\pi r^2)^{-1}[-0.5R_{02}^2+0.3795R_{03}^2+0.1205R_{11}^2]. \quad (C6)$$

Thus, using (C5) and (C6) and including the fact that the probability for deformation is 20%, the total density correction from the deformed admixture is

$$\Delta\rho=(10\pi r^2)^{-1}[-0.0067R_{00}^2-0.0200R_{01}^2-0.5833R_{02}^2-0.0067R_{10}^2+0.3795R_{03}^2+0.1205R_{11}^2+0.0267R_{12}^2+0.0900R_{04}^2]. \quad (C7)$$

This correction is extremely small and is graphed in Fig. 24.

[83] S. G. Nilsson, Kgl. Danske Videnskab. Selskab, Mat.-Fys. Medd. **29**, No. 16 (1955).

PHYSICAL REVIEW C VOLUME 1, NUMBER 4 APRIL 1970

Coulomb Distortion in Heavy-Ion Reactions

A. S. JENSEN* AND C. Y. WONG

The Niels Bohr Institute, University of Copenhagen, Denmark and *Oak Ridge National Laboratory, Oak Ridge, Tennessee 37830*†

(Received 24 November 1969)

The dynamics of nuclear distortion is studied for two spherical nuclei under the influence of their mutual Coulomb interactions. Both the quadrupole and the octupole degrees of freedom are considered. Realistic stiffness and effective-mass parameters are employed. It is found that the energy needed to bring the two nuclei into contact increases as a result of the distortions. However, in the most favorable case, the increase is only a few percent. This is much smaller than previous estimates using either the liquid-drop model or the adiabatic model.

I. INTRODUCTION

PREVIOUS estimates of the increase in the Coulomb-barrier height were obtained by studying the dynamics of distortion using the liquid-drop model,[1,2] or by using an adiabatic model with realistic stiffness parameters.[3] A very large increase in the Coulomb-barrier height was obtained. The use of liquid-drop parameters to describe the vibrational properties of a nucleus is inappropriate, however, as they do not reproduce the experimental excitation energies and the transition rates for the first-quadrupole vibrational state. On the other hand, the distortion estimated by considering the deformation potential alone, as done in Ref. 3, would be correct only if the

* Present address: Atomic Energy of Canada Limited, Chalk River, Ont., Canada.

† Research sponsored in part by The U.S. Atomic Energy Commission under contract with Union Carbide Corporation.

[1] R. Beringer, Phys. Rev. Letters **18**, 1006 (1967).

[2] J. Maly and R. Nix, J. Phys. Soc. Japan Suppl. **24**, 678 (1968).

[3] C. Y. Wong, Phys. Letters **26B**, 120 (1968).